博士学位論文

Studies on the mode of action of neurotoxic insecticides and insecticide resistance

平 田 晃 一

博士学位論文

Studies on the mode of action of neurotoxic insecticides and insecticide resistance

平成 29 年 11 月 6 日

平 田 晃 一

Contents

General Introduction **1**

Chapter 1 **8**

A single crossing-over event in voltage-sensitive Na^+ channel genes may cause critical failure of dengue mosquito control by insecticides

Chapter 2 **30**

Association between the R81T mutation in the nicotinic acetylcholine receptor β1 subunit of *Aphis gossypii* and the differential resistance to acetamiprid and imidacloprid

Chapter 3 **49**

The R81T mutation in the nicotinic acetylcholine receptor of *Aphis gossypii* is associated with neonicotinoid insecticide resistance with differential effects for cyano- and nitro-substituted neonicotinoids

Chapter 4 **75**

Studies on *Aphis gossypii* cytochrome P450s CYP6CY22 and CYP6CY13 using an in vitro system

Summary **94**

Reference **97**

Acknowledgements

Publications

General Introduction

Crop protection and insecticides

By 2050, the United Nations estimates that the global population will reach 9.7 billion people (World Population Prospects 2015). It is estimated that only slight increases are to be expected in the amount of arable farmland over the next several decades (World Population Prospects 2015). Insecticides are essential tools for preventing or minimizing insect damage to, and significantly increasing the quality and quantity of crops, as well as for improving the quality of life of humans. There are currently more than 20 different mechanisms, or modes of action, by which various commercial insecticides control insects by disrupting specific vital biological processes. Many of the commercially available insecticides, such as pyrethroids, neonicotinoids, and some other natural products, target the nervous system of insects and affect the voltage-sensitive sodium channel (Vssc) and nicotinic acetylcholine receptor (nAChR), which are transmembrane proteins that play an important role in signal transduction in the nervous system, and are important targets of insecticides.

Voltage-sensitive sodium channel (Vssc)

The Vssc is composed of α- and β-subunits; the α-subunit is composed of four domains, each containing six transmembrane segments (S1–S6) (Figure 1). The α-subunit is the main functional subunit, while the β-subunit supports it (Feng et al., 1995). The Vssc opens due to an increase or decrease in the membrane potential, which causes an influx of sodium ions into the cell and subsequent depolarization. The Vssc is affected by various compounds, and is a target of pyrethroids, as well as tetrodotoxin,

which is also known as fugutoxin. These compounds are classified according to the site of interaction; ten sites of interaction have been identified to date, and the pyrethroids are known to act on site 7 (Zlotkin, 1999). Pyrethroids exhibit insecticidal activity by causing a delay in inactivation and stabilize the open state of the Vssc (Bloomquist, 1996; Narahashi, 1996, 2000). Pyrethroids are grouped into two categories (Type I and Type II) based on their distinct poisoning symptoms, effects on nerve preparations, and chemical structures (Gammon et al., 1981; Lawrence and Casida, 1982; Narahashi, 1986) . Type I pyrethroids lack an α-cyano group, which is present at the phenoxybenzyl alcohol moiety of Type II pyrethroids (Figure 2). Type I pyrethroids also cause repetitive discharges in response to a single stimulus, whereas Type II pyrethroids cause membrane depolarization accompanied by suppression of cellular excitability (Narahashi, 1986) .

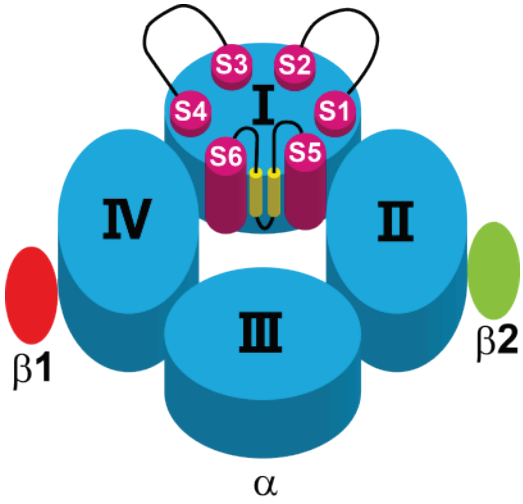

Figure 1. Schematic representation of voltage-sensitive sodium channel (Vssc). The Vssc is composed of α- and β-subunits. The α-subunit is composed of four domains, each containing six transmembrane segments (S1–S6).

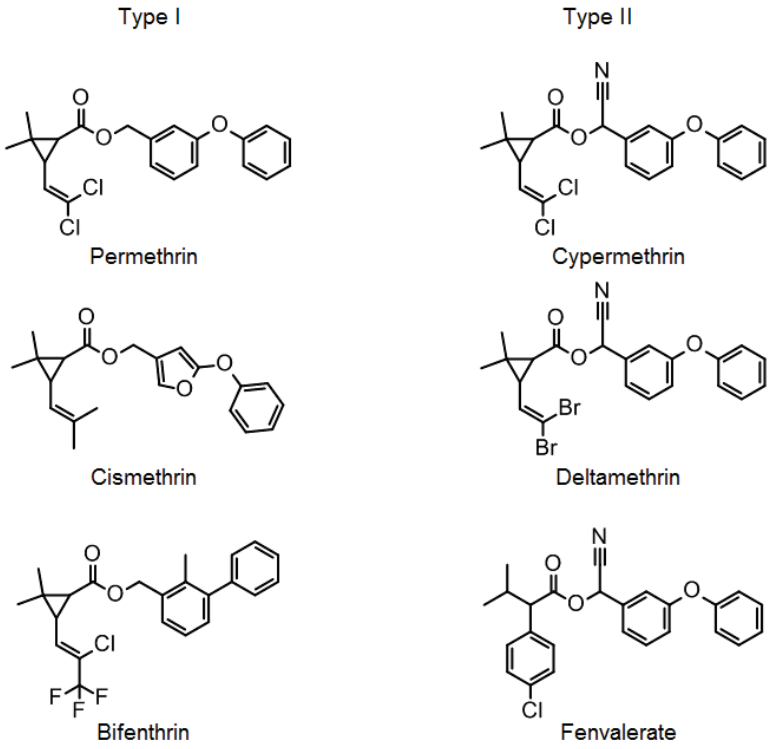

Figure 2. Chemical structures of Type I and Type II pyrethroid insecticides.

Nicotinic acetylcholine receptor (nAChR)

nAChR, inhibitory-aminobutyric acid receptor, inhibitory glutamic acid receptor, and glycine receptor belong to the cys-loop ligand-gated ion channel superfamily (Karlin, 2002). nAChR is composed of five subunits having four-transmembrane structures to form homomers or heteromers (Tomizawa and Casida, 2001) (Figure 3); upon binding with its ligand acetylcholine (ACh), this channel opens and allows cations to penetrate. Natural products such as nicotine or neonicotinoids (Figure 4) act on nAChR, bind to it, and exhibit an agonistic effect (Matsuda et al., 1998; Matsuda et al., 2001; Matsuda et al., 2005; Tomizawa and Casida, 2005). Neonicotinoids are a family of insecticides acting on neuronal nAChRs with higher selective toxicity for insects

over vertebrates, and show excellent control for a wide range of insect pests due to their systemic distribution in crop plants (Matsuda et al., 2001).

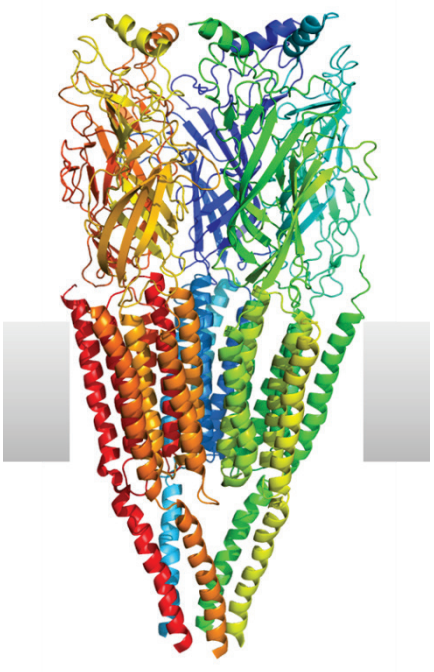

Figure 3. Schematic representation of the nicotinic acetylcholine receptor (nAChR). The nAChR is composed of five subunits having four-transmembrane structures to form homomers or heteromers.

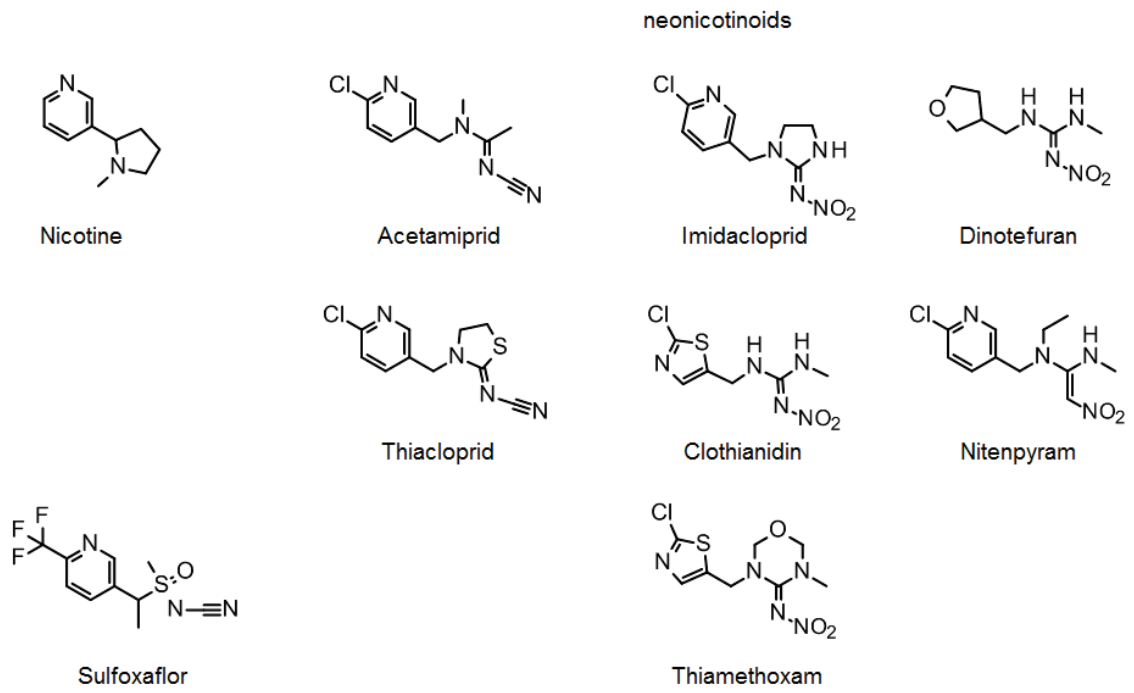

Figure 4. Chemical structures of nicotine, neonicotinoids and sulfoxaflor

Methods for studying the mode of action of compounds having neurotoxic insecticidal activity

A range of methods are available for studying the mechanism of action of compounds having neurotoxic insecticidal activity, including molecular biology and biochemical approaches, binding assays, optical methods using fluorescent dye, and electrophysiological methods. Among these, electrophysiological methods are the most suitable for detailed testing of the effects of actions or mechanisms of action of receptors or ion channels because such approaches identify the effects of the compound by detecting changes in current. There are three different types of electrophysiological method. One is the two-electrode voltage-clamp method (TEVC), which uses *Xenopus* oocytes. This method is suitable for the expression and analysis of receptors of a wide range of biological strains, especially for the analysis of variants (Shimomura et al.,

2006). Another method is the patch clamp method; this enables various measurements, is particularly applicable to the nerve cells of insects, and enables evaluation of the effects or activities of a compound on the expression of receptors in an insect's body. The third method is the automatic patch clamp method. This was developed to improve the low throughput of electrophysiological methods, which is one of their drawbacks, is labor-saving, and can be used to analyze a large number of compounds, while utilizing the benefits of electrophysiological features.

Insecticide resistance

The development of resistance to insecticides is one of the most important problems encountered during insect pest management. Since the late 1940s, the number of cases of insecticide resistance, and the number of species and compounds involved has been continually increasing (Sparks and Nauen, 2015). Detoxification by P450 for example, mutation of an amino acid residue at the site of activity, and a decrease in the permeability of an insecticide due to an increased cuticle surface area are known to be involved in such resistance (Bass et al., 2014; Casida and Durkin, 2013; Scott, 1999). In most cases, cytochrome P450-mediated detoxification plays a primary role in insecticide resistance in a variety of insects (Rauch and Nauen, 2003; Scott, 1999; Zhao et al., 2000) . Cytochrome P450 is found widely in nature and plays roles in many biological processes, including hormone synthesis and the metabolism of exogenous compounds. In insects, cytochrome P450 has been implicated in providing resistance to insecticides via degrading foreign compounds to more soluble and less toxic forms (Scott, 1999) . This is accomplished via either up-regulated cytochrome P450 expression or structural changes that may alter the substrate profile or catalytic activity

of the enzyme (Amichot et al., 2004b; Bergé et al., 1998; Bogwitz et al., 2005; Feyereisen et al., 1989; Nikou et al., 2003; Pridgeon and Liu, 2003).

Aim of this thesis

The author believe that the findings of studies on the mechanisms of action of neurotoxic insecticides and resistance to them will contribute to the research and development of new insecticides, including ones effective against insecticide-resistant insects, and to the establishment of appropriate and effective measures for avoiding resistance. Therefore, in the present study, the author investigated the mechanism of action of the compound that acts on Vssc and nAChR, and the associated mechanism of resistance, mainly using an electrophysiological method. In chapter 1, the author expressed several types of *Aedes aegypti* Vssc in *Xenopus* oocytes and examined the effect of amino acid substitutions in Vssc on pyrethroids susceptibilities. In chapter 2, the author attempted to identify the mechanisms of neonicotinoid resistance of *Aphis gossypii* using an insecticidal assay with and without piperonyl butoxide (PBO) pretreatment, along with sequencing of the nAChR gene and electrophysiology. In chapter 3, two-electrode voltage-clamp electrophysiological analyses and molecular modeling were employed to investigate the differential effects of the R81T mutation of *A. gossypii* nAChR on cyano- and nitro-substituted neonicotinoids and sulfoxaflor. In chapter 4, the author used next-generation sequencing (NGS) to identify P450 family members involved in the metabolism of neonicotinoids insecticides of *A. gossypii*. Further, molecularly cloned P450 cDNAs and expressed to study P450-mediated insecticide metabolism.

Chapter 1

A single crossing-over event in voltage-sensitive Na^+ channel genes may cause critical failure of dengue mosquito control by insecticides

Introduction

Aedes aegypti is the major mosquito vector of dengue fever (DF), yellow fever, and chikungunya fever. DF causes more illness and death in humans than any other arboviral disease (Gubler, 1998). Mosquito control is mainly achieved by pyrethroids because of the high and rapid activity of this class of insecticides in insects, and its low toxicity to mammals. However, intensive and frequent use of these chemicals has resulted in the development of resistance in *A. aegypti* (Hemingway et al., 2004; Vontas et al., 2012).

Pyrethroid insecticides target the voltage-sensitive Na^+ channel (Vssc) (Davies et al., 2007). Some amino acid substitutions alter the affinity of Vssc for pyrethroids and they confer resistance to this class of insecticide in insects (Davies et al., 2007). Understanding how mutations alter interaction of pyrethroids with Vssc is important for improving our understanding of the pyrethroid mechanism of action and for constructing appropriate control strategies against pest insects. Previous studies have shown that additional amino acid substitutions concomitantly occurring in Vssc can further reduce an insect's susceptibility to pyrethroids. For instance, houseflies harboring Vssc with the L1014F substitution cause reduction in the affinity of Vssc for pyrethroids (so-called knockdown resistance or kdr), while the double mutation

L1014F+M918T further reduces the susceptibility of the insects to pyrethroids (so-called super-kdr) (Vais et al., 2000).

In Southeast Asia, one of the largest DF endemic areas, two major Vssc haplotypes confer pyrethroid resistance to *A*. *aegypti*, i.e., S989P+V1016G and F1534C. *A*. *aegypti* with these two haplotypes are widely and sympatrically distributed in this area (Kasai et al., 2014; Kawada et al., 2009; Stenhouse et al., 2013). Neurophysiological studies have revealed that V1016G and F1534C single mutations each confer resistance to pyrethroids (Du et al., 2013). The F1534C mutation has also been confirmed from another dengue vector, *Aedes albopictus* (Kasai et al., 2011). S989P is usually accompanied by V1016G (Srisawat et al., 2010), but its contribution to pyrethroid resistance is unclear. Vssc harboring triple amino acid substitutions (i.e., S989P+V1016G+F1534C) has not been recorded from a field population of *A*. *aegypti* although heterozygous form of these two haplotypes was confirmed (Kawada et al., 2009; Stenhouse et al., 2013). Such a haplotype, however, can be generated by a single crossing-over event of the above two major resistance Vssc haplotypes. Moreover, the sensitivity of such a triple-mutated Vssc to pyrethroids has not yet been investigated.

In this study, the author analyzed the pyrethroid sensitivity of Vssc harboring triple substitutions, using a two-electrode voltage-clamp method, and we discussed the effect thereof on the control of the dengue mosquito vector by pyrethroids. We also investigated the synergistic effect of S989P on the sensitivity of Vssc harboring the V1016G mutation to pyrethroid insecticides.

Materials and Methods

Mosquito strains

Two strains of *A. aegypti* were used: SMK, a laboratory reference strain susceptible to pyrethroid insecticides, and SP, originally collected from Singapore in 2009, which has developed a high level of resistance to permethrin (1650-fold in adult females) after permethrin selection for 10 generations (Kasai et al., 2014). Mosquitoes were reared as described previously (Kasai et al., 1998).

In vitro metabolism and synergistic studies revealed that both reduced permethrin susceptibility and enhanced metabolic enzyme activity, via cytochrome P450 monooxygenases, confer the high level of resistance in strain SP (Kasai et al., 2014). Previous study confirmed that this strain possesses both S989P and V1016G mutations in Vssc homozygously (Kasai et al., 2014). The full length of Vssc cDNA in the SP strain, however, has not yet been sequenced.

Chemicals

Permethrin (purity > 99.1%) and deltamethrin (purity > 99.0%) were purchased from LGC Standards (Teddington, UK) and Wako Pure Chemical Industries, Ltd. (Osaka, Japan), respectively. The stock solutions of insecticides (100 mM) were prepared in dimethyl sulfoxide (DMSO). Working solutions were prepared in standard oocyte saline (SOS; 100 mM NaCl, 2 mM KCl, 1.8 mM $CaCl_2$, 1 mM $MgCl_2$, 5 mM HEPES, pH 7.6) immediately prior to experiments. The DMSO concentration in the final solution was < 0.1% and it did not affect the function of Na^+ channels in the experiments (data not shown).

Sequencing full-length Vssc cDNA from SMK and SP strains

Total RNA was extracted from 10 three-day-old females using ISOGEN (Nippon Gene Co., Ltd., Tokyo, Japan). Genomic DNA was removed by digesting the total RNA samples with DNase I using TURBO DNase (Life Technologies Co., Carlsbad, Ca, USA). cDNA was synthesized using RNA and QT primer (Table 1-1) and reverse transcriptase ReverTra Ace (Toyobo, Osaka, Japan) according to the manufacturer's instructions. The full-length cDNAs of *A*. *aegypti* Vssc were amplified by PCR using PrimeStar GXL DNA polymerase (Takara Bio Inc., Shiga, Japan) and the primers aegSCF1 and aegSCR2. Cycling conditions for PCR were as follows: 95 ℃ for 2 min, followed by 35 cycles of each consisting of 98 ℃ for 10 s, 60 ℃ for 15 s, and 68 ℃ for 6 min. Nested PCR was performed under the same conditions, but using the primers aegSCF3 and aegSCR4. PCR products were purified by agarose gel electrophoresis and inserted into the pTA2 plasmid using the TArget Clone -Plus system (Toyobo, Osaka, Japan). The insert sequence was confirmed using the following primers: T7b, aegSCF5, aegSCF9, aegSCR8, AaSCF3, aegSCF7, AaSCR21, aegSCF10, AaSCR8, AlSCR8, aegSCR6, and T3b. Eight and six clones of full-length Vssc cDNAs from the SMK and the SP strains, respectively, were sequenced. Nucleotide polymorphisms that were confirmed only in a single clone were considered to reflect polymerase errors.

Site-directed mutagenesis and cloning of tipE cDNA

Site-directed mutagenesis was performed by PCR using PrimeStar GXL DNA polymerase and primers that were designed based on the 5' and 3' end sequences of *A*. *aegypti* Vssc (AaNavS2, DDBJ accession number: AB909019), which was isolated from insecticide susceptible SMK strain as described below. The forward primer

aegSCF13 and reverse primer aegSCR14 included *Eco*RI and *Stu*I restriction sites (underlined), respectively, to facilitate cloning (Table 1-1). Full-length cDNAs encoding the substitutions V1016G (AaNavR6), F1534C (AaNavR7), S989P (AaNavR8), S989P+V1016G (AaNavR9), and S989P+V1016G+F1534C (AaNavR10) in Vssc were amplified, as shown in Figure 1-1. In this study, we numbered the amino acid position according to the sequence of the most abundant splice variant of the house fly Vssc (GenBank accession nos. AAB47604 and AAB47605). Starting with AaNavS2 (wild-type), each fragment containing the smallest number of polymorphisms were subjected to oligonucleotide-mediated mutagenesis following a standard protocol (Ho et al., 1989), using the primers aegSCF15, aegSCR16, aegSCF17, aegSCR18, aegSCF19, and aegSCR20. Amplified PCR products were digested with restriction enzymes and cloned into the pTS1 vector (Nippon Gene Co., Ltd, Tokyo, Japan). Clones were fully sequenced and each amino acid substitution was confirmed. *Drosophila melanogaster* temperature-induced paralytic E (tipE) cDNA was also amplified and cloned into pcDNA3.1(+) (Invitrogen, Carlsbad, CA, USA) using published primer sequences (Feng et al., 1995). The compatibility of *Drosophila* tipE with Vssc of other insects has been well documented (Burton et al., 2011; Du et al., 2009; Hu et al., 2011; Tan and Tong, 2004).

Table 1-1. Primer sequences used in this study.

Name	Sequence (5' to 3')	Restriction enzymes	Purpose
QT	CCAGTGAGCAGAGTGACGAGGACTCGTGCTCAAGCT		cDNA synthesis
aegSCF1	ATGACCGAAGACTCCGATTCGA		PCR amplification of Aae Vssc
aegSCR2	TCAGACATCCGCCGATCGT		
aegSCF3	ATGACCGAAGACTCCGATTCGATAT		PCR amplification of Aae Vssc
aegSCR4	TCAGACATCCGCCGATCGTGAA		
T7b	CGTAATACGACTCACTATAGGGC		Sequencing of Aae Vssc
aegSCF5	GTCGAATCTACCGAGGTGAT		
aegSCF9	TGGTGTTACGATCAGCTGGA		
aegSCR8	CAGCCCTCTTGGAAGTAGTA		
AaSCF3	GTGGAACTTCACCGACTTCA		
aegSCF7	GAGGCGTTCAATCGGATATC		
AaSCR21	GCAATCTGGCTTGTTAACTTG		
aegSCF10	CGTTTCAGCTCATCGAGAAC		
AaSCR8	TAGCTTTCAGCGGCTTCTTC		
AlSCR8	AACAGCAGGATCATGCTCTG		
aegSCR6	TGCCTGAACTTCACCCAGTT		
T3b	CGCAATTAACCCTCACTAAAGGGA		
aegSCF13	CGGAATTCATGACCGAAGACTCCGATTCGATAT	*Eco*RI	PCR amplification of Aae Vssc
aegSCR14	GAAGGCCTTCAGACATCCGCCGATCGTGAA	*Stu*I	
aegSCF15	GGAAATCTAGTAGGACTTAACCTTTTCTTAGC		Site-directed mutagenesis
aegSCR16	GCTAAGAAAAGGTTAAGTCCTACTAGATTTCC		
aegSCF17	CTTCATCATCTGCGGGTCGTTCTT		
aegSCR18	AAGAACGACCCGCAGATGATGAAG		
aegSCF19	AGTGGATCGAACCCATGTGGGATT		
aegSCR20	AATCCCACATGGGTTCGATCCACT		
pTS1_cRNA_F	GCGCATAATACGACTCACTATAGGGAG		cRNA synthesis template
pTS1_cRNA_R	AGCTGTGCGCGCAAATTAACCCTC		

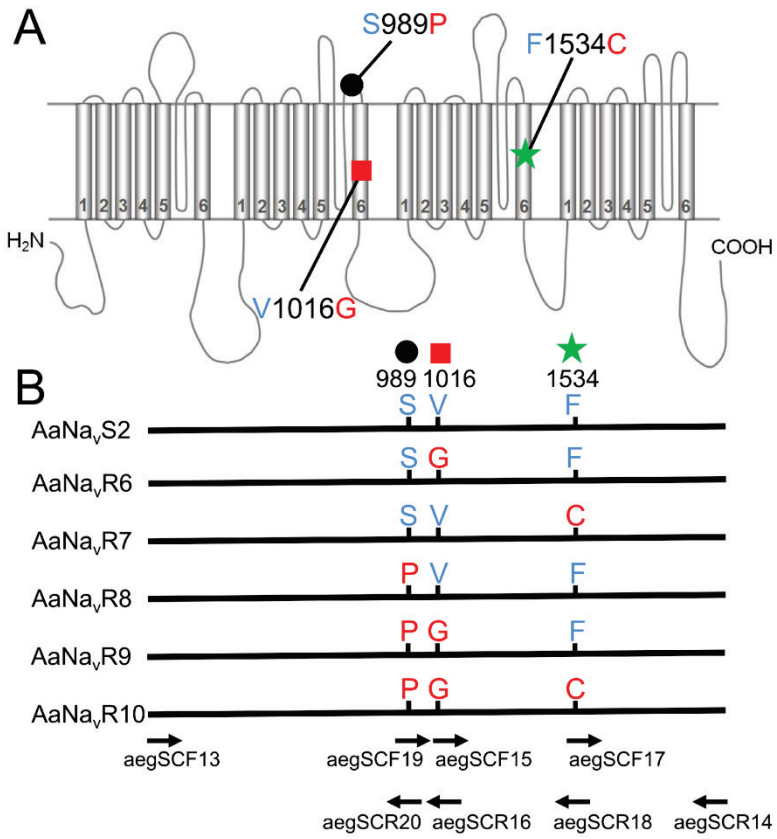

Figure 1-1. Mutations of *Aedes aegypti* Vssc investigated in this study.

(A) Schematic illustration of the locations of the Vssc mutations assessed. Positions are numbered according to the amino acid sequence of the most abundant splice variant of housefly Vssc (GenBank accession nos. AAB47604 and AAB47605). (B) Six Vssc types investigated in this study and the positions of primers used for site-directed mutagenesis are shown. Primer sequences are listed in Methods. AaNavS2 is the wild-type Vssc of which the cDNA was isolated from the insecticide-susceptible SMK strain.

Preparation of cRNA

Templates for in vitro transcription were PCR-amplified from plasmids using KOD plus Neo (Toyobo) and the primers pTS1_cRNA_F and pTS1_cRNA_R (Table 1-1). Capped RNA transcripts were synthesized using the mMessage mMachine T7 Ultra Kit (Life Technologies, Carlsbad, CA, USA). The quantity and quality of cRNAs

were verified by agarose gel electrophoresis and absorption spectroscopy, and cRNAs were stored at −80°C until required for use.

Expression of A. aegypti Vssc in Xenopus oocytes

Female *Xenopus laevis* were purchased from Hamamatsu Seibutsukyozai (Shizuoka, Japan) and maintained in dechlorinated water at 18 °C. Oocytes were surgically obtained following anesthesia of a *Xenopus* frog using 0.03% benzocaine (Sigma-Aldrich, Tokyo, Japan), and enzymatically defolliculated by incubating them for 1–1.5 h in a Ca^{2+}-free SOS containing 1 mg/ml collagenase (Wako Pure Chemical Industries, Osaka, Japan). Vssc cRNA and tipE cRNA (0.9 ng each) were co-injected into healthy stage V–VI oocytes, which were incubated at 18 °C in SOS medium supplemented with 50 μg/ml gentamycin, 100 U/ml penicillin, 100 μg/ml streptomycin, 2.5 mM Na pyruvate, and 4% horse serum, for 2–4 days after injection. The medium was replaced daily and unhealthy oocytes were discarded. It is generally recognized that the knockdown resistance is a recessive trait (Gao et al., 2003; Huang et al., 2004). Since we injected mRNA of a single Vssc haplotype into *Xenopus* oocytes, theoretically we reproduced the environment of the homozygous Vssc form in the cell.

Electrophysiological recording environment

Na^+ currents were recorded using a TEV-200A (Dagan Corporation, Minneapolis, MN, USA) amplifier and digitized at 40 kHz with PowerLab 8/30 (AD Instruments, Nagoya, Japan). Signals were filtered at 2 kHz using a Bessel four-pole filter (Dagan Corporation, Minneapolis, MN, USA). The P/N method was used to subtract capacitive transient currents (Bezanilla and Armstrong, 1977). Recording electrodes were prepared

from borosilicate glass tubes (GC150TF-10; Warner Instruments, Hamden, CT, USA) using a P-1000 puller (Sutter Instruments, Novato, CA, USA). Electrodes were filled with 3 M KCl and had a resistance of 0.5–2.0 MΩ when measured in SOS. Oocytes were continuously perfused with SOS throughout the recording session, at a rate of 5 ml/min using a gravity-fed system. Experiments were performed at 18–19 °C.

Voltage protocols and data analysis

Methods for Na^+-current recordings were performed using standard two-electrode voltage clamping, as described by Du et al. (Du et al., 2009). Na^+ currents were elicited by a 20-ms test pulse from a holding potential of −120 mV to −20 mV. The peak current ensuing from 20-ms step depolarization, in response to a test potential (V) in the range of −80 mV to +40 mV, in 5-mV increments, from a holding potential, at 10-s intervals was measured. The voltage dependence of activation was then calculated by dividing by $(V - V_{rev})$, where V_{rev} is the reversal potential as determined from the current-voltage curves. Peak conductance values were plotted against V and fitted with the Boltzmann equation to obtain the half-maximal activation voltage. The voltage dependence of Vssc inactivation was determined using a 200-ms pre-pulse in the range of −100 mV to 0 mV, in 5 mV increments, followed by a 20-ms test pulse at −20 mV. Data were plotted as normalized current vs. inactivation pre-pulse voltage, and fitted with the Boltzmann equation to obtain the half-maximal inactivation voltage. Application of permethrin and deltamethrin were conducted using the disposable perfusion system (Tatebayashi and Narahashi, 1994). Pyrethroid-induced tail currents were recorded during a 100-pulse train of 5-ms depolarizations from a holding potential (−120 mV) to −20 mV at 10-ms intervals (Du et al., 2009). The amplitude of tail currents was used to establish the

percentage of modified channels, as previously described (Burton et al., 2011; Tan and Tong, 2004; Tatebayashi and Narahashi, 1994; Vais et al., 2000). The decays of tail currents were fitted with single functions to determine the time constant (Tau values). The sensitivity of Vssc to each insecticide was defined as the concentration of insecticide at which 25% of channels were modified (EC_{25}).

Statistical analysis

The recorded data were analyzed using GraphPad Prism 5.04 software (GraphPad Software, Inc., La Jolla, CA, USA). Voltage dependences (both activation and inactivation of $V_{1/2}$) were compared statistically between wild-type and mutant channels using one-way ANOVA followed by Dunnett's multiple comparison tests. The decays of tail currents were fitted with single functions to determine time constants (Tau values). Statistical comparisons (one-way ANOVA followed by Dunnett's multiple comparison test) were made for time constants of the decays between the wild-type and the mutant channels at $P<0.05$. Tukey-Kramer HSD (Honestly significant difference) procedure was used to test for the percentage differences of modified channels among Vssc haplotypes after the treatment of insecticides.

Results

Cloning and sequencing the full-length Vssc cDNA from A. aegypti

Eight clones of full-length Vssc cDNA obtained from a pyrethroid-susceptible SMK strain were sequenced. The Vssc cDNA (six clones) of SP was also sequenced to determine if S989P and V1016G were the only substitutions present in Vssc in this strain. The SMK strain harbored two polymorphisms that both generated a substitution at amino acid 427 (R or K). K427 was not confirmed in the Vssc of strain SP. It is known that Vsscs have two mutually exclusive alternative exons (c and d) (Thackeray and Ganetzky, 1995); the expression of both exons was confirmed in both the SMK and SP strains. These two exons are 54 amino acids long and differ at two residues (V922+T952 and M922+I952 for exons c and d, respectively). In the SMK strain, the ratio of exon c and d were 0.54 and 0.46 (based on 13 clones), and we therefore concluded that these polymorphisms were not responsible for pyrethroid resistance. For electrophysiology studies, we used SMK-derived AaNavS2 (DDBJ accession number: AB909019, consisted of 2109 amino acid residues), which contains R427 and exon c, as does the wild-type Vssc. We also confirmed that S989P and V1016G are the only amino acid substitutions present in the full-length Vssc cDNA in the SP strain.

Functional analysis of AaNavS2 in Xenopus *oocytes*

The wild-type *A. aegypti* Vssc (AaNavS2) and *Drosophila* tipE, which is required for robust expression of insect Vssc, were co-expressed in *Xenopus* oocytes. No peak current was detected in oocytes that had not been injected with cRNA (data not shown). A peak current of approximately 0.5–3 μA was detected on days 2–4 in most oocytes

that had been co-injected with wild-type AaNavS2 and tipE cRNA. A representative trace is shown in Figure 1-2A. Currents were completely inhibited by 10 nM tetrodotoxin (Figure 1-2B), confirming that they were Na^+ currents. Oocytes were clamped at a holding potential of −120 mV, then depolarized to test potentials from −80 mV to +40 mV in 5-mV increments (Figure 1-2C). Na^+ currents through AaNavS2 were detected at approximately −40 mV, and peaked at −15 mV (Figure 1-2C). The half-maximal activation voltage of wild-type AaNavS2 was −31.1±0.4 mV and the slope factor was 3.9±0.3 mV (Table 1-2). To assess the voltage dependence of steady-state inactivation, oocytes were held at −120 mV and depolarized with a series of 200-ms inactivating pre-pulses, from −100 mV to 0 mV in 5-mV increments, followed by a 20-ms test pulse at −20 mV. The half-maximal inactivation voltage was −48.8±0.5 mV and the slope factor was 5.5±0.4 mV (Table 1-2, Figure 1-2C).

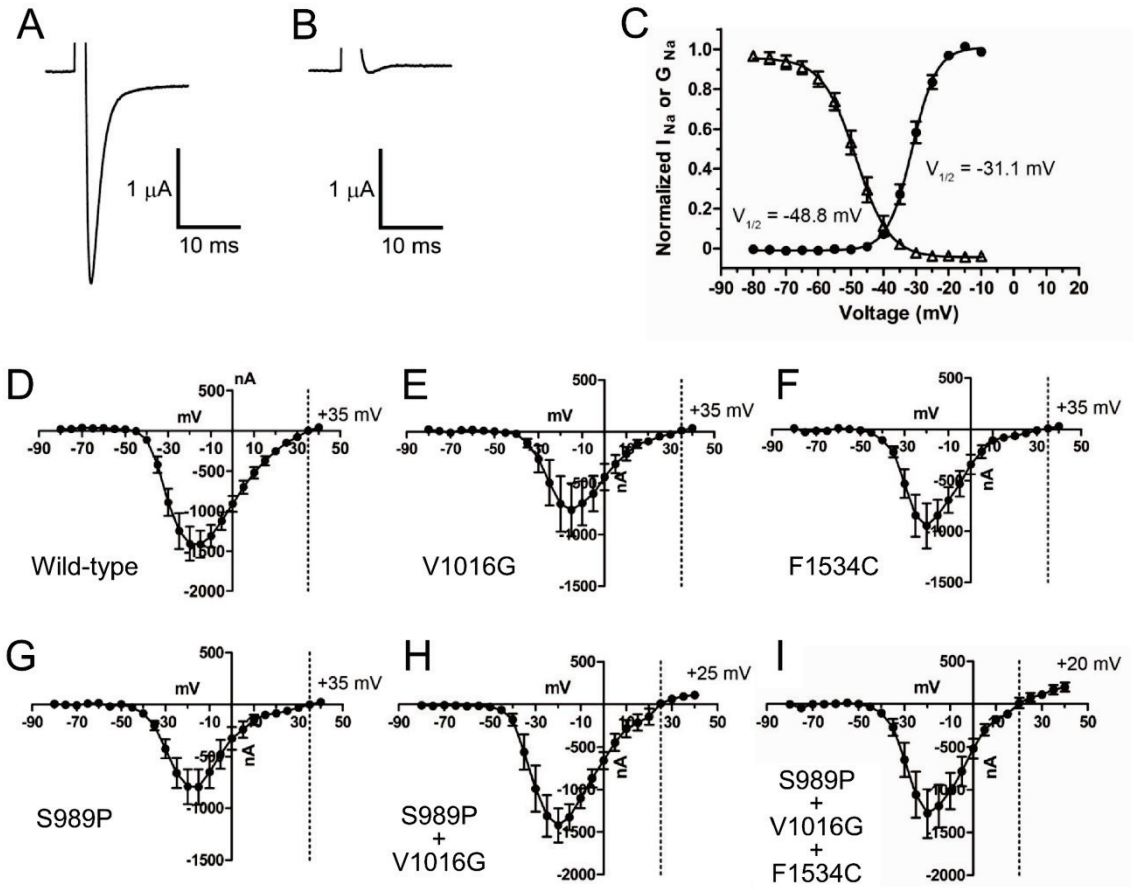

Figure 1-2. Mutations of *Aedes aegypti* Vssc investigated in this study.

(A) The cloned AaNavS2 (wild-type) channel was expressed in *Xenopus* oocytes and a Na^+ current trace was recorded. (B) The Na^+ current was blocked by the application of 10 nM tetrodotoxin, verifying that this was a Na^+ current. (C) Normalized voltage-conductance and inactivation curves of AaNavS2. The peak current was plotted against the depolarizing voltage (solid circles). The peak current amplitude was plotted as a function of the pre-pulse potential (triangles). Error bars indicate standard errors for 7–9 oocytes (D–I). Na^+ current-voltage curves for 6 Vssc types. Error bars indicate standard errors for 7–9 oocytes. Reversal potentials were: (D) wild-type (+35 mV); (E) V1016G single mutation (+35 mV); (F) F1534C single mutation (+35 mV); (G) S989P single mutation (+35 mV); (H) S989P+V1016G double mutation (+25 mV); and (I) S989P+V1016G+F1534C triple mutation (+20 mV).

Table 1-2. Voltage-dependence of activation and inactivation of *Aedes aegypti* sodium channels and sensitivity of mutant channels to pyrethroids.

	Voltage dependence						Pyrethroid susceptibility					
Vssc type (mutations)	Activation			Inactivation			Permethrin			Deltamethrin		
	n[a]	$V_{1/2}$ (mV)	*k* (mV)	n[a]	$V_{1/2}$ (mV)	*k* (mV)	n[a]	EC_{25} (μM)	Ratio	n[a]	EC_{25} (μM)	Ratio
$AaNa_vS2$ (Wild-type)	8	−31.1±0.4	3.9±0.3	7	−48.8±0.4	5.5±0.4	4	0.002	-	4	0.01	-
$AaNa_vR6$ (V1016G)	7	−27.5±0.7*	4.2±0.5	8	−47.1±0.6	4.6±0.5	5	0.2	100	8	0.02	2
$AaNa_vR7$ (F1534C)	7	−28.7±0.3*	4.0±0.2	7	−49.2±0.9	5.4±0.8	4	0.05	25	4	0.01	1
$AaNa_vR8$ (S989P)	7	−28.4±0.4*	4.3±0.3	8	−48.5±0.4	3.9±0.4	4	0.002	1	4	0.01	1
$AaNa_vR9$ (S989P+V1016G)	8	−32.0±0.4	3.5±0.4	7	−47.3±0.5	4.6±0.5	4	0.2	100	4	0.1	10
$AaNa_vR10$ (S989P+V1016G+F1534C)	9	−29.4±0.8	5.0±0.7	7	−47.8±0.7	4.9±0.6	4	2.2	1100	4	0.9	90

Data were fitted with the Boltzmann equation to determine $V_{1/2}$, the voltage of half-maximal conductance or inactivation, and *k*, the slope factor. Values represent the mean ± standard errors. Voltage dependences were compared statistically between wild-type and mutant channels using one-way ANOVA by Dunnett's multiple comparison test.

*$P<0.05$. Ratios were calculated by EC_{25} (mutant)/EC_{25} (wild-type).

[a]n, number of biological replications for each insecticide concentration tested.

Effect of Vssc mutations on gating properties of channels

The expression of all five modified Vssc was confirmed in *Xenopus* oocytes. The effects of three substitutions (S989P, V1016G, and F1534C), alone or in combination, on the voltage dependence of activation, steady-state inactivation, and reversal potential were evaluated. Na^+ currents recorded in oocytes expressing mutant channels exhibited voltage-dependent activation and inactivation, similar to those expressing the wild-type AaNavS2 (Figures 1-2D–I, Table 1-2). The reversal potentials of AaNavR9 (S989P+V1016G) and AaNavR10 (S989P+V1016G+F1534C) mutants were slightly shifted, from +35 mV in the wild-type (Figure 1-2D) to +25 mV (Figure 1-2H) and +20 mV (Figure 1-2I) in the respective mutants. Three mutant channels, AaNavR6 (V1016G), AaNavR7 (F1534C), and AaNavR8 (S989P) significantly ($P<0.05$ by one-way ANOVA followed by Dunnett's multiple comparison test) shifted the voltage-dependence of activation in the depolarizing direction (Table 1-2). None of the

Vssc mutants changed the voltage dependence of inactivation significantly (Table 1-2).

Effects of amino acid substitutions on the sensitivity of Vssc to permethrin

Pyrethroid-induced tail currents were elicited with a train of 100 depolarizing pulses (Burton et al., 2011; Tan et al., 2002; Tatebayashi and Narahashi, 1994; Vais et al., 2000). Currents were recorded 10 min after application of permethrin (Figure 1-3). In the wild-type channel AaNavS2, 100 nM permethrin induced large tail currents that recovered to baseline values within 3 s (Figure 1-3A). In all five mutant channels, the same concentration of permethrin induced only a small tail current that quickly recovered to baseline (Table 1-3, Figures 1-3B–F). The S989P mutation had no effect on permethrin sensitivity on its own (AaNavR8), or in combination with V1016G (AaNavR9) (Figure 1-4A). The V1016G and F1534C substitutions independently reduced sensitivity of Vssc to permethrin by 100- and 25-fold, respectively (Table 1-2, Figure 1-4A). The combination of three substitutions, viz., S989P+V1016G+F1534C (AaNavR10), exhibited 1100-fold more resistance, which represents an 11-fold reduction (1100/100) and a 44-fold (1100/25) reduction in Vssc sensitivity to permethrin as compared to Vssc harboring S989P+V1016G or F1534C, respectively. This suggested that these substitutions acted synergistically (Table 1-2, Figure 1-4A).

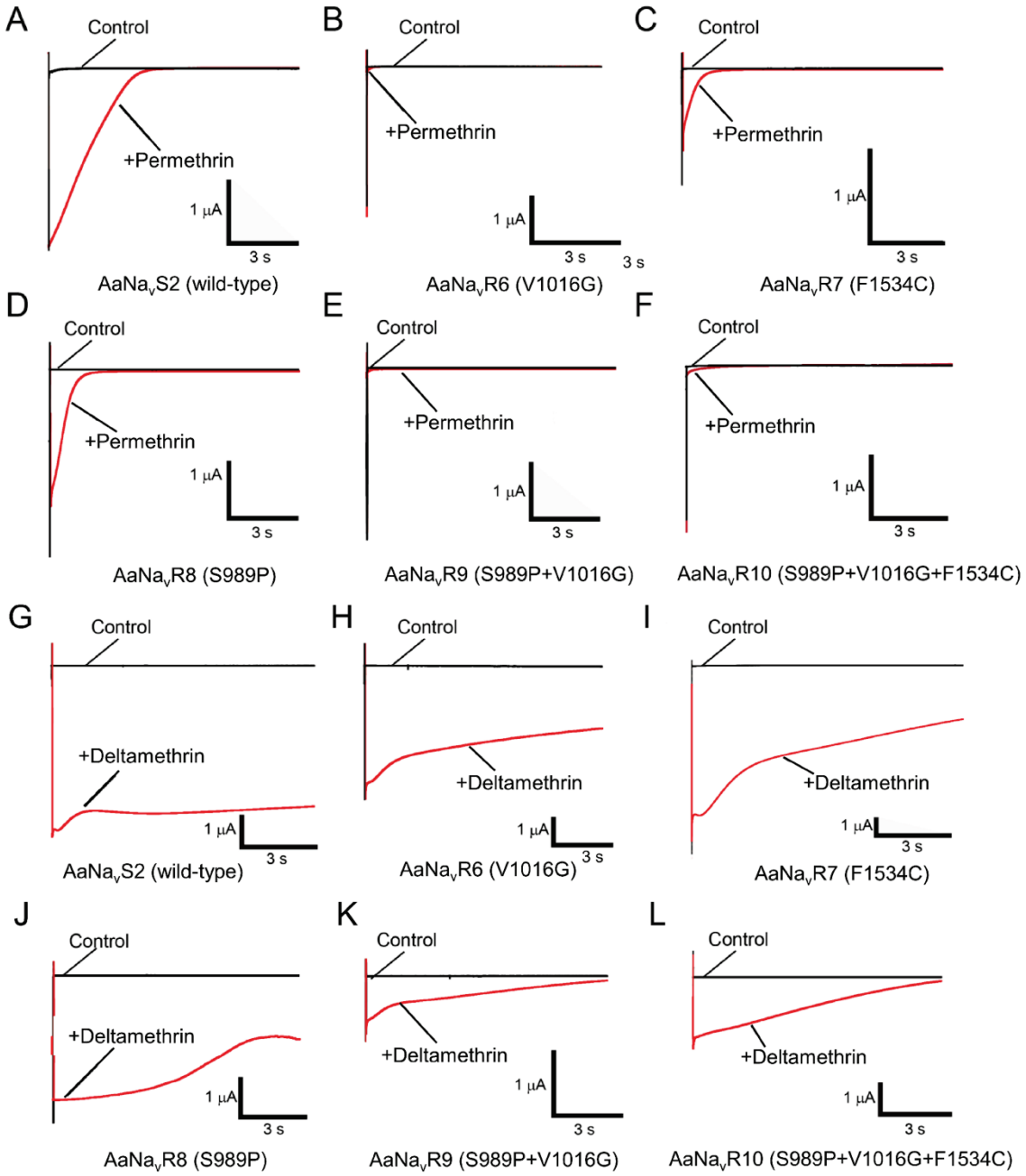

Figure 1-3. Pyrethroid-induced tail currents from oocytes injected with various types of Vssc.

(A, G) AaNavS2 (wild-type); (B, H) AaNavR6 (V1016G); (C, I) AaNavR7 (F1534C); (D, J), AaNavR8 (S989P); (E, K), AaNavR9 (S989P+V1016G); (F, L) AaNavR10 (S989P+V1016G+F1534C) in the absence (control) or presence of 100 nM permethrin (A–F) or 100 nM deltamethrin (G–L).

Table 1-3. Time constants of the decay (τ_{decay}) of pyrethroid-induced tail currents.

Vssc type	Mutations	Permethrin	Deltamethrin
		τ_{decay} (s)	τ_{decay} (s)
$AaNa_vS2$	Wild-type	2.0±0.2	9.7±1.5
$AaNa_vR6$	V1016G	0.15±0.01*	3.6±1.1*
$AaNa_vR7$	F1534C	0.33±0.10*	3.3±0.3*
$AaNa_vR8$	S989P	0.60±0.08*	4.0±0.4*
$AaNa_vR9$	S989P+V1016G	0.22±0.13*	3.8±2.0*
$AaNa_vR10$	S989P+V1016G+F1534C	0.21±0.02*	N. D.

The decays of tail currents were fitted with single functions to determine time constants (Tau values). Values represent the mean ± standard errors. Statistical comparisons (one-way ANOVA followed by Dunnett's multiple comparison test) were made for time constants of the decays between the wild-type and the mutant channels at *P<0.05. N.D., not determined because the tail current tended to keep recovering to base line.

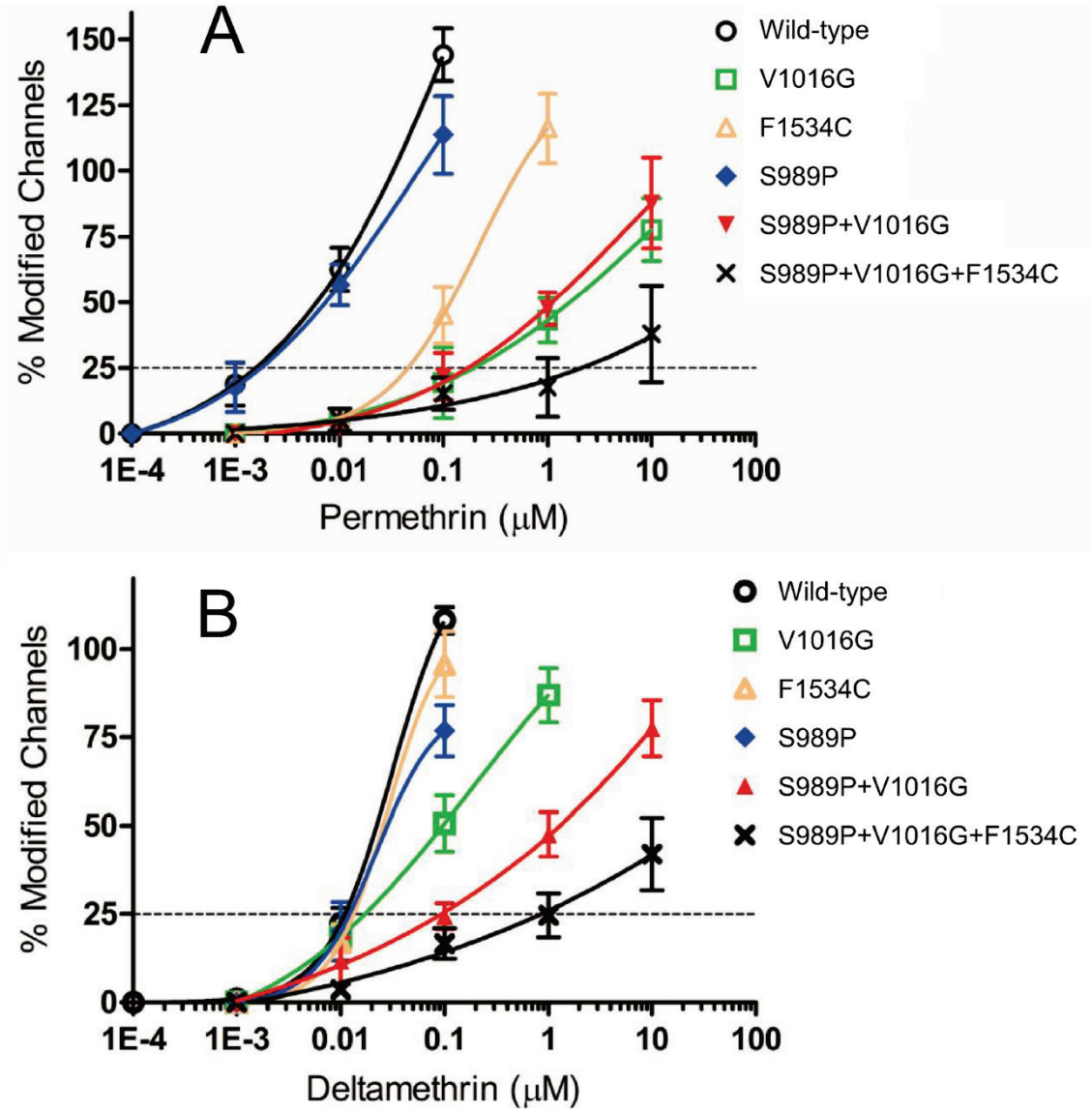

Figure 1-4. Sensitivity of *Aedes aegypti* Vsscs to permethrin and deltamethrin.

The percentages of modified channels were plotted against different concentrations of permethrin (A) and deltamethrin (B), and fitted to a four-parameter logistic equation. Error bars indicate standard errors for 4–8 oocytes. The percentages of modified channels were significantly different between AaNavR6 (V1016G) and AaNavR9 (S989P+V1016G) at deltamethrin concentration of 1.0 μM (P=0.0091 by Tukey-Kramer test) in Figure 1-4B.

Effects of amino acid substitutions on the susceptibility of Vssc to deltamethrin

Deltamethrin-induced tail currents initially increased, and then gradually recovered in the wild-type channel (Figure 1-3G). However, the current in AaNavR10 (S989P+V1016G+F1534C) had a lower amplitude and recovered to baseline more rapidly than did the wild-type (Figure 1-3L). As compared with wild-type Vssc, deltamethrin-induced tail currents of four mutant channels (AaNavR6, -R7, -R8, and -R9) decayed very quickly (Table 1-3, Figures 1-3H–K). We could not estimate the actual time constant for AaNavR10 (S989P+V1016G+F1534C) because the tail current tended to keep recovering to baseline. The deltamethrin-induced tail current of AaNavR10, however, clearly decayed faster than that of the wild-type. V1016G reduced the sensitivity of Vssc to deltamethrin by 2-fold, while F1534C alone exerted no effect on Vssc sensitivity (Table 1-2, Figure 1-4B). S989P alone (AaNavR8) had no effect on deltamethrin sensitivity, but the combination of S989P and V1016G (AaNavR9) reduced deltamethrin-sensitivity of Vssc by 10-fold (Table 1-2), which was a 5-fold reduction in deltamethrin-sensitivity over that induced by V1016G alone. The percentage of modified channels were significantly different between AaNavR6 and AaNavR9 at deltamethrin concentration of 1.0 μM (P=0.0091 by Tukey-Kramer test). Furthermore, S989P+V1016G+F1534C (AaNavR10) exhibited a 90-fold greater resistance than wild-type. This represents a 9-fold (90/10) and 90-fold (90/1) greater reduction in sensitivity than that induced by S989P+V1016G and F1534C, respectively, indicating a strong synergistic effect of the triple substitutions (Table 1-2). The percentage of modified channels were significantly different between AaNavR9 and AaNavR10 at deltamethrin concentration of 10 μM (P=0.034).

Discussion

To date, the V1016G mutation (usually accompanied by S989P) of Vssc has been confirmed only in *A*. *aegypti* distributed in Southeast Asia, including Thailand (Srisawat et al., 2010; Stenhouse et al., 2013), Vietnam (Kawada et al., 2009), Taiwan (Lin et al., 2013), Singapore (Kasai et al., 2014), and the Philippines (Yukiko Higa, personal communications). F1534C mutation of Vssc has also been confirmed from all of above regions except for Taiwan (Kasai et al., 2014; Kawada et al., 2009; Stenhouse et al., 2013). These two haplotypes were confirmed as heterozygous form as well (Kawada et al., 2009; Stenhouse et al., 2013). A previous study revealed that Vssc harboring V1016G exhibited a greater reduction in permethrin susceptibility than did Vssc harboring F1534C, which was in agreement with our findings. Surprisingly, the combination of S989P, V1016G, and F1534C altered the sensitivity of the S989P+V1016G mutant to permethrin and deltamethrin by 11-fold (1100/100) and 9-fold (90/10), respectively. Theoretically, this haplotype can be generated as the result of a single crossing-over event involving two resistant haplotypes (i.e., S989P+V1016G and F1534C), which are widely and sympatrically distributed throughout Southeast Asia. Pyrethroid insecticides may lose their efficacy in the control of *A*. *aegypti* if such a new type of Vssc emerges in the field population of this mosquito species. Therefore, we strongly emphasize the importance of surveying of the triple mutations in Vssc in the field population of this key mosquito vector. Early detection of this unique haplotype may assist in vector control strategies by providing early warning of insecticide insensitivity.

The likelihood of occurrence of such a Vssc with triple mutations may depend on

its fitness cost. In this study, we observed that the reversal potential of AaNavR10 (S989P+V1016G+F1534C) shifted slightly, although there were no statistically significant differences in the voltage dependence of activation or in the voltage dependence of steady-state inactivation between AaNavR10 and the wild-type AaNavS2. In North and South America, where no V1016G mutation has been confirmed in the Vssc of *A*. *aegypti* to date, V1016I is widely distributed (Aponte et al., 2013; Harris et al., 2010; Marcombe et al., 2012). The double mutations V1016I+F1534C have already been detected in some of these regions (Marcombe et al., 2012) and this fact implies the possibility that S989P+V1016G+F1534C triple mutations can also emerge. According to a neurophysiological study, V1016I does not alter the susceptibility of Vssc to pyrethroid (Du et al., 2013) while in another study quantitative trait loci (QTL) that affects permethrin resistance was mapped close to the Vssc gene with this mutation (Saavedra-Rodriguez et al., 2008). Anyway, the synergistic effect of V1016I on the pyrethroid-susceptibility of Vssc with F1534C is intriguing. In our study, we focused on characterization of triple mutations that can be generated by a single crossing-over event between two major resistant Vssc haplotypes, but the pyrethroid-susceptibility of Vssc harboring V1016G+F1534C or S989P+F1534C double mutations may also elucidate the synergistic effects of these mutations.

These results exhibited that S989P has a synergistic effect on the sensitivity of V1016G-harboring Vssc to deltamethrin, but not to permethrin (Figure 1-4). This result contradicts with an earlier observation that S989P does not synergize with V1016G (Du et al., 2013). The discrepancy between these two reports may be due to the use of different evaluation methods. The author measured the Na^+ currents of each Vssc at five concentrations of deltamethrin, with at least 4 independent replications, and used EC_{25}

values as a measure of sensitivity. The percentages of modified channels were significantly different between AaNavR6 (V1016G) and AaNavR9 (S989P+V1016G) at deltamethrin concentration of 1.0 μM (P=0.0091 by Tukey-Kramer test; Figure 1-4B). In contrast, previous studies used the ratios of modified channels at only one concentration of the chemical; it is possible that this may have led to an underestimation of the effect of S989P. These findings highlight the need for genotyping S989P mutation as well as V1016G and F1534C for better understanding the pyrethroid susceptibility of the field population of *A*. *aegypti* collected especially in Southeast Asia.

Chapter 2

Association between the R81T mutation in the nicotinic acetylcholine receptor β1 subunit of *Aphis gossypii* and the differential resistance to acetamiprid and imidacloprid

Introduction

The cotton aphid, *Aphis gossypii*, is an important sucking pest that causes severe crop losses, both in the field and in greenhouses. Neonicotinoid insecticides (Fig. 2-1), which show excellent control of *A. gossypii*, target insect nicotinic acetylcholine (ACh) receptors (nAChRs) (Matsuda et al., 2001; Matsuda et al., 2005; Thany et al., 2007; Tomizawa and Casida, 2005). nAChRs are members of the cys-loop superfamily of ligand-gated ion channels that conduct fast-moving excitatory cholinergic neurotransmission (Karlin, 2002). Targeting nAChRs has raised concerns about mammalian toxicity, yet neonicotinoids show highly selective toxicity to insects over vertebrates (Matsuda et al., 2001; Matsuda et al., 2005; Tomizawa and Casida, 2005). Insecticide resistance is a major hindrance to the effective control of insect pests worldwide. Neonicotinoids have been used for more than 20 years to protect economically important crops (Elbert et al., 2008; Jeschke and Nauen, 2008; Nauen et al., 2008). However, although resistance to neonicotinoids has developed relatively slowly, it is now recognized as an emerging issue (Nauen and Denholm, 2005). In most cases, P450-mediated detoxification plays a primary role in insecticide resistance in a variety of insects, including the whitefly (*Bemisia tabaci*) and the Colorado potato

beetle (*Leptinotarsa decemlineata*) (Rauch and Nauen, 2003; Zhao et al., 2000). On the other hand, laboratory selection of *Nilaparvata lugens* with imidacloprid resulted in an α-subunit Y151S mutation that was responsible for the acquisition of neonicotinoid resistance (Liu et al., 2005; Liu et al., 2006). However, this mutation has not been identified in any pest in the field. Instead, a mutation in the nAChR β1 subunit was found to be a major factor in imidacloprid resistance in a field population of *Myzus persicae* (Bass et al., 2011).

Previously reported the emergence of neonicotinoid resistance in the aphid and recently isolated an *A. gossypii* (Kushima) clone in Miyazaki Prefecture, Japan, that exhibited relatively high neonicotinoid resistance (Matsuura and Nakamura, 2014). Interestingly, the level of the Kushima clone's resistance to neonicotinoids with nitro substituents (e.g., imidacloprid) was higher than for those with cyano substituents (e.g., acetamiprid; see Figure 1-1 for the structures). However, the mechanisms of neonicotinoid resistance remain unknown.

In this study, we attempted to identify the mechanisms of neonicotinoid resistance using an insecticidal assay with and without piperonyl butoxide (PBO) pretreatment, along with sequencing of the nAChR gene and voltage-clamp electrophysiology. These results suggest that a mutation in the β1 subunit is the main mechanism of resistance and that differences in resistance levels are probably associated with differential interactions between nitro- and cyano-type neonicotinoids and nAChRs.

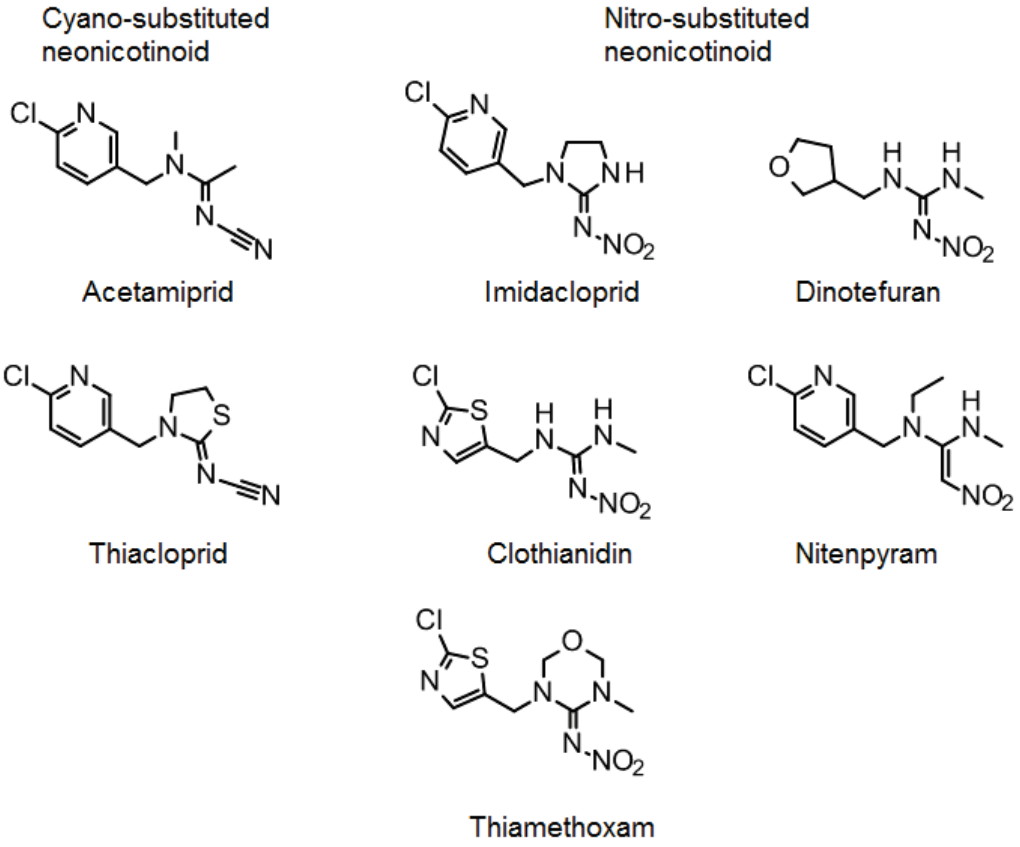

Figure 2-1. Chemical structures of neonicotinoid insecticides.

Materials and Methods

Insects

In this study, we used a field-isolated clone of *A*. *gossypii* (Kushima) and a susceptible clone that has been maintained since 1993 at the Odawara Research Center, Nippon soda Co., Ltd. (Odawara, Kanagawa, Japan). The Kushima clone was collected from a field in Miyazaki Prefecture, Japan, in 2012. The Kushima clone was reared for four months and used for insecticide bioassays without insecticide selection. These aphid clones were reared on cucumber seedlings at 25 ℃ and a relative humidity (RH) of 60% under a 16:8-hr light:dark photoperiod.

Chemicals

Acetamiprid and other neonicotinoids were synthesized at the Odawara Research Center. ACh chloride was purchased from Sigma-Aldrich (Tokyo, Japan). The purity of imidacloprid and acetamiprid was >99.9%.

Insecticide bioassays

All compounds were dissolved in a 5% N,N,-dimethylformamide aqueous solution and then diluted with distilled water and 2×10^{-4}% (v/v) of the surfactant RABIDEN 3S (which is a trade name: 1.4% sodium dioctylsulfosuccinate, 8% polyoxyethylene alkyl ether, and 3% polyoxyethylene fatty acid ester). Wingless female *A*. *gossypii* (n = 5-10) were incubated on cucumber seedlings at the first- to second-leaf stage of development. One day later, they were removed, and the test solutions were sprayed on the offspring, while the leaves were maintained under the same conditions

(25 °C, 60% RH, and a 16:8-hr light:dark photoperiod). Seventy-two hr after application, the effects of the compounds were assessed using median lethal dose (LC_{50}) values calculated by probit analysis. Each compound was tested in duplicate.

To assess the effects of the synergist PBO, aphids were sprayed with PBO solution (250 ppm, 5% N,N,-dimethylformamide aqueous solution) 5 hr prior to application of the insecticide solution. Each compound was tested in duplicate.

Sequence analysis of the* A. gossypii *nAChR α1, α2, and β1 subunits

Total RNA was isolated from adult aphids using TRIzol Reagent (Invitrogen Corporation, Carlsbad, CA, USA) in accordance with the manufacturer's instructions. First strand cDNA was synthesized from total RNA using the Transcriptor First Strand cDNA Synthesis Kit (Roche Diagnostics, K.K., Tokyo, Japan) with oligo-dT primers. PCR amplification was performed using KOD plus Neo polymerase (Toyobo Co., Ltd., Osaka, Japan) and the following gene-specific primers: Ago nAChR β1-F, Ago nAChR β1-R, Ago nAChR α1-F, Ago nAChR α1-R, Ago nAChR a2-F, and Ago nAChR a2-R (Table 2-1). PCR amplification was performed under the following cycling conditions: 2 min at 94 °C, followed by 35 cycles of 10 sec at 98 °C, 30 sec at 56 °C, and 1 min at 68 °C. Amplicons of the expected size were purified using the QIAquick PCR Purification Kit (Qiagen GmbH, Hilden, Germany) and directly sequenced in both directions using the BigDye Terminator V3.1 Cycle Sequencing Kit (Applied Biosystems, Foster City, CA, USA). The direct sequences were confirmed using the following primers: Ago nAChR β1S-F and Ago nAChR β1S-R for subunit β1, Ago nAChR α1S-F and Ago nAChR α1S-R for subunit α1, and Ago nAChR α2S-F and Ago nAChR α2S-R for subunit α2.

Table 2-1. Primer sequences used in this study.

Name	Sequence (5' to 3')	Restriction enzymes	Purpose
Ago nAChR β1-F	CAACAAACTAATCAGACCTGTCC		PCR amplification of β1 subunit
Ago nAChR β1-R	GGCAAGTAGAACACTAGCACGC		
Ago nAChR α1-F	CTACAATCGGTTGATCAGGC		PCR amplification of α1 subunit
Ago nAChR α1-R	CTAACACCGTCATGAATGTC		
Ago nAChR α2-F	CTAGTAAGGCCTGTGCTCAAC		PCR amplification of α2 subunit
Ago nAChR α2-R	GGAAGGTAAAATACAAGTATCG		
Ago nAChR β1S-F	CAGACCTGTCCAGAACATGACC		Direct sequencing of nAChR subunit
Ago nAChR β1S-R	ATGAGGACCGTGGGCAGTATC		
Ago nAChR α1S-F	CAGTCCAAAACCATTCAGAG		
Ago nAChR α1S-R	GTAGAACAAAGTCTTGCGTCG		
Ago nAChR α2S-F	CAGTACGGATTAAGCTCAAAC		
Ago nAChR α2S-R	GGTATGATCAGATTTACTGTG		
Dme nAChR α2-F	GGTACCATGGCTCCTGGCTGCTGCACCAC	*Kpn*I	PCR amplification of Dme α2 subunit
Dme nAChR α2-R	GGGCCCTTAATTCTTCTTCTCGGTTAG	*Apa*I	
Gga nAChR β2-F	GGGGTACCGCCACCATGGCGCTGCTCCGCGTCCTC		PCR amplification of Gga β2 subunit
Gga nAChR β2-R	GGGAATTCCCTATTTGGAGGTGGGGGTGCCCTGGC		
pcDNA3 cRNA-F	CTCTCTGGCTAACTAGAGAACC		cRNA synthesis template
pcDNA3 cRNA-R	CTAGAAGGCACAGTCGAGGCTG		

Isolation of cDNA clones encoding nAChRs

cDNA encoding *Drosophila melanogaster* nAChR α2 subunit (Dα2) was amplified from first strand cDNA synthesized from larval total RNA using the Transcriptor First Strand cDNA Synthesis Kit with oligo-dT primers. PCR amplification was performed using the following primers: Dme nAChR α2-F and Dme nAChR α2-R (Table 2-1). PCR amplification was performed under the following cycling conditions with KOD plus Neo: 2 min at 94 °C, followed by 30 cycles of 10 sec at 98 °C, 30 sec at 56 °C, and 2 min at 68 °C. Amplicons were purified using the QIAquick Gel Extraction Kit (Qiagen GmbH) and cloned into pTA2 vectors (Toyobo Co., Ltd.). Several clones containing the Dα2 gene were sequenced. One clone identical to a published sequence (GenBank accession number X53583) was excised from the pTA2 vector using the restriction endonucleases *Kpn*I and *Apa*I and then ligated into the pcDNA3.1(+) vector (Life Technologies, Japan, Tokyo, Japan).

The chicken nAChR β2 subunit was amplified from first strand cDNA

synthesized from chicken total RNA obtained from BioChain Institute, Inc. (Newark, CA, USA). PCR was performed using KOD-plus-Neo polymerase with the gene-specific primers Gga nAChR β2-F and Gga nAChR β2-R. PCR amplification was performed under the following cycling conditions: 2 min at 94 °C, followed by 30 cycles of 10 sec at 98 °C, 30 sec at 56 °C, and 1.5 min at 68 °C. Amplicons were cloned into pTA2 vectors (Toyobo Co., Ltd.) and sequenced, while the β2 gene was cloned into the pcDNA3.1(+) vector.

Preparation of Dα2 and chicken β2 cRNA

Templates for in vitro transcription were obtained by PCR amplification of each plasmid using KOD-plus-Neo polymerase and the gene-specific primers pcDNA3 cRNA-F and pcDNA3 cRNA-R (Table 2-1). The capped RNA transcripts were synthesized using the T7 polymerase included with the mMessage mMachine T7 Ultra Kit (Life Technologies). The quality and quantity of cRNAs were verified by agarose gel electrophoresis and absorption spectroscopy. The cRNA was stored at −80 °C for further use.

nAChR expression in* Xenopus *oocytes by cRNA injection and electrophysiology

All experiments were performed at 18–19 °C. Female *Xenopus laevis* were purchased from Hamamatsu Seibutsukyozai (Shizuoka, Japan) and maintained in tap water. Oocytes were surgically obtained using 0.03% benzocaine (Sigma-Aldrich) and then enzymatically defolliculated by incubation for 1–1.5 hr in Ca^{2+}-free Standard Oocyte Saline (SOS) solution (100 mM NaCl, 2.0 mM KCl, 1.0 mM $MgCl_2$, 5.0 mM HEPES, pH 7.6) (Ihara, 2003) containing 1 mg/mL collagenase (Wako Pure Chemical

Industries, Ltd., Osaka, Japan). Healthy stage V–VI oocytes were injected with equivalent amounts (10 ng each) of cRNA encoding Dα2 and chicken β2 using the Nanoject II Auto-Nanoliter Injector (Drummond Scientific Company, Broomall, PA, USA) and then incubated in SOS solution supplemented with 50 μg/mL gentamycin, 100 U/mL penicillin, 100 μg/mL streptomycin, 2.5 mM sodium pyruvate, and 4% horse serum for 1–4 days. The medium was replaced daily and unhealthy oocytes were discarded.

Two-electrode voltage clamp electrophysiological analysis was performed as described by Ihara et al. (Ihara, 2003) Currents were recorded using the TEV-200A amplifier (Dagan Corporation, Minneapolis, MN, USA) and digitized at 1 kHz using the PowerLab 8/30 data acquisition and analysis system (ADInstruments, Nagoya, Japan). Signals were filtered at 50 Hz using a 4-pole Bessel filter. Recording electrodes were prepared from borosilicate glass tubes (CG150TF-10; Warner Instruments, Hamden, CT, USA) using a P-1000 Puller (Sutter Instruments, Novato, CA, USA). Electrodes were filled with 3 M KCl and had resistance of 0.5–2.0 MΩ when measured in SOS solution. Oocytes were continuously perfused with SOS solution throughout the recording session at a rate of 5 mL/min using a gravity-fed system (Ihara, 2003) and voltage-clamped at −100 mV, while those with excessive leak currents (>-1000 nA) were not used for further analysis.

Test compounds were first dissolved in dimethyl sulfoxide (DMSO) and later diluted to the appropriate test concentration in SOS solution (100 mM NaCl, 2.0 mM KCl, 1.0 mM $MgCl_2$, 1.8 mM $CaCl_2$, 5.0 mM HEPES, pH 7.6) containing 0.5 μM atropine. The concentration of DMSO was maintained at < 0.1% (v/v) to avoid the effects of the channel or cell. A solution of ACh and SOS was prepared by adding ACh

chloride directly to the atropine-SOS solution immediately before use.

The LabChart 7 (ADInstruments, Nagoya, Japan) and GraphPad Prism 5 (GraphPad Software, Inc., La Jolla, CA, USA) software packages were used for data analysis and the preparation of graphs. Normalized concentration-response data were analyzed by nonlinear regression using GraphPad Prism to obtain I_{max} (the maximum normalized response), EC_{50} (the concentration inducing the half-maximal normalized response), and pEC_{50} ($-\log EC_{50}$). The peak amplitude of the current recorded in response to each challenge was normalized to the maximum amplitude of the response to ACh. Data from the Dα2β2, T77R, and T77R + E79V mutants were normalized to the response to 1 mM ACh.

Results

Neonicotinoid insecticide bioassays

The *A. gossypii* (Kushima) clone, which was discovered in Miyazaki Prefecture, Japan, exhibited resistance to neonicotinoid insecticides as compared with a susceptible clone (Table 2-2), which was associated with resistance factors (RFs) 23.8–394. Additionally, the Kushima clone had a high level of resistance (RFs 216–394) to nitro-substituted neonicotinoids (Figure 2-1), such as imidacloprid. In contrast, the Kushima clone exhibited low to moderate levels of resistance (RFs 23.8 and 65.4) to cyano-substituted neonicotinoids (e.g., acetamiprid).

When PBO was used as a pretreatment synergist with the Kushima clone, the LC_{50} value decreased (Table 2-2). The LC_{50} values of acetamiprid and imidacloprid to the Kushima clone without PBO pretreatment were 6.54 and 75.7 ppm, but 1.91 and 7.01 ppm with PBO pretreatment, respectively. The synergistic factor (SF) of acetamiprid was lower than that for imidacloprid (3.4 vs. 11, respectively). These results indicate that the Kushima clone acquired a resistance mechanism other than an enhanced oxidative metabolism.

Table 2-2. Insecticidal activity of neonicotinoids to susceptible aphids and Kushima clone with and without pretreatment with piperonyl butoxide (PBO)

Compound	Susceptoble strain		*Kushima* strain		RF[b]
	LC_{50} (ppm)	95% confidense limit of LC_{50}	LC_{50} (ppm)	95% confidense limit of LC_{50}	
Acetamiprid	0.10	0.080-0.12	6.54	4.62-9.73	65.4
Thiacloprid	0.30	0.20-0.61	7.15	4.40-11.8	23.8
Imidacloprid	0.35	0.20-0.85	75.7	44.7-193	216
Clothianidin	0.10	0.061-0.18	39.4	28.0-58.5	394
Thiamethoxam	0.19	0.12-0.31	56.0	40.6-73.7	295
Dinotefuran	0.66	0.40-1.04	167	114-285	253
Nitenpyram	0.30	0.19-0.54	71.0	27.5-103	237
Acetamiprid+PBO	0.028	0.016-0.048	1.91	1.03-3.08	3.4
Imidacloprid+PBO	0.050	0.028-0.079	7.01	3.46-12.0	11

Experiments were performed in duplicate.

[a] Resistance factor (LC_{50} Kushima clone/LC_{50} susceptible clone).

[b] Synergistic factor (LC_{50} Kushima clone/LC_{50} Kushima clone with PBO).

Sequence analysis of A. gossypii *nAChR subunit genes*

The N-terminal regions of the *A. gossypii* (Kushima clone) nAChR β1, α1, and α2 subunits, which encompass the conserved domains (loop A-F) that comprise the ACh and neonicotinoid binding sites, were PCR-amplified and then sequenced. Although a limited number of silent single-nucleotide polymorphisms were detected, no amino acid changes were observed in the α1 and α2 subunits. In contrast, a single point mutation, Arg81 (AGA) to Thr (ACA), was detected in the β1 subunit (Figure 2-2). Additionally, the mutation was detected heterozygously (data not shown).

Species	Amino acid number of *Gallus gallus* β2 subunit 73	74	75	76	77	78	79	80	81	82	83
Homo sapiens β2	N	V	W	L	**T**	Q	E	W	E	D	Y
Gallus gallus β2	N	V	W	L	**T**	Q	E	W	E	D	Y
Rattus norvegicus β2	N	V	W	L	**T**	Q	E	W	E	D	Y
	Amino acid number of *Aphis gossypii* β1 subunit										
	77	78	79	80	81	82	83	84	85	86	87
Drosophila melanogaster β1	C	V	W	L	**R**	L	V	W	Y	D	Y
Bemisia tabaci β1	N	V	W	L	**R**	L	V	W	N	D	Y
Myzus persicae β1	N	V	W	L	**R**	L	V	W	R	D	Y
Aphis gossypii β1	N	V	W	L	**R**	L	V	W	R	D	Y
Aphis gossypii Kushima β1	N	V	W	L	**T**	L	V	W	R	D	Y

Figure 2-2. Alignment of amino acid sequences in loop D of the agonist binding region of vertebrate and insect nicotinic ACh receptor subunits (nAChRs). *Homo sapiens* (human), *Gallus gallus* (chicken), *Rattus norvegicus* (rat), *Drosophila melanogaster* (fruit fly), *Bemisia tabaci* (sweet potato whitefly), *Myzus persicae* (peach-potato aphid), *Aphis gossypii* (cotton aphid).

Agonist activity of ACh

A concentration-response curve of ACh to *Drosophila melanogaster* Dα2-chicken β2 nAChRs was used as a control in this study. We used the Dα2-vertebrate β2 hybrid receptor for the following reasons: Insect nAChR functional expression is difficult, but the Dα2-chicken β2 hybrid receptor has been well established for assaying neonicotinoids. The I_{max} and pEC_{50} values of ACh for Dα2β2 nAChR were 1.08 ± 0.03 and 4.60 ± 0.04, respectively. The ACh values of the Dα2β2 nAChR were similar to those in previous reports (Ihara, 2003; Shimomura et al., 2005; Shimomura et al., 2006) (Figure 2-3, Table 2-3).

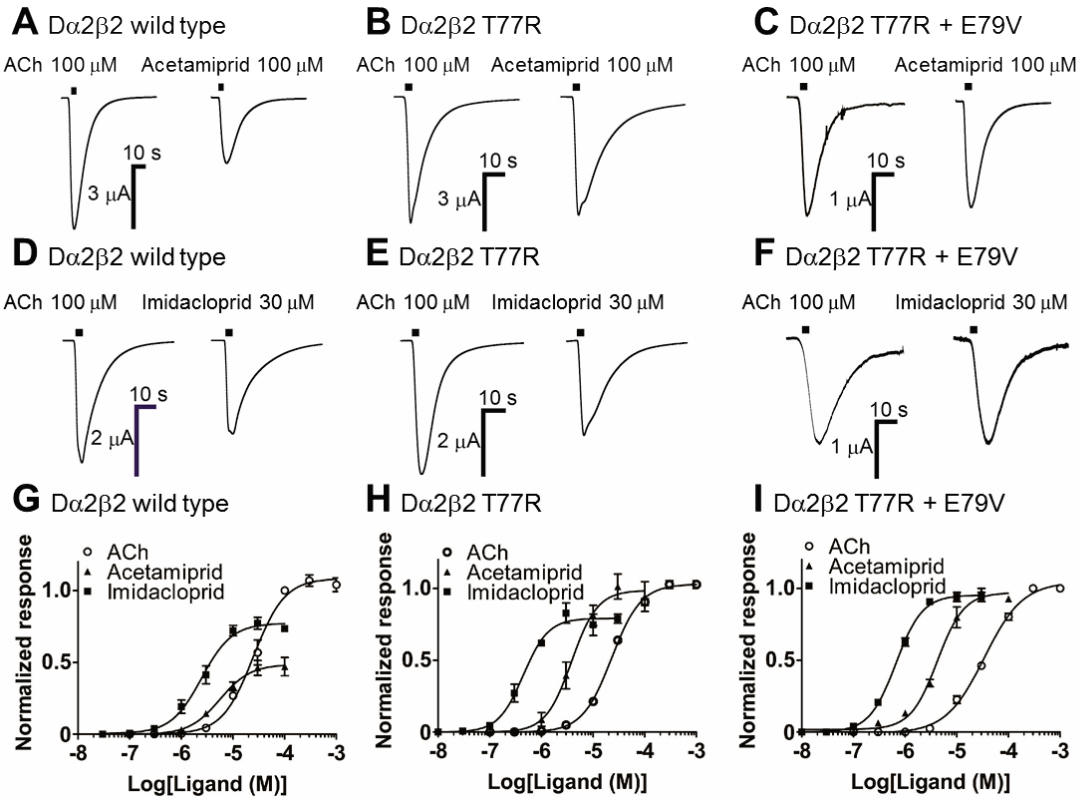

Figure 2-3. Response to acetamiprid of Dα2Gβ2 nicotinic ACh receptors (nAChRs). (A, B, C) Responses of oocytes expressing WT Dα2β2 nAChRs (A), the T77R single mutation (B), and the T77R + E79V double mutation (C) to 100 μM ACh and 100 μM acetamiprid. (D, E, F) Responses of oocytes expressing the WT (D), the T77R single mutation (E), and the T77R + E79V double mutation Dα2β2 nAChRs (F) to 100 μM ACh and 30 μM imidacloprid. Concentration-response curves of ACh, acetamiprid, and imidacloprid of the WT (G), the T77R single mutation (H), and the T77R + E79V double mutation (I) Dα2Gβ2 nAChRs. Each point represents the mean ± S.E.M. of four experiments (n = 4). The peak amplitude of the current recorded in response to each challenge was normalized to the maximum amplitude of the response to ACh. Data from the Dα2β2, T77R, and T77R + E79V mutants were normalized to the response to 1 mM ACh.

Table 2-3. pEC_{50} and I_{max} values of ACh, acetamiprid and imidacloprid for wild-type, T77R, T77R+E79V Dα2β2 nAChRs.

Compounds	Dα2β2 wild-type		Dα2β2 T77R		Dα2β2 T77R+E79V	
	pEC_{50}	I_{max}	pEC_{50}	I_{max}	pEC_{50}	I_{max}
ACh	4.60±0.04	1.08±0.03	4.64±0.07	1.03±0.01	4.47±0.03	1.04±0.02
Acetamiprid	5.26±0.09	0.49±0.03	5.42±0.06	0.99±0.04*	5.38±0.04	0.97±0.03*
Imidacloprid	5.61±0.06	0.77±0.03	6.35±0.06*	0.79±0.03	6.18±0.02*	0.96±0.02*

Values shown are the results of a fit of the concentration-response data (mean ± S.E.M, $n = 4$) illustrated in Figure 2-3. Statistical test (one-way ANOVA, Dunnett's multiple-comparison test) is for significant differences from the wild-type data. *$p < 0.05$. The peak amplitude of the current recorded in the response to each challenge was normalized to the maximum amplitude of the response to ACh. Data from the Dα2β2, T77R, and T77R + E79V mutants were normalized to the response to 1 mM ACh.

Effect of mutation in the nAChR β subunit on neonicotinoid sensitivity

To examine the effects of the R81T mutation in loop D of the β1 subunit on neonicotinoid agonist activity, we constructed an equivalent single mutant (T77R) of the chicken β2 subunit (Figure 2-2). We also evaluated the T77R + E79V double mutant because the cotton aphid nAChR β1 subunit has Val (Val83) at the equivalent amino acid residue of the chicken β 2 subunit (E79). The E79 residue of the chicken β 2 subunit may suppress interactions between the nitro group of neonicotinoids and Arg 77 through the negative electrostatic forces of Glu79 (Shimomura et al., 2006). The I_{max} and pEC_{50} values of ACh for Dα2β2 nAChR T77R were 1.03 ± 0.01 and 4.64 ± 0.07, respectively. The I_{max} and pEC_{50} values of ACh for Dα2β2 nAChR with the double mutation T77R + E79V were 1.04 ± 0.02 and 4.47 ± 0.03, respectively. The T77R and T77R + E79V mutations did not significantly affect the pEC_{50} and Imax values for the natural agonist ACh (Table 2-3, Figure 2-3), as compared with the wild type (WT) Dα2β2 nAChR, in accordance with the findings of previous report (Shimomura et al.,

2006). The pEC_{50} values of acetamiprid and imidacloprid for WT Dα2β2 nAChR were 5.26 ± 0.09 and 5.61 ± 0.06, respectively. On the other hand, the pEC_{50} values of acetamiprid and imidacloprid for the Dα2β2 nAChR single mutant (T77R) were 5.42 ± 0.06 and 6.35 ± 0.06, and 5.38 ± 0.04 and 6.18 ± 0.02 for the Dα2β2 nAChR double mutant (T77R + E79V), respectively. The pEC_{50} value of imidacloprid was significantly shifted relative to that of the WT, but that for acetamiprid exhibited no significant change. The I_{max} values of acetamiprid and imidacloprid for the WT, T77R, and T77R + E79V Dα2β2 nAChRs were, respectively, 0.49 ± 0.03 and 0.77 ± 0.03, 0.99 ± 0.04 and 0.79 ± 0.03, and 0.97 ± 0.03 and 0.96 ± 0.02. Unexpectedly, and importantly, neither the T77R nor the T77R + E79V mutations induced significant changes in the pEC_{50} values of acetamiprid, whereas significant changes were observed in the Imax values (Figure 2-3, Table 2-3). On the other hand, the T77R + E79V double mutant induced significant changes in both the pEC_{50} and the I_{max} values of imidacloprid. In addition, the T77R and T77R + E79V mutations did not significantly affect the maximum amplitudes of the ACh-induced current as compared with the WT (data not shown).

Discussion

In this study, we characterized a field isolate of *A. gossypii* (Kushima clone) that exhibited levels of neonicotinoid resistance (23.8–394-fold) high enough to impair field performance. Sequencing of the nAChR gene of the Kushima clone showed that it had at least one point mutation (R81T) in the loop D region of the nAChR β1 subunit. The ACh binding site contains loop D (Grutter and Changeux, 2001) and many experimental studies have indicated that the amino acid residue at position 81 within this loop is a key determinant of neonicotinoid binding to nAChRs (Ihara et al., 2008; Shimomura et al., 2006; Talley et al., 2008). In addition, an R81T mutation in *Myzus persicae* was previously reported to be responsible for reduced sensitivity to neonicotinoids and affinity of nAChR to imidacloprid (Bass et al., 2011).

P450-mediated detoxification has been implicated in resistance mechanisms through the use of PBO. The LC_{50} values of acetamiprid and imidacloprid to the Kushima strain pretreated with PBO were 1.91 and 7.01 ppm, respectively, which were reduced by 3.4–11-fold. PBO pretreatment also reduced the LC_{50} values of the susceptible clone to acetamiprid and imidacloprid (0.028 and 0.050 ppm, respectively). The synergistic factors of acetamiprid and imidacloprid were 3.6 and 6.0, respectively. PBO reduced the LC_{50} values of acetamiprid and imidacloprid to the Kushima clone as well as to the susceptible clone. These findings suggest that enhanced oxidative metabolism is not the main mechanism of neonicotinoid resistance (Puinean et al., 2010).

The Kushima clone exhibited high levels of neonicotinoid resistance and different RFs between the nitro- and cyano-substituted neonicotinoids. Specifically, the cyano-substituted neonicotinoid (Figure 2-1) had smaller RFs than did the

nitro-substituted ones (Table 2-2). We assessed the effect of the R81T mutation (WT Dα2β2, T77R single mutant, and T77R + E79V double mutant nAChRs) on the activity of a neonicotinoid agonist using electrophysiological methods. The Thr 77 residue of the chicken β2 subunit corresponds to the Arg 81 residue of the cotton aphid β1 subunit (Figure 2-2). Interestingly, the T77R and T77R + E79V mutations did not significantly affect the pEC_{50} value of the natural agonist ACh (Table2-3, Figure 2-3), as previously reported (Shimomura et al., 2006). The R81T mutation, which had no effect on the pEC_{50} values of ACh, may enable both a high level of resistance to neonicotinoids and a low fitness cost.

The pEC_{50} value of imidacloprid to the Dα2β2 nAChR T77R single mutant significantly shifted compared with that of the WT Dα2β2 nAChR. Furthermore, the T77R + E79V double mutant induced significant changes in the pEC_{50} and I_{max} values of imidacloprid (Figure 2-3,Table 2-3). The pEC_{50} value of imidacloprid for the Dα2β2 nAChR T77R mutant was 443 nM, which is close to the value determined for native nAChRs on the native neurons of the cockroach (Periplaneta americana) (Ihara et al., 2006) On the other hand, the T77R and T77R + E79V mutants did not significantly change the pEC_{50} value of acetamiprid, whereas a significant change was observed in the I_{max} value. Although the effect of the T77R + E79V double mutation on imidacloprid agonist activity has been previously reported (Shimomura et al., 2006; Toshima et al., 2009) the present study is the first to show its effect on acetamiprid activity. Although it remains unclear whether insecticidal activity is dependent on either the pEC_{50} or I_{max} value, differences in the RFs between nitro- and cyano-substituted neonicotinoids were likely due to the effect of the R81T mutation on agonist affinity. The crystal structures of imidacloprid and thiacloprid complexed with AChBP (Ihara et

al., 2014b; Talley et al., 2008) showed that the nitro- and cyano-substituted neonicotinoids had almost identical interactions. Homology modeling of *Myzus persicae* nAChR with imidacloprid showed its similarity to the crystal structure of AChBP with imidacloprid (Matsuda et al., 2009). However, the cyano-substituted neonicotinoid (thiacloprid) had an additional water bridge with the cyano group, which presumably enhanced interactions with loop C (Talley et al., 2008). Recent studies have indicated that the binding characteristics of thiacloprid are distinct from those of nitro-substituted neonicotinoids (Ihara et al., 2014a), and the binding characteristic of acetamiprid are probably the same as those of thiacloprid. In addition, electrophysiological studies, photoaffinity labeling experiments, and homology modeling have indicated that the cyano group of neonicotinoids may interact with loop C in the agonist binding domain of the α subunit (Matsuda et al., 2009; Shimomura et al., 2004). Furthermore, recent electrophysiological experiments have indicated that the cyano group of thiacloprid may have unique interactions as compared with the nitro group of imidacloprid (Toshima et al., 2008). Accordingly, the different effects of acetamiprid and imidacloprid, as indicated by the pEC_{50} values, are probably due to their slightly different interactions with aphid nAChRs.

In conclusion, we have shown that the Kushima clone harbors an R81T mutation that conveys a high level of resistance to neonicotinoids. In addition, we investigated the effect of the R81T mutation on neonicotinoid affinity. An important finding of this study was the significant changes in the pEC_{50} values of imidacloprid for the Dα2β2 nAChR T77R single mutant and the T77R + E79V double mutant, whereas those of acetamiprid showed no change. In this study, we used Dα2 and chicken β2 hybrid nAChRs. To elucidate further the effect of mutations on neonicotinoid agonist activities,

further studies with aphid nAChR or complete insect nAChRs are required. Here, we have analyzed the sequences of the aphid nAChR α1, α2, and β1 subunits. However, aphids may carry additional mutations in other nAChR subunit genes or different genes altogether. Therefore, whole-genome analyses of both susceptible aphid strains and the Kushima clone are necessary to investigate other possible resistance mechanisms. Additionally, the mutation of Arg81 (AGA) to Thr (ACA) was detected heterozygously. However, the inheritance pattern remains unclear. Elucidation of this is necessary for understanding the mechanism of resistance. We trust that the findings obtained in this study will contribute to a better understanding of the different modes of action of nitro- and cyano-substituted neonicotinoids to improve resistance management.

Chapter 3

The R81T mutation in the nicotinic acetylcholine receptor of *Aphis gossypii* is associated with neonicotinoid insecticide resistance with differential effects for cyano- and nitro-substituted neonicotinoids

Introduction

The cotton aphid, *Aphis gossypii* Glover, is one of the most agriculturally important insect pests. Neonicotinoid insecticides and sulfoxaflor (Figure 4) excellently control *A. gossypii* and function via selective interaction with insect nicotinic acetylcholine receptors (nAChRs) (Jeschke and Nauen, 2008; Wang et al., 2016). The nAChRs are members of the Cys-loop superfamily of ligand-gated ion channels, and neuronal nAChRs play a central role in fast cholinergic neurotransmission in both vertebrates and invertebrates (Changeux, 2012; Hurst et al., 2013). The nAChRs are composed of five-subunit proteins and form a pentagonal assembly. Subunit proteins consist of an extracellular ligand-binding domain (LBD) and four transmembrane regions (TMs), the latter of which line integral ion channels. Agonist binding sites are formed at the subunit interfaces of the LBD, where they are involved in agonist binding; these sites are named loops A–F (Corringer et al., 2000). The binding of ACh to nAChRs triggers gating of the integral cation channel to mediate cholinergic neurotransmission (Unwin and Fujiyoshi, 2012). The functional properties of neonicotinoid insecticides have been studied using both native and cloned nAChR subunits. For example, commercially available neonicotinoid insecticides have been

shown to be agonists or partial agonists of insect nAChRs (Bai et al., 1991; Kagabu et al., 2002; Matsuda et al., 2001; Nishiwaki et al., 2003; Tan et al., 2007).

Resistance to neonicotinoid insecticides has developed relatively slowly, but it is now a major problem (Nauen and Denholm, 2005). It has been reported in a number of species, such as whiteflies (*Bemisia tabac*i and *Trialeurodes vaporariorum*) (Elbert and Nauen, 2000; Gorman et al., 2007; Nauen and Denholm, 2005), the brown planthopper (*Nilaparvata lugens*) (Zewen et al., 2003), the Colorado potato beetle (*Leptinotarsa decemlineata*) (Zhao et al., 2000), and the western flower thrips (*Fraklinealla occidentalis*) (Zhao et al., 1995). Resistance to neonicotinoid insecticides has in some cases been attributed to mutations in nAChR or to increased rates of insecticide detoxification. With regard to the target site, resistance to neonicotinoid insecticides in *Myzus persicae* and *Aphis gossypii* may be associated with a point mutation (R81T) in the β1 subunit of nAChR (Bass et al., 2011; Hirata et al., 2015). Many experimental studies have indicated that the amino acid residue affected by this mutation is a key determinant of the binding of neonicotinoid insecticides to nAChR (Ihara et al., 2008; Shimomura et al., 2006; Talley et al., 2008). In most cases, cytochrome P450-mediated detoxification plays a primary role in insecticide resistance in a variety of insects (Rauch and Nauen, 2003; Scott, 1999; Zhao et al., 2000). Cytochrome P450 is found widely in nature and plays roles in many biological processes, including hormone synthesis and the metabolism of exogenous compounds. In insects, cytochrome P450 has been implicated in providing resistance to insecticides via degrading foreign compounds to more soluble and less toxic forms (Scott, 1999). This is accomplished via either up-regulated cytochrome P450 expression or structural changes that may alter the substrate profile or catalytic activity of the enzyme (Amichot et al., 2004a; Bergé et al.,

1998; Bogwitz et al., 2005; Feyereisen et al., 1989; Nikou et al., 2003; Pridgeon and Liu, 2003).

The author previously characterized a field-collected *A. gossypii* (Kushima clone) that exhibited 23.8- to 394-fold resistance to neonicotinoid insecticides (Hirata et al., 2015). This Kushima clone showed higher resistance to nitro-substituted neonicotinoids, such as imidacloprid, than to cyano-substituted neonicotinoids, such as acetamiprid (Figure 4). This clone harbors the R81T mutation that confers resistance to neonicotinoid insecticides. The R81T mutation was revealed to lead to a significant shift in the pEC_{50} value of imidacloprid for the *Drosophila melanogaster* Dα2chickenβ2 nAChR, while barely affecting the pEC_{50} values of acetylcholine and acetamiprid. In addition, piperonyl butoxide (PBO) pretreatment reduced the LC_{50} values of neonicotinoid insecticides, for which the synergistic factors of acetamiprid and imidacloprid were 3.6 and 6.0, respectively. These findings suggested that cytochrome P450-mediated detoxification is not the main mechanism of neonicotinoid insecticide resistance. In the present study, two-electrode voltage-clamp electrophysiological analyses and molecular modeling were employed to investigate the differential effects of the R81T mutation of *A. gossypii* nAChR on cyano- and nitro-substituted neonicotinoids and sulfoxaflor. The obtained findings provided an explanation for the Kushima clone exhibiting distinct levels of resistance to cyano- and nitro-substituted neonicotinoid insecticides.

Materials and methods

Insects

The Kushima resistant clone was collected from a green pepper in Miyazaki Prefecture, Japan in 2012 (Matsuura and Nakamura, 2014). The clone harbors the R81T mutation in the nAChR β1 subunit that confers a high level of resistance to neonicotinoids. The Nippon-soda susceptible clone, which was also used in this study, has been maintained since 1993 at the Odawara Research Center, Nippon-soda Co., Ltd. (Odawara, Kanagawa, Japan). These clones were reared on cucumber seedlings at 25 °C and relative humidity (RH) of 60% under a 16:8-hr light:dark photoperiod without insecticide selection.

Chemicals

All tested neonicotinoids and sulfoxaflor were synthesized at the Odawara Research Center. The purity of the test compounds (Figure 4) was > 99%.

RNA-seq and data analysis

Sequences of nAChR genes were manually identified based on the results of tblastn searches against the generated contigs by using sequences of known insect nAChRs (Hirata et al., 2017).

Synthesis of cDNA clones encoding **A. gossypii** *nAChR*

Total RNA was isolated from adult aphids using ISOGEN with Spin Columns (Nippon Gene Co., Ltd., Tokyo, Japan) in accordance with the manufacturer's

instructions. First-strand cDNA was synthesized from total RNA using the Transcriptor First Strand cDNA Synthesis Kit (Roche Diagnostics K.K., Tokyo, Japan) with oligo-dT primers. PCR amplification was performed using KOD Plus Neo Polymerase (Toyobo Co., Ltd., Osaka, Japan) and gene-specific primers, which are listed in Table 3-1. PCR amplification was performed under the following cycling conditions: 2 min at 94 °C followed by 35 cycles of 10 s at 98 °C and 55 s at 68 °C. Amplicons were digested with restriction enzymes, and fragments of expected size were purified using the QIAquick Gel Extraction Kit (Qiagen). Purified amplicons were ligated into the pcDNA3.1(+) vector (Thermo Fisher Scientific K.K., Tokyo, Japan). Each cDNA clone was sequenced using the BigDye Terminator V3.1 Cycle Sequencing Kit (Applied Biosystems, Foster City, CA, USA).

Table 3-1. Primer sequences used in this study.

Name	Sequence (5' to 3')	Restriction enzymes	Purpose
Agoα1-F	ATAGGATCCGCCACCATGGAAATCCTTTGCGCGGT	*BamH*I and *Eco*RI	PCR amplification of Agoα1
Agoα1-R	ATAGAATTCTCATAAAATGGCTTGCAATTTCT		
Agoα2-F	ATAGGTACCGCCACCATGGCGTCAATCGACCCCGTC	*Kpn*I and *Apa*I	PCR amplification of Agoα2
Agoα2-R	ATAGGGCCCCTATTCCATATCAGACATTGGAGAAAA		
Agoβ1-F	GGTACCGCCACCATGGACACTCCCGTCGGACT	*Kpn*I and *Apa*I	PCR amplification of Agoβ1
Agoβ1-R	GGGCCCTTATTTTCCACCGTAGATTTCGA		
Agoα4-F	ATAGGTACCGCCACCATGGGGCCGAAATTTGCATTTCTTGG	*Kpn*I and *Apa*I	PCR amplification of Agoα4
Agoα4-R	ATAGGGCCCTTATGTGGTTTGGTATTCGCTGA		
Agoα8-F	GGTACCATGGATATTTTATATATCCTCCCGT	*Kpn*I and *Apa*I	PCR amplification of Agoα8
Agoα8-R	GGGCCCTTAATCGGCACCGTACGTGC		
pcDNA3.1-F	TAATACGACTCACTATAGGG		Sequencing
Agoα1-S1	TGAGGAACCGTACCTGGACA		Sequencing of Agoα1
Agoα1-S2	TACTTGGGCTACAATCGCGG		Sequencing of Agoα1
Agoα2-S1	TAACTCTGAGGCGGAGGACT		Sequencing of Agoα2
Agoβ1-S1	CTTGCTGCTAGCCGAGATCA		Sequencing of Agoβ1
Agoα4-S1	CGGACAGCGGTGAAAAAGTG		Sequencing of Agoα4
Agoα8-S1	CTTGCTGCTAGCCGAGATCA		Sequencing of Agoα8
pcDNA cRNA-F	CTCTCTGGCTAACTAGAGAACC		cRNA synthesis template
pcDNA cRNA-R	CTAGAAGGCACAGTCGAGGCTG		cRNA synthesis template

Preparation of Ago nAChR and chicken β2 cRNA

Templates for in vitro transcription were obtained by PCR amplification of each plasmid using the KOD Plus Neo polymerase and primers pcDNA cRNA-F and pcDNA cRNA-R (Table 3-1). Chicken β2 cDNA (wild type and T77R + E79V mutant) was used as described previously (Hirata et al., 2015). The capped RNA transcripts were synthesized using the T7 polymerase included with the mMessage mMachine T7 Ultra Kit (Thermo Fisher Scientific K.K.). The cRNA were purified using the RNeasy Mini Kit (Qiagen). The quality and quantity of cRNA were verified by agarose gel electrophoresis and absorption spectroscopy. The cRNA was stored at -80 °C until further use.

Functional expression of nAChR

Female *Xenopus laevis* were purchased from Hamamatsu Seibutsukyozai (Shizuoka, Japan) and maintained in tap water. Oocytes were surgically obtained using 0.03% benzocaine (Sigma-Aldrich) to reduce animal suffering as much as possible. The oocytes were treated with type IA collagenase (Sigma-Aldrich) in Ca^{2+}-free Standard Oocyte Saline (SOS) solution (100 mM NaCl, 2.0 mM KCl, 1.0 mM $MgCl_2$, and 5.0 mM HEPES, pH 7.6). Then, the follicle layer was removed manually using fine forceps in Ca^{2+}-containing SOS (100 mM NaCl, 2.0 mM KCl, 1.8 mM $CaCl_2$, 1.0 mM $MgCl_2$, and 5.0 mM HEPES, pH 7.6). Healthy V–VI stage oocytes were injected with equivalent amounts (10 ng each) of cRNA encoding Agoα1, α2, β1, and chicken β2 using the Nanoject II Auto Nanoliter Injector (Drummond Scientific Company, Broomall, PA, USA) and then incubated in SOS solution supplemented with 50 μg/mL gentamycin, 100 U/mL penicillin, 100 μg/mL streptomycin, 2.5 mM sodium pyruvate,

and 4% horse serum for 1–4 days. The medium was replaced daily, and unhealthy oocytes were discarded.

Two-electrode voltage-clamp (TEVC) electrophysiological recording

The two-electrode voltage-clamp (TEVC) method was conducted as previously reported (Hirata et al., 2015). In brief, *Xenopus* oocytes were placed in a recording chamber and superfused at 5 mL/min by a gravity-fed system with SOS including 0.5 μM atropine to suppress any contribution of endogenous muscarinic responses (Kusano et al., 1982). All experiments were performed at 18-19 °C. Membrane currents were recorded using 3.0 M KCl-filled electrodes (resistance 0.5-2.0 MΩ), and the membrane potential was clamped at -100 mV by using a TEV-200A amplifier (Dagan Corporation, Minneapolis, MN, USA) and digitized at 1 kHz using the PowerLab8/30 data acquisition and analysis system (ADInstruments, Nagoya, Japan). Signals were filtered at 50 Hz using a four-pole Bessel filter. Test compounds were dissolved in dimethyl sulfoxide (DMSO) at a concentration of 100 mM, and DMSO stock solution was diluted in SOS containing 0.5 μM atropine. ACh was directly dissolved in the atropine-containing SOS. Intervals of 3–5 min were allowed to pass between each agonist application to prevent the attenuation of response amplitude by desensitization. To determine antagonism by the test compounds, the oocytes were first challenged by 3 s applications of 1 μM ACh three times to confirm the integrity of the ACh-induced currents. They were then perfused with SOS containing various concentrations of test compounds for 1 min.

The LabChart 7 (ADInstruments) and GraphPad Prism 5 (GraphPad Software Inc., La Jolla, CA, USA) software packages were used for data analysis and the preparation

of graphs. Normalized concentration-response data were analyzed by nonlinear regression using GraphPad Prism to obtain I_{max} (the maximum normalized response), EC_{50} (the concentration including the half-maximal normalized response), IC_{50} (the concentration including the half-inhibition normalized response), pEC_{50} ($-\log EC_{50}$), and pIC_{50} ($-\log IC_{50}$).

Homology modeling of* A. gossypii *α1β1 nAChRs and ligand docking

Crystal structures of insect nAChRs are not presently available. Homology models of nAChRs based on the acetylcholine binding protein (AChBP) are used in computational studies (Shimomura et al., 2006; Wang et al., 2016). In this study, an *A. gossypii* α1β1 nAChR homology model was constructed from the crystal structure of *Lymnaea stagnalis* AChBP (PDB ID: 1UW6). This model was built using the Prime homology modeling program (ver. 4.3; Schrödinger LLC). Sequence alignment between *L. stagnalis* AChBP and *A. gossypii* α1 and β1 subunits was also performed using the Prime homology modeling program. The α1β1 combination corresponds to *M. persicae* α2β1, which was previously used in *M. persicae* nAChR modeling (Matsuda et al., 2009; Wang et al., 2016). In the mutant receptor model, R81T of the β1 subunit was replaced with mutated residues in the alignment. The structure was then energy-minimized using the OPLS_2005 force field.

The protein structure was prepared for docking simulations using the Prepare Protein Wizard (ver. 4.3; Schrödinger LCC) with a minimized root mean square deviation (RMSD) of 0.3 Å by applying the OPLS_2005 force field. The ligands used in this study were prepared using the LigPrep module (ver. 3.7; Schrödinger LCC). Ligand docking studies were carried out using GLIDE (ver. 7.0; Schrödinger LCC). All ligands

were docked into the *A. gossypii* α1β1 homology model in SP mode. A total of 30 binding poses were generated for each docked ligand. The most likely binding pose was selected for each molecule based on known X-ray poses for AChBP and their docking energy scores. All selected binding poses were used for further analysis.

Calculation of binding free energies using the molecular mechanics-generalized Born surface area method

The molecular mechanics-generalized Born surface area (MM-GBSA) method was used to estimate the binding free energy of receptor-ligand complexes (Massova and Kollman, 2000; Wang et al., 2013; Wang et al., 2001). All simulations used the OPLS_2005 force field and were performed using Prime/MM-GBSA (Lyne et al., 2006). The docked poses were minimized, and the energy of each complex was calculated using the OPLS_2005 force field and the generalized-Born surface area (GBSA) continuum solvent model. Flexible residue distance was defined using all ligands with the processed distance from a ligand set to 10 Å.

Results

Identification of A. gossypii *genes encoding nAChR α1, α2, and β1 subunits and cloning of full-length coding sequences*

Transcriptome sequences of 78,101 contigs (70,470,579 bp in total) were generated by de novo assembly using the RNA-seq reads of the Nippon-soda clone (21,772,148,022 bp in total). Sequences of *A. gossypii* nAChR genes were identified from the generated contigs by tblatn search using sequences of the known *A. gossypii* genes, and then nAChR α1, α2 and β1 subunits were manually identified. The author also manually identified nAChR α4-1, α4-2, and α8.

Full length coding sequences (CDS) of *A. gossypii* (Ago) nAChR α1, α2, and β1 subunits were cloned using degenerate gene-specific primers designed from the sequences of corresponding RNA-seq contigs. As a result, the full length CDS (1776 bp) of Agoα1 was identified (LC215865). The Agoα1 protein was found to be 69.8% identical to the *Drosophila melanogaster* Dα1 (× 07194) polypeptide sequence and 97.8% identical to that of *M. persicae* Mpα2 (× 81887). The full length CDS (1752 bp) of Agoα2 was also identified (LC215866). The findings revealed the Agosα2 protein to be 70.7% identical to the *D. melanogaster* Dα2 (× 53583) polypeptide sequence and 95.1% identical to that of *M. persicae* Mpα1 (× 81887). Furthermore, the full length CDS (1530 bp) of Agoβ1 was identified (LC215870) and shown to be 70.7% identical to the *D. melanogaster* Dβ1 (CAA27641) polypeptide sequence and 95.1% identical to that of *M. persicae* Mpβ1 (AJ251838). Thus, the *A. gossypii* nAChR subunits exhibited high identity to the *M. persicae* nAChR subunit.

Sequences of these *A. gossypii* nAChR subunits possessed typical features such as

an extracellular N-terminal domain with loops A–F, which are involved in ligand binding; a cysteine loop that consists of two disulfide bond-forming cysteines separated by 13 amino acid residues; four transmembrane domains (TM–TM4); and a large, highly variable intracellular loop between TM3 and TM4 (Figure 3-1). The presence of two adjacent cysteines in loop C signified that this is an α-subunit (Kao et al., 1984). Construction of a Clustal Omega-based molecular tree of the polypeptide sequences (Figure 3-2) showed that the Agoα1 subunit forms a cluster with the corresponding protein (insect nAChR α1 subunit), while the same was observed for the Agoα2 and Agoβ1 subunits, which form a cluster with the corresponding proteins (insect nAChR α2 and β1 subunits).

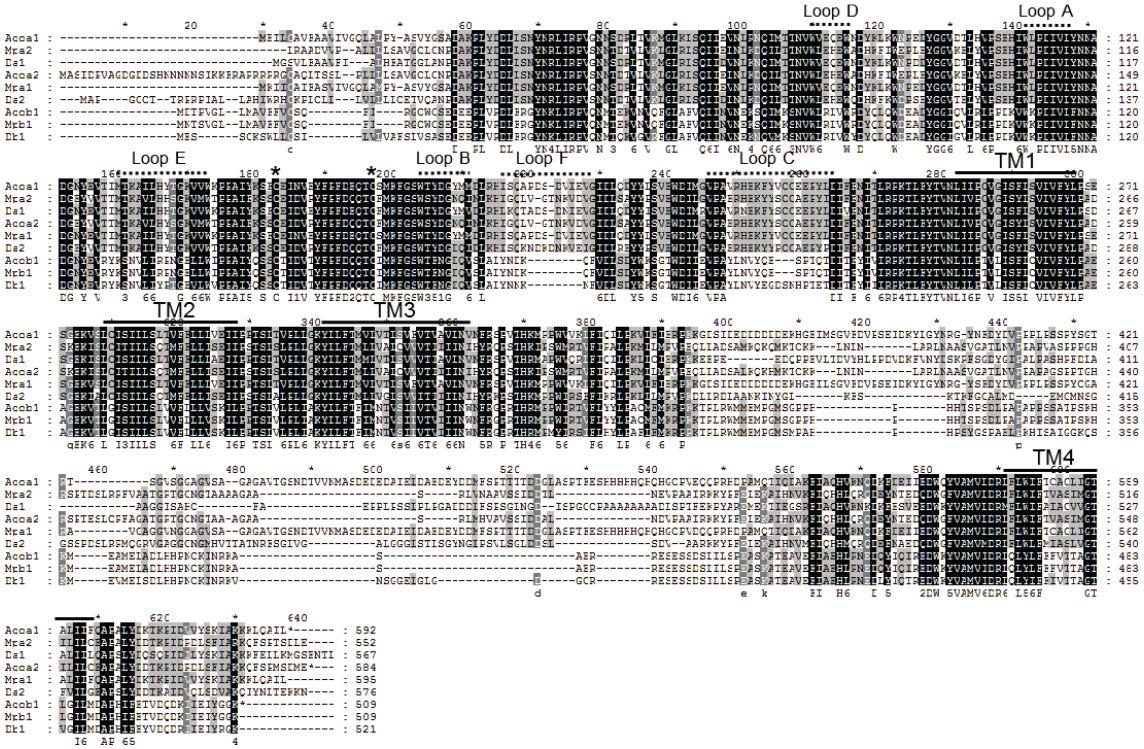

Figure 3-1. Multiple alignment of protein sequence of the insect nicotinic acetylcholine receptor (nAChR) α1, α2, and β1 subunits. *Aphis gossypii* (Ago) α1, α2, and β1; *Myzus persicae* (Mp) α1, α2, and β1; *Drosophila melanogaster* (Dm) α1, α2, and β1. The positions of loops (loops A–F) implicated in ligand binding and four transmembrane domains (TM1–4) are indicated. The sites of cysteine residues involved in the Cys-loop are marked with asterisks.

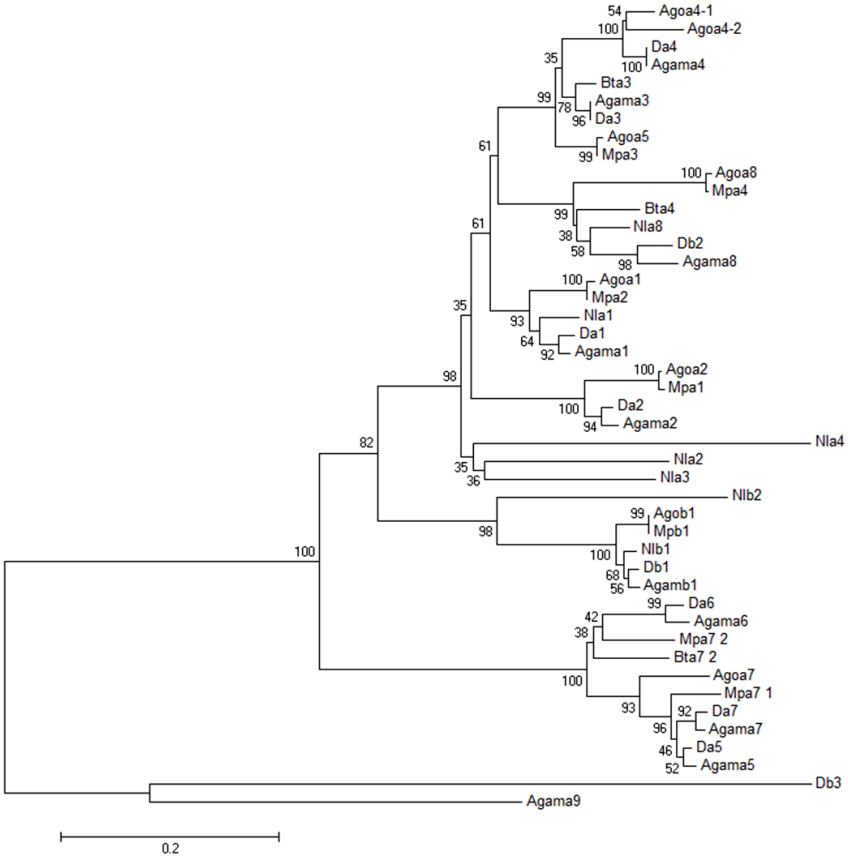

Figure 3-2. Phylogenetic analysis of the *Aphis gossypii* nicotinic acetylcholine receptor (nAChR) subunits. Sequences were aligned using Clustal Omega (http://www.ebi.ac.uk/Tools/msa/clustalo/). The phylogenetic tree was constructed using protein sequences with the neighbor-joining (NJ) method using MEGA version 6 (Tamura et al., 2013). Scale bar represents an estimate of the number of amino acid substitutions per site and numbers represent bootstrap values with 1000 replications. Accession and database sequence identifiers are the following: *Drosophila melanogaster*- Dα1 (X07194), Dα2 (X53583), Dα4 (CAA75688), Dα5 (AF272778), Dα6 (AF321445), Dα7 (AY036614), Dβ1 (CAA27641), Dβ2 (CAA39211), and Dβ3 (CAC48166); *Myzys persicae*- Mpα1 (X81887), Mpα2 (X81888), Mpα3 (AJ236786), Mpα4 (AJ236787), Mpα7-1 (AY500239), Mpα7-2 (AJ880086), and Mpβ1 (AJ251838); *Bemisia tabaci*- Btα3 (AJ880081), Btα4 (AJ880082), and Btα7-2 (AJ880083); *Nilaparvata lugens*- Nlα1 (AY378698), Nlα2 (AY378702), Nlα3 (AY378700), Nlα4 (AY378699), Nlα8 (FJ481979), Nlβ1 (FJ358493), and Nlβ2 (AY378703); *Anopheles gambiae*- Agamα1 (AY705394), Agamα2 (AY705395), Agamα3 (AY705396), Agamα4 (AY705397), Agama5 (AY705399), Agamα6 (AY705400), Agamα7 (AY705402), Agamα8 (AY705403), Agamα9 (AY705404), and Agamβ1 (AY705405); and *Aphis gossypii*- Agoα1 (LC215865), Agoα2 (LC215866), Agoα3 (AF527783), Agoα4-1 (LC215867), Agoa4-2 (LC215868), Agoα7 (JN989962), Agoα8 (LC215869), and Agoβ1 (LC215870).

Functional expression of* A. gossypii *nAChR α1, α2, β1, and chicken β2 subunits in X. laevis *oocytes

The application of 1 mM ACh to oocytes injected with Agoα1 alone or Agoα1β1 and clamped at − 100 mV resulted in no inward current (Figure 3-3A, B). In contrast, the application of 10 μM ACh to oocytes injected with Agoα1 chickenβ2 (Gβ2) resulted in strong inward currents of up to 4 μA (Figure 3-3C). Similarly, the application of 1 mM ACh to oocytes injected with Agoα2, Agoα2β1, or Agoα2Gβ2 resulted in no inward current (Figure 3-3D, E) or a very weak one (Figure 3-3F), respectively. In addition, for oocytes injected with Agoα4 and Agoα8, there was no inward current or only a weak one (Figure 3-4, 3-5). Accordingly, we investigated the differential effects of the R81T mutation of *A. gossypii* nAChR using the Agoα1Gβ2 nAChR.

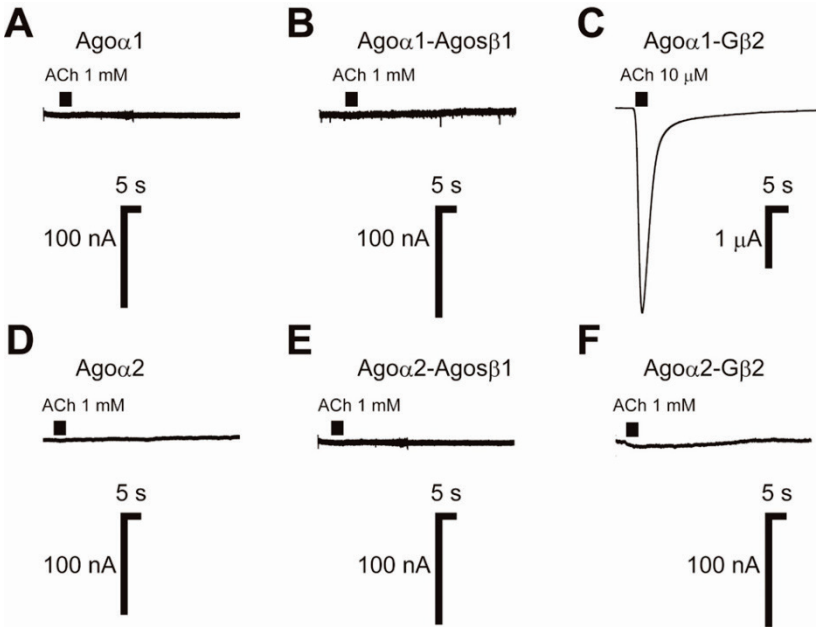

Figure 3-3. Responses to acetylcholine of various nicotinic acetylcholine receptors (nAChRs). Responses of oocytes expressing Agoα1 alone (A), Agoα1β1 (B), or Agoα1-chicken β2 (Gβ2) (C) to 1 mM ACh or 10 μM ACh. Responses of oocytes expressing Agosα2 alone (D), Agoα2β1 (E), or Agoα2-chicken β2 (F) to 1 mM ACh or 10 μM ACh.

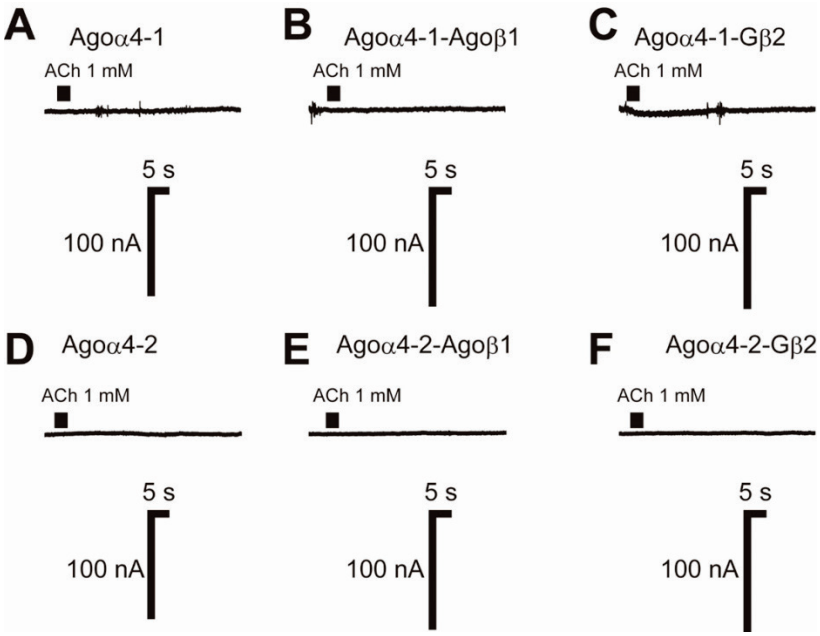

Figure 3-4. Responses to acetylcholine of various nicotinic acetylcholine receptors (nAChRs). Responses of oocytes expressing Agoα4-1 alone (A), Agoα4-1-β1 (B), and Agoα4-1-β1-chicken β2 (Gβ2) (C) to 1 mM ACh. Responses of oocytes expressing Agosα4-2 alone (D), Agoα4-2-β1 (E), and Agoα4-2-chicken β2 (F) to 1 mM ACh.

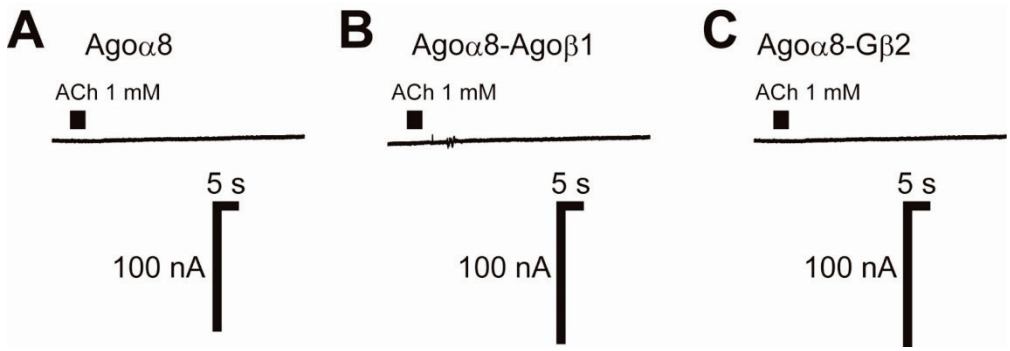

Figure 3-5. Responses to acetylcholine of various nicotinic acetylcholine receptors (nAChRs). Responses of oocytes expressing Agoα8 alone (A), Ago α8-β1 (B), or Ago α8-chicken β2 (Gβ2) (C) to 1 mM ACh.

Effect of R81T mutation in Agoα1Gβ2 nAChR expressed in* X. laevis *oocytes on cyano- and nitro-substituted neonicotinoids and sulfoxaflor

When Agoα1Gβ2 wild-type receptors were used, ACh, acetamiprid, sulfoxaflor, and clothianidin induced inward currents, however, there was no inward current for imidacloprid (Figure 3-6). Additionally, ACh and sulfoxaflor induced inward currents in a concentration-dependent manner (Figure 3-7A). The I_{max} and pEC_{50} values of ACh were 1.05 ± 0.04 and 6.19 ± 0.06 (0.64 μM), respectively (Table 3-2). The I_{max} and pEC_{50} values of sulfoxaflor were 0.10 ± 0.007 and 5.83 ± 0.17 (1.5 μM), respectively (Table 3-2). Acetamiprid and clothianidin were not determined because the inward currents were very weak.

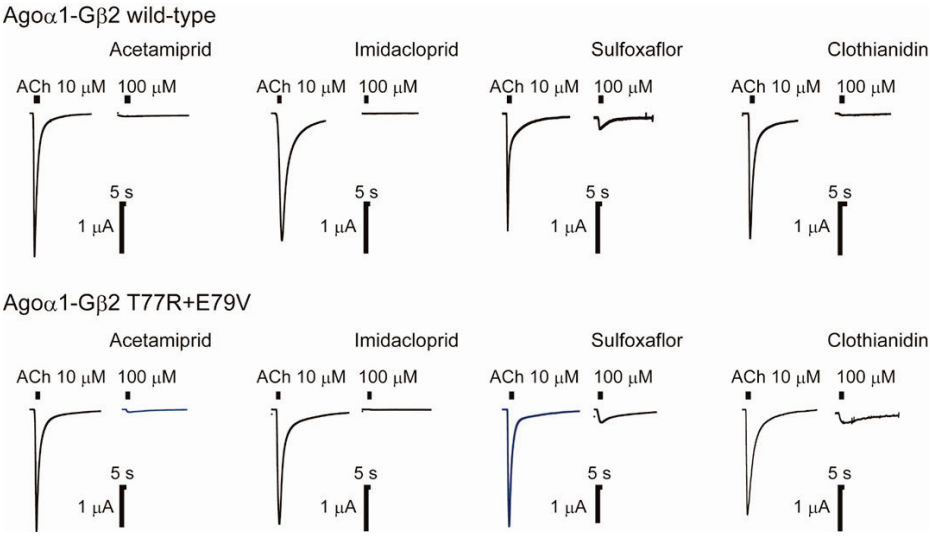

Figure 3-6. Responses to 10 mM ACh and 100 mM acetamiprid, imidacloprid, sulfoxaflor, and clothianidin of oocytes expressing Agosα1Gβ2 wild-type and T77R+E79V mutant.

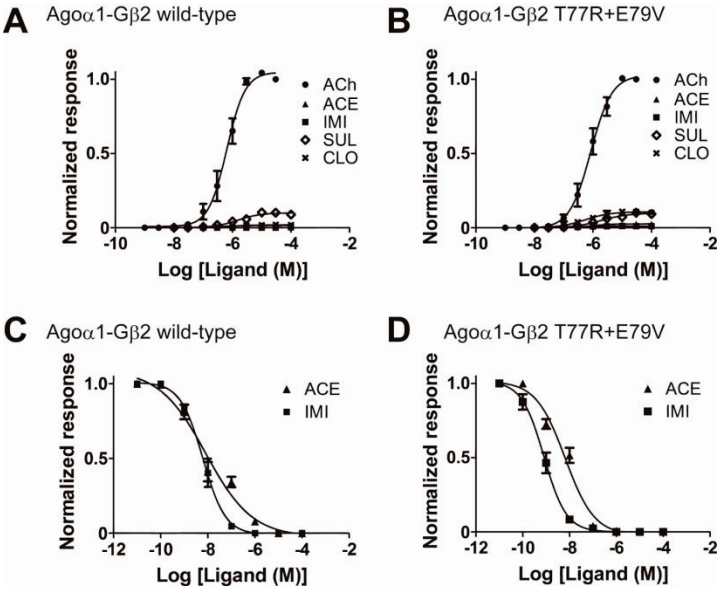

Figure 3-7. Concentration-response curves of ACh, acetamiprid, imidacloprid, sulfoxaflor, and clothianidin of wild-type (A) and T77R+E79V Agoα1Gβ2 (B). Concentration-response curves for acetamiprid and imidacloprid for the inhibition of wild-type Agoα1Gβ2 in the presence of 1 μM ACh (C) and those for T77R+E79V mutant (D). Each point represents the mean ± S.E.M. of at least four experiments (n = 4).

Table 3-2. pEC_{50}, I_{max}, and pIC_{50} of ACh, acetamiprid, sulfoxaflor, imidacloprid, and clothianidin for wild-type and T77R+E79V mutant Agoα1Gβ2 receptors.

Ligands	Wild-type			T77R+E79V			
	pEC_{50}	I_{max}	pIC_{50}	pEC_{50}	I_{max}	pIC_{50}	RF[a]
ACh	6.19 ± 0.06	1.05 ± 0.04	n.t.	6.08 ± 0.06	1.03 ± 0.03	n.t.	65.4
Acetamiprid	n.d.	0.02 ± 0.001	8.09 ± 0.17	n.d	0.03 ± 0.002	8.18 ± 0.08	23.8
Sulfoxaflor	5.83 ± 0.17	0.10 ± 0.007	n.t.	5.74 ± 0.17	0.10 ± 0.01	n.t.	22.6
Imidacloprid	n.d.	n.d.	8.21 ± 0.07*	n.d	0.01 ± 0.002	9.09 ± 0.06*	216
Clothianidin	n.d.	0.02 ± 0.001*	n. t.	6.26 ± 0.22	0.11 ± 0.01*	n.t.	394

Values shown are the results of a fit of the concentration-response data (mean ± S.E.M., at least n = 4) illustrated in Figure 3-6. Statistical tests (one-way ANOVA, Dunnett's multiple-comparison test) were performed to determine the significance of differences from the wild-type data. *$p<0.05$. The peak amplitude of the current recorded in the response to each challenge was normalized to the maximum amplitude of the response to ACh.

[a]Resistance factor as previously tested (Hirata et al., 2015).

To examine the effects of R81T mutation in loop D of the β1 subunit on neonicotinoid and sulfoxaflor agonist activity, we used an equivalent double mutant (T77R + E79V) of the chicken β2 subunit. The E79 residue of the chicken β2 subunit may suppress interactions between the nitro group of neonicotinoids and Arg77 through the negative electrostatic forces of Glu79 (Shimomura et al., 2006). Using Agoα1Gβ2 T77R + E79V receptors, ACh and all test compounds induced inward currents, whereas the current for imidacloprid was very weak (Figure 3-6). ACh, sulfoxaflor, and clothianidin induced inward currents in a concentration-dependent manner (Figure 3-7B). The I_{max} and pEC_{50} values of ACh were 1.03 ± 0.03 and 6.08 ± 0.06 (0.84 μM), respectively (Table 3-2), which were not significantly different compared with those of the wild type. The I_{max} values of sulfoxaflor and clothianidin were 0.10 ± 0.01 and 0.11 ± 0.01 (Table 3-2), while their pEC_{50} values were 5.74 ± 0.17 (1.8 μM) and 6.26 ± 0.22 (0.55 μM), respectively (Table 3-2). The I_{max} and pEC_{50} values of sulfoxaflor exhibited no significant change. On the other hand, the I_{max} and pEC_{50} values of clothianidin exhibited greater change than those of sulfoxaflor (Figure 3-7, Table 3-2).

Acetamiprid and imidacloprid induced inward currents, but they were very weak (Figure 3-6). For this reason, the effects of the R81T mutation on acetamiprid and imidacloprid were tested via assessing the antagonistic actions on the Agoα1Gβ2 wild-type and T77R + E79V receptors. These compounds were applied alone for 1 min prior to co-application with ACh at 1 μM, a concentration close to the EC_{50} of ACh. These test compounds suppressed the ACh-induced current of the Agoα1Gβ2 wild-type receptors at 1 μM ACh. The pIC_{50} values of acetamiprid and imidacloprid were 8.09 ± 0.17 (8.2 nM) and 8.21 ± 0.07 (6.2 nM), respectively (Table 3-2, Figure 3-7, 3-8). Additionally, acetamiprid and imidacloprid suppressed the ACh-induced current of the

Agoα1Gβ2 T77R + E79V. The pIC_{50} values of acetamiprid and imidacloprid were 8.18 ± 0.08 (6.5 nM) and 9.09 ± 0.06 (0.81 nM), respectively (Table 3-2, Figure 3-7D, 3-8). The pIC_{50} value of imidacloprid was significantly different compared with values of the wild-type and T77R + E79V receptors for that of acetamiprid, which did not differ significantly. However, Agoα1-Gβ2 T77R + E79V demonstrated resistance to these two pesticides (Table 3-2).

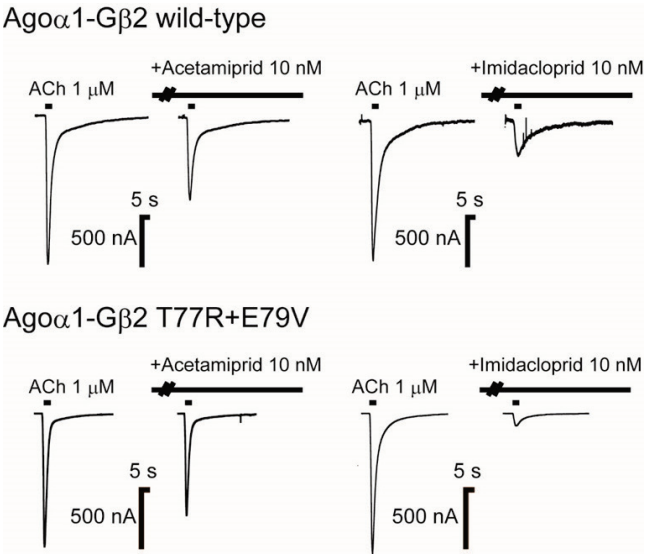

Figure 3-8. Neonicotinoid binding in the Agoα1Gβ2 nAChR protein pocket. (A) imidacloprid in the wild type, (B) imidacloprid in the R81T mutant, (C) acetamiprid in the wild type, and (D) acetamiprid in the R81T mutant.

Agoα1β1 nAChR modeling and effects of R81T mutation on cyano- and nitro-substituted neonicotinoids and sulfoxaflor regarding binding free energy

To verify the effects of the R81T mutation, three-dimensional models of the ligand binding site of Agoα1β1 wild-type and R81T nAChRs were constructed. Neonicotinoid insecticides and sulfoxaflor were docked into the binding site of the Agoα1β1 nAChR model. The most likely docking poses for neonicotinoids were

determined on the basis of X-ray poses in the AChBP and docking scores. The binding free energy of receptor-ligand complexes (ΔG) using the most likely docking poses was estimated for each test compound and Prime MM-GBSA. The wild-type models (Figure 3-9A, C) showed Arg81 in close proximity to the cyano group of acetamiprid and the nitro group of imidacloprid. In addition, the cyano group of acetamiprid and the nitro group of imidacloprid underwent electrostatic interactions with Arg81. In contrast, the electrostatic interaction was lost upon replacement with threonine (Figure 3-9B, D). In the wild-type model, the ΔG values of acetamiprid and imidacloprid were shown to be − 67.28 and − 89.63 kcal/mol, respectively (Table 3-3). In the R81T model, these values were instead − 64.01 and − 80.67 kcal/mol, respectively (Table 3-3). The differences in the ΔG values (ΔGwild − ΔGR81T) for acetamiprid and imidacloprid between these two models were thus − 3.27 and − 8.97 kcal/mol, respectively (Table 3-3, Figure 3-10A). This is potentially due to the smaller Thr residue, which leads to the lack of a strong nitro/cyano-Arg hydrogen bond interaction. The change of ΔG values of imidacloprid was greater than that of acetamiprid. Among the six neonicotinoids and sulfoxaflor, the difference of ΔG values for acetamiprid was the smallest, while the largest difference was observed for clothianidin (Table 3-3). In addition, the differences of ΔG values for nitro-substituted neonicotinoids were greater than those for cyano-substituted neonicotinoids and sulfoxaflor (Table 3-3, Figure 3-10A). These differences for ΔG values were strongly correlated with the resistance factor of the Kushima clone (Figure 3-10B), with an R^2 value of 0.71.

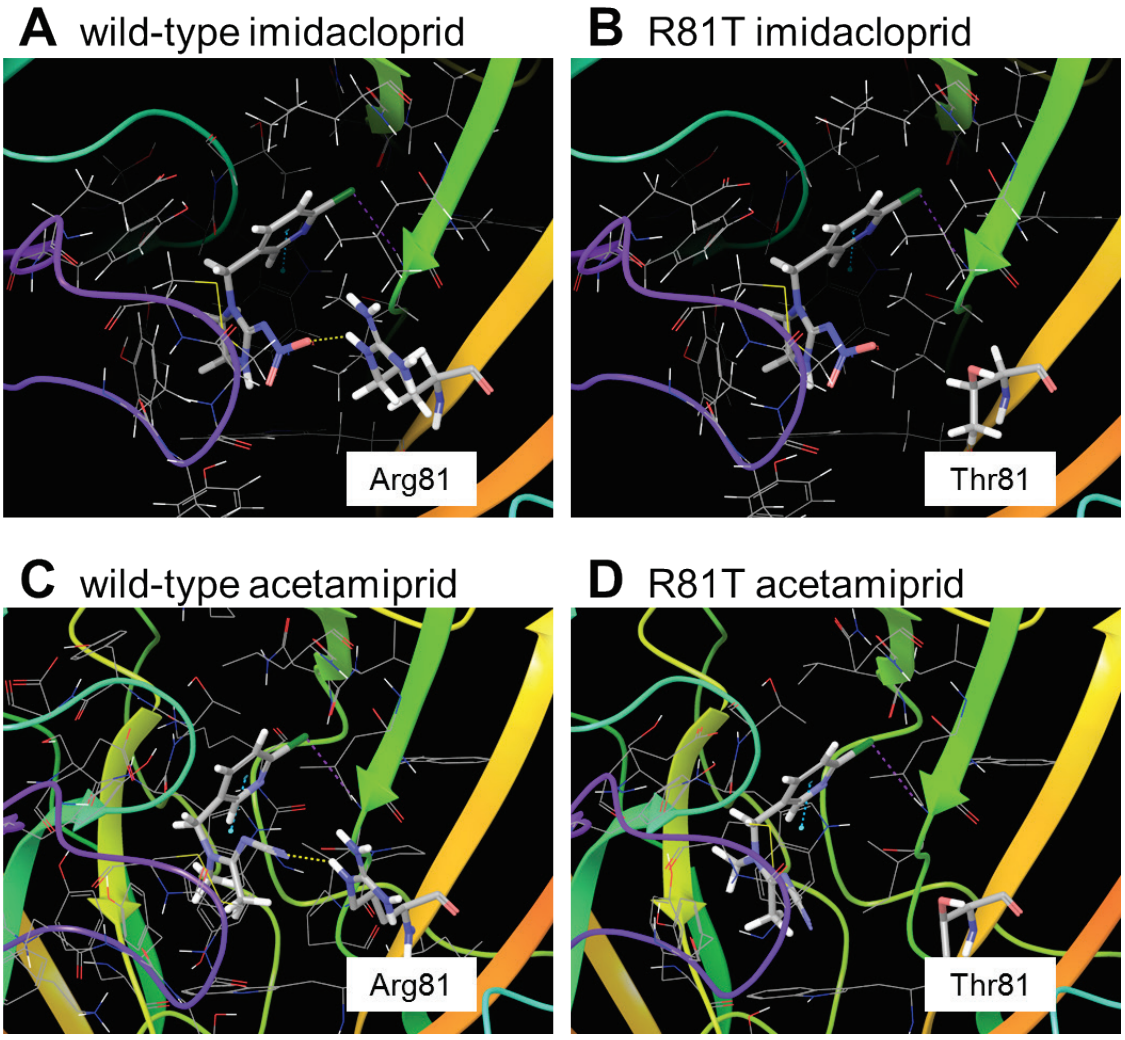

Figure 3-9. Neonicotinoid binding in the Agoα1Gβ2 nAChR protein pocket. (A) imidacloprid in the wild type, (B) imidacloprid in the R81T mutant, (C) acetamiprid in the wild type, and (D) acetamiprid in the R81T mutant.

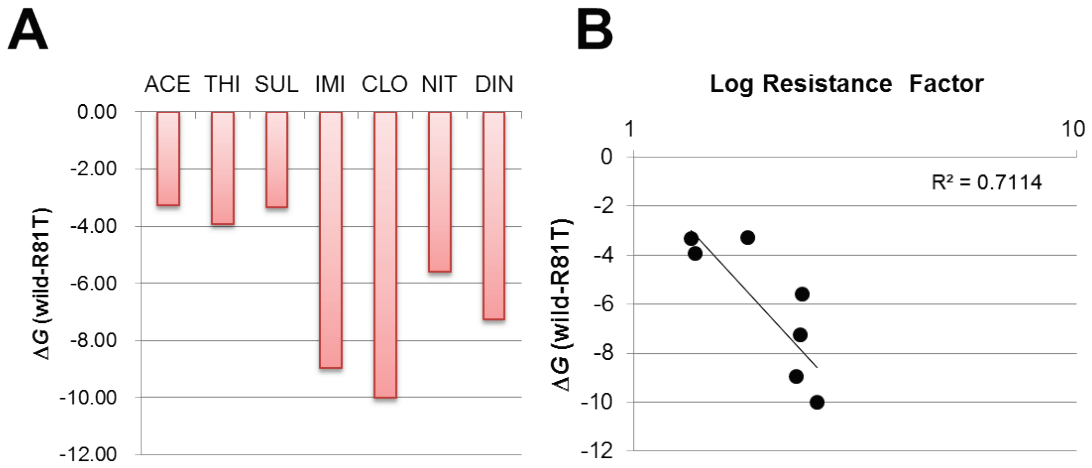

Figure 3-10. A comparison of the difference of Δ*G* values (Δ*G*wild – Δ*G*R81T) for neonicotinoids and sulfoxaflor from modeling and correlation of the difference of Δ*G* values with the resistance factor of neonicotinoid insecticides in the Kushima clone. A comparison of the modeled changes of Δ*G* values (Δ*G* wild – Δ*G* R81T) for neonicotinoids and sulfoxaflor (A). ACE = acetamiprid; THI = thiacloprid; SUL = sulfoxaflor; IMI = imidacloprid; CLO = clothianidin; NIT = nitenpyram; DIN = dinotefuran. (B) Correlation of the differences of Δ*G* values with the resistance factor (Log) of neonicotinoid insecticides in the Kushima clone (r^2 = 0.711).

Table 3-3. A comparison of the changes of Δ*G* values for neonicotinoids and sulfoxaflor for wild-type versus the R81T mutant.

	Ago nAChR α1β1 MM-GBSA		
	Wild	R81T	Δ
	kcal/mol	kcal/mol	kcal/mol
	Δ*G*	Δ*G*	WT-R81T
Acetamiprid	-67.28	-64.01	-3.27
Thiacloprid	-84.16	-80.24	-3.92
Sulfoxaflor	-51.73	-48.40	-3.33
Imidacloprid	-89.63	-80.67	-8.97
Clothianidin	-78.37	-68.36	-10.01
Nitenpyram	-77.17	-71.58	-5.59
Dinotefuran	-66.38	-59.11	-7.26

Discussion

In this study, we investigated the differential effects of the R81T mutation of *A. gossypii* nAChR on cyano- and nitro-substituted neonicotinoids and sulfoxaflor. We identified, cloned, and demonstrated functionality of genes from the *A. gossypii* Kushima clone, namely, those encoding the Agoα1, α2, and β1 subunits. Based on phylogenetic analysis (Figure 3-2) and multiple alignment analysis (Figure 3-1), the Agoα1, α2, and β1 subunit genes studied belonged to the insect nAChR α1, α2, and β1 subunits, respectively.

Functional expression and two-electrode voltage-clamp studies on Agoα1, α2, and β1 cRNA injected into *Xenopus* oocytes demonstrated that the Agoα1 gene with the Gβ2 (chicken) product acts as an nAChR receptor. In contrast, Agoα1 alone and Agoα1 with the Agoβ1 gene product did not perform this functional role when these cRNAs were injected into *Xenopus* oocytes (Figure 3-3). Similarly, the Agoα4 and Agoα8 gene products did not function when these cRNAs were injected into Xenopus oocytes (Figure 3-4, 3-5). In addition, the translated ORF of Agoα1 is 69.8% identical to *Drosophila melanogaster* Dα1 (× 07194) and 97.8% identical to *M. persicae* Mpα2 (× 81887). Dα1 and Mpα2 have already been classified as insect nAChR α1 subunits (Millar and Denholm, 2007). For the Agoα1Gβ2 nAChR, ACh induced inward currents at a low concentration (Figure 3-7). The pEC_{50} value of ACh to wild-type Agoα1Gβ2 nAChR was 6.19 ± 0.06 (0.64 μM), which was close to the value determined for Dα1Gβ2 nACh (6.12 ± 0.06, 0.76 μM). In addition, the pEC_{50} value of ACh to Dα2Gβ2 nAChRs was much smaller than that of Dα1Gβ2 nAChR (4.79 ± 0.03, 16 μM) (Ihara et al., 2003). Neither sulfoxaflor nor any test compounds in this study were highly

efficacious as acting as agonists on Agoα1Gβ2 nAChRs, with responses to the most efficacious compound, sulfoxaflor, producing currents that were at most only 10% of the maximal currents (Table 3-2, Figure 3-6). Sulfoxaflor and clothianidin were determined to have super-agonistic actions on Dα2Gβ2 receptors (Brown et al., 2006; Ihara et al., 2004; Tan et al., 2007; Watson et al., 2011), whereas sulfoxaflor and all test compounds exhibited low efficacy to Dα1Gβ2 nAChRs (Watson et al., 2011). These agonist activities of Agoα1Gβ2 represented significant insect α1 subunit-like features of ACh and the test compounds.

We assessed the effect of the R81T mutation (wild-type Agoα1Gβ2 and T77R + E79V mutant) on the activity of neonicotinoids and sulfoxaflor. The Thr77 residue of the Gβ2 subunit corresponds to the Arg81 residue of the *A. gossypii* nAChR β1 subunit (Hirata et al., 2015). Interestingly, T77R + E79V mutations did not significantly affect the pEC_{50} values of ACh (Table 3-2, Figure 3-7), as previously reported (Shimomura et al., 2006). Moreover, T77R + E79V mutations did not significantly affect the pEC_{50} values of sulfoxaflor (Table 3-2, Figure 3-6, 3-7). However, the I^{max} value of clothianidin to the T77R + E79V mutant was greater than that of wild-type nAChRs (Table 4-2, Figure 4-6). Additionally, the pEC_{50} value of clothianidin was only determined in the T77R + E79V mutant. The pIC_{50} values of acetamiprid and imidacloprid were 8.09 ± 0.17 (8.2 nM) and 8.21 ± 0.07 (6.2 nM), respectively (Table 3-2, Figure 3-7C, D). The pIC_{50} value of imidacloprid was close to that of Dα1Gβ2 nAChR(Ihara et al., 2003). The pIC_{50} value of imidacloprid to Agoα1Gβ2 T77R + E79V nAChR significantly shifted compared with that of the wild-type Agoα1Gβ2 nAChR (Table 3-2, Figure 3-7C, D). On the other hand, the T77R + E79V mutations did not significantly change the pIC_{50} value of acetamiprid. These results were similar to

those obtained in a previous study (Hirata et al., 2015). The data indicated that the R81T mutation exhibits resistance to these compounds, but the mutation likely has differential effects on cyano- and nitro-substituted neonicotinoid insecticides and sulfoxaflor.

The R81T mutation in nAChR has been shown to be associated with target-site resistance to neonicotinoids in both M. persicae and *A. gossypii* (Bass et al., 2011; Hirata et al., 2015). This is explained by the fact that Arg81 within loop D is a key determinant of neonicotinoid binding to nAChRs (Ihara et al., 2008; Shimomura et al., 2006; Talley et al., 2008). In addition, the R81T mutation in *M. persicae* conferred reduced affinity of nAChR to imidacloprid (Bass et al., 2011). In the present study, the difference of ΔG values for cyano-substituted neonicotinoids and sulfoxaflor was smaller than that for nitro-substituted neonicotinoids (Table 3-3, Figure 3-10A), which is similar to the changes in the electrostatic energy component in neonicotinoid binding between wild-type M. persicae nAChRα2β1 and R81T (Wang et al., 2016). Among the six neonicotinoids and sulfoxaflor, acetamiprid showed the smallest difference in changes of ΔG values (Table 3-3, Figure 3-10A). Within the limits of the current dataset, the difference in changes of ΔG values between wild-type Agoα1β1 and R81T nAChR (Figure 3-10B) appears to be a reasonable predictor of resistance in the Kushima clone. The difference of ΔG values correlated with the resistance factor of the Kushima clone (Figure 3-10B), for which the r^2 value was 0.71. For example, among the test compounds, clothianidin showed the largest changes in difference of ΔG values (Table 3-3, Figure 3-10A), namely, − 10.01 kcal/mol; clothianidin indicated the highest resistance factor of the Kushima clone.

In conclusion, we revealed the R81T mutation has resistance to neonicotinoids in the nAChRs, and the mutation distinctly affects cyano- and nitro-substituted

neonicotinoids. In addition, we have investigated the effect of R81T of Agoα1β1 nAChR on neonicotinoid binding free energy via modeling (ΔG) using Prime MM-GBSA. Importantly, the small difference of ΔG values for the cyano-substituted neonicotinoids and sulfoxaflor between the wild-type and R81T nAChR models also provides a potential explanation for the rather modest differences in the resistance of the Kushima clone between cyano- and nitro-substituted neonicotinoids.

Chapter 4

Studies on Aphis gossypii *cytochrome P450s CYP6CY22 and CYP6CY13 using an in vitro system*

Introduction

The cotton aphid (*Aphis gossypii*) is an important sucking pest that causes severe crop losses in fields and greenhouses. Neonicotinoid insecticides (Figure 4), which achieve excellent control of *A. gossypii*, target nicotinic acetylcholine (ACh) receptors (nAChRs) of insects (Matsuda et al., 2001; Matsuda et al., 2005; Thany et al., 2007; Tomizawa and Casida, 2005). Resistance to neonicotinoid insecticides has developed relatively slowly; however, it is recognized as an important issue (Nauen and Denholm, 2005), particularly because of the resistance of numerous species such as whiteflies (*Bemisia tabaci* and *Trialeurodes vaporariorum*) (Elbert and Nauen, 2000; Gorman et al., 2007; Nauen and Denholm, 2005), brown planthoppers (*Nilaparvata lugens*) (Zewen et al., 2003), Colorado potato beetles (*Leptinotarsa decemlineata*) (Zhao et al., 2000), and western flower thrips (*Frankliniella occidentalis*) (Zhao et al., 1995). Resistance to neonicotinoid insecticides is attributed in some cases to mutations in nAChRs or to increased rates of insecticide detoxification. Target-site insensitivity occurs in field-caught peach potato aphids (*Myzus persicae*) and *A. gossypii* (Bass et al., 2011; Hirata et al., 2015). These aphids harbor a point mutation (R81T) in the loop D region of the nAChR β1 subunit. Moreover, numerous studies indicate that R81 within this loop is a key determinant required for the binding of neonicotinoid insecticides to

nAChRs (Ihara et al., 2008; Rauch and Nauen, 2003; Shimomura et al., 2006; Talley et al., 2008).

In most cases, cytochrome P450-mediated detoxification plays a primary role in the resistance to insecticides of diverse insects (Rauch and Nauen, 2003; Scott, 1999; Zhao et al., 2000). Cytochrome P450 (CYP) occurs widely in nature and plays roles in many biological processes, such as hormone synthesis and the metabolism of xenobiotics. In insects, P450 is implicated in resistance to insecticides through the degradation of these foreign compounds to more soluble and less toxic forms (Scott, 1999). This is accomplished via an increase in P450 expression or structural changes that may alter substrate-specificity profiles or catalytic activities (Amichot et al., 2004b; Bergé et al., 1998; Bogwitz et al., 2005; Feyereisen et al., 1989; Nikou et al., 2003; Pridgeon and Liu, 2003).

We previously characterized a field-isolated *A. gossypii* [Kushima resistant (KR) clone] that is resistant to nicotinoid insecticides (23.8- to 394-fold) conferred by the nAChR β1 subunit R81T mutation (Hirata et al., 2015). Further, piperonyl butoxide (PBO) pretreatment reduces LC_{50} values of neonicotinoid insecticides through synergizing with acetamiprid and imidacloprid (synergistic factors = 3.6 and 6.0, respectively). Therefore, we used next-generation sequencing (NGS) to identify P450 family members involved in the metabolism of neonicotinoid insecticides. Further, we molecularly cloned P450 cDNAs of *A. gossypii* KR clone and expressed. The functional recombinant P450s provide further evidence of the involvement of P450s in the metabolism of neonicotinoid insecticides.

Materials and Methods

Insects

KR and Miyazaki susceptible (MS) clones were collected from a green pepper and a cucumber, respectively, in Miyazaki Prefecture, Japan, in 2012 (Matsuura and Nakamura, 2014). The Nippon soda susceptible clone (NS clone) has been maintained since 1993 at the Odawara Research Center, Nippon Soda Co., Ltd. (Odawara, Kanagawa, Japan). These clones were reared on cucumber seedlings at 25 °C and 60% relative humidity under a 16:8-hr light:dark photoperiod in the absence of insecticides.

Chemicals

Acetamiprid and other neonicotinoids were synthesized at the Odawara Research Center. The purities of the test compounds (Figure 4) were >99%.

RNA-seq and data analysis

Aphids were treated with acetamiprid (0.08 ppm for susceptible NS and MS clones and 5 ppm for the KR clone) or vehicle (Hirata et al., 2015). Three biological replicates were performed using each condition. Total RNA of each biological replicate was extracted from the bodies of 10–15 wingless, viviparous females using TRizol reagent (Thermo Fisher Scientific K.K., Tokyo, Japan) and an RNeasy Mini Kit (QIAGEN K.K., Tokyo, Japan), in accordance with the manufacturer's instructions.

cDNA libraries were prepared from the total RNAs and nucleotide sequencing using an Illumina HiSeq 2000 sequencer (paired-end, 101 bp) by Macrogen Japan Corp. (Kyoto, Japan). RNA-seq raw reads of each replicate were filtered using Trimmomatic

(Bolger et al., 2014). The filtered reads of the KR clone were merged and assembled de novo using Trinity (Grabherr et al., 2011). The contigs were used as reference transcript sequences for further analysis. Each contig was annotated with a description of the top protein hit in the NCBI nr database using Blastx (e-value threshold: $1e^{-03}$). Coding sequence (CDS) prediction was performed using TransDecoder bundled with Trinity, and the predicted CDSs were annotated with a description of the homologous domains of the Pfam protein family database acquired using an HMMER3 search (Eddy, 2011).

The sequences of genes involved in insecticide resistance, such as those that encode detoxification enzymes (cytochrome P450s, glutathione S-transferases [GSTs], and carboxylesterases [COEs]), were identified according to the results of the Blastx and HMMER3 searches. For each sample, expression levels (tag count and TMM-normalized FPKM) of all genes (Trinity components) of the three replicates were calculated by aligning the filtered reads to the reference sequences using align_and_estimate_abundance.pl and abundance_estimates_to_matrix.pl bundled with Trinity. Differentially expressed gene (DEG) analysis of each susceptible and resistant clone was performed using iDEGES/edgeR, which is a statistical DEG analysis method that employs the tag counts of the two groups of RNA-seq data (three biological replicates for each group (Sun et al., 2013). Threshold values for identifying DEGs were a false discovery rate (FDR) of 0.05 and a fold change ≥2. The raw RNA-seq reads of the six samples were deposited in the DDBJ under accession number DRA005446.

Isolation of cDNA clones encoding A. gossypii *P450s*

Total RNA was isolated from adult aphids using ISOGEN and Spin Columns (Nippon Gene Co., Ltd., Tokyo, Japan), in accordance with the manufacturer's

instructions. First-strand cDNA was synthesized from total RNA using the Transcriptor First Strand cDNA Synthesis Kit (Roche Diagnostics K.K., Tokyo, Japan) with oligo-dT primers (Table 4-1). PCR amplification was performed using KOD -Plus- Neo polymerase (TOYOBO Bio-Technology Co., Ltd., Osaka, Japan) and gene-specific primers as follows: c21228_g1-F, c21228_g1-R, c21368_g1-F, and c21368_g1-R. PCR amplification was performed using the following cycling conditions: 2 min at 94 °C, followed by 35 cycles for 10 s at 98 °C and 50 s at 68 °C. Amplicons of the c21228_g1 gene were digested with *Kpn*I and *Apa*I, and those of the c21368_g1 gene were digested using *Eco*RI and *Apa*I. Amplicons of the expected sizes were purified using the QIAquick Gel Extraction Kit (QIAGEN). Purified amplicons were ligated to the pAc5.1(+) vector (Thermo Fisher Scientific K.K., Tokyo, Japan). Each cDNA clone was sequenced using the BigDye Terminator V3.1 Cycle Sequencing Kit (Applied Biosystems, Foster City, CA, USA). The sequences were confirmed using the following primers: pAc5.1-F, c21228_g1-S1 and c21228_g1-S2 for c21228_g1, and c21368_g1-S1 and c21368_g1-S2 for c21368_g1.

Table 4-1. Primer sequences used in this study.

Name	Sequence (5' to 3')	Restriction enzymes	Purpose
c21228_g1-F	ATAGGTACCCAAAATGATATCGTATCTGACCAACTTGT	*Kpn*I	PCR amplification of c21228_g1
c21228_g1-R	ATAGGGCCCATGTTCAATGATCGGTCTAAATT	*Apa*I	
c21368_g1-F	ATAGAATTCCAAAATGATTTCGTGGACGATCGATTG	*Eco*RI	PCR amplification of c21368_g1
c21368_g1-R	ATAGGGCCCAACCGCAACGACTGGCTTTAGAC	*Apa*I	
pAc5.1-F	ACACAAAGCCGCTCCATCAG		Sequencing of g21228
c21228_g1-S1	TTCGTACTTCACCGACCACG		
c21228_g1-S2	TGCAGGCGCGTAAAGAATTG		
c21368_g1-S1	AAGACTTTGCGCACTTCACG		Sequencing of g21368
c21368_g1-S2	GGAACGATGTGGCACAAACA		

Expression of* A. gossypii *P450 and metabolic studies

Drosophila melanogaster S2 cells were maintained at 28 °C in a T-75 flask in Insectagro DS2 medium (Corning Inc., Corning, NY, USA) supplemented with 4 mM Ala-Glu (Sigma-Aldrich, Tokyo, Japan). The transient expression of *A. gossypii* P450 was performed using S2 cells seeded 24 hr before transfection in six-well plates (8×10^5 cells per well) incubated at 28 °C. The transfection mixture in each well contained 3.6 μg of *A. gossypii* P450 DNA, 0.4 μg of *D. melanogaster* NADPH-cytochrome P450 reductase (CPR), and 4 μL of X-tremeGENE HP DNA Transfection Reagent (Roche Diagnostics K.K., Tokyo, Japan) in a final volume of 100 μL of Insectagro DS2 medium. *D. melanogaster* CPR (GenBank accession number Q27597) was synthesized by FASMAC (Kanagawa, Japan) and inserted into the pAc5.1 vector.

The medium was exchanged with serum-free CYP expression medium (supplemented with 0.1 mM ferric citrate, 0.1 mM 5-aminolevulinic acid, and 4 mM Ala-Glu in Insectagro DS2 medium) 6 hr after transfection. Next, the medium was exchanged with 2 mL of CYP expression medium 48 hr after transfection; test compounds (35 μL each) were added to a well and then sampled immediately (0 hr) and 72 hr later. All incubations were performed at 28 °C. Test compounds were dissolved in dimethyl sulfoxide to prepare a 40,000 ppm stock, which was then diluted to 400 ppm with phosphate-buffered saline (final concentration = 7 ppm).

After incubation, samples from the wells were transferred to 15-mL centrifuge tubes and diluted with an equal volume of acetonitrile (final volume 2 mL). The samples were vortexed for 10 sec, centrifuged at 14,000 × g for 5 min at room temperature, and then filtered through a 0.45-μm filter. The extracts were analyzed using high-performance liquid chromatography (HPLC) (Shimazu LC20A system;

Shimadzu Corporation, Kyoto, Japan) with an Inertsil ODS-5, 150 × 4.6 mm, 5-μm particle column (GL Sciences Inc., Tokyo, Japan), with UV detection at 254 nm. Samples were separated using gradient elution with a mobile phase comprising 0.1% (v/v) formic acid, 5 mM ammonium acetate in HPLC-grade water, and methanol at 1.0 mL/min for 40 min. The gradient elution conditions were as follows: 0 min methanol:water 10:90, 10 min methanol:water 10:90, 30 min methanol:water 70:30, 32 min methanol:water 10:90, and 40 min methanol:water 10:90. The injection volume was 25 μL. Each well of a six-well plate was analyzed three times.

Electrospray-ionization mass spectrometry (ESI-LC-MS spectra) was performed using a TSQ Vantage (Thermo Fisher Scientific K.K., Tokyo, Japan) operated in positive-ion mode. High-purity nitrogen (450 °C) was used as the sheath gas, and argon served as the collision gas. After 72 hr incubation, potential metabolites of acetamiprid and imidacloprid were analyzed using LC-MS, as indicated by the detection of extracted ions of the parents (223+ for acetamiprid and 256+ for imidacloprid) and metabolites (209+ for acetamiprid and 272+ for imidacloprid). Separation was performed using an Inertsil ODS-5 column (150 × 2.1 mm, 5-μm-diameter particle) and a gradient (same conditions as for the HPLC analysis above, except that the mobile phase comprised 0.1% [v/v] formic acid and 5 mM ammonium acetate in HPLC water and acetonitrile) delivered at 1.0 mL/min. The injection volume was 25 μL.

An EzRIPA Lysis Kit (Atto Corporation, Tokyo, Japan) was used to prepare samples from the cells in each well for Western blotting analysis. The samples were added to equal volumes of 2 × Laemmli sample buffer and heated at 100 °C for 5 min. The samples were then separated using a 10% SDS-PAGE gel and transblotted onto a polyvinylidene fluoride membrane. The membrane was probed with an anti-V5

antibody, subsequently incubated with an anti-IgG2a-HRP antibody, and the immunocomplexes were visualized using EzWestBlue (Atto Corporation).

Results

RNA-seq and DEG analysis of A. gossypii *genes encoding detoxification enzymes*

The numbers of RNA-seq paired-end reads (raw reads, filtered reads, and reads mapped to reference transcriptome sequences) of each clone are shown in Table 4-2. Reference transcriptome sequences of 81,316 contigs (70,664,259 bp in total) were generated using de novo assembly of the RNA-seq paired-end reads of the KR clone (21,070,670,904 bp). The reference contigs represented 65,692 genes (Trinity components) encoding at least one isoform (contigs).

Nine genes encoding *A. gossypii* detoxification enzymes were expressed at significantly higher levels by the KR clone as compared with those of the two insecticide-susceptible clones (Table 4-3). The nine genes encode cytochromes P450 according to annotation information acquired from the NCBI-nr and Pfam databases. In contrast, the transcriptional levels of genes encoding detoxification enzymes such as GST and COE were not significantly upregulated in the KR clone as compared with those of the susceptible clones. Transcriptional levels of the P450, GST, and COE genes were not significantly upregulated in the KR clone or the two insecticide-susceptible clones treated with acetamiprid vs. the control. Two of the nine P450 genes, c21228_g1 and c21368_g1 (Trinity IDs), were highly upregulated under the four conditions. The respective fold changes in the expression levels of the c21228_g1 and c21368_g1 genes were 46.21 and 7.46 for the KR/NS clones and 4.35 and 3.32 for the KR/MS clones in the absence of acetamiprid. Similarly, the respective values of the two genes were 38.05 and 8.22 for the KR/NS clones and 3.71 and 2.48 for the KR/MS clones in the presence of acetamiprid. The amino acid sequences of c21228_g1 (513 aa) and c21368_g1 (513

aa) are similar to those of CYP6CY22 (94.15% identical) and CYP6CY13 (99.61% identical) of *Aphid gossypii*, respectively.

Table 4-2. The number of RNA-seq paired-end reads acquired for the three *A. gossypii* clones (NS, MS, and KR).

Sample Id[a)]	Replicate ID	No. of RNA-seq paired-end reads[b)]		
		Raw	Filtered	Mapped to reference
NS (N)	rep1	36,807,970	29,952,366	23,732,526
	rep2	36,718,120	29,131,314	23,566,250
	rep3	36,417,536	29,158,596	23,333,644
NS(T)	rep1	33,581,112	27,099,350	22,090,390
	rep2	34,283,634	27,316,198	22,119,944
	rep3	37,757,450	30,506,432	23,567,262
MS (N)	rep1	38,883,482	30,185,406	26,480,438
	rep2	30,302,292	23,917,022	20,556,194
	rep3	32,049,156	25,433,864	21,541,656
MS (T)	rep1	38,463,596	33,257,728	28,917,210
	rep2	36,832,066	31,746,908	27,596,414
	rep3	35,566,136	30,776,962	26,170,864
KR (N)	rep1	35,392,952	30,615,400	25,700,126
	rep2	37,300,282	29,893,988	21,960,964
	rep3	35,562,908	28,725,344	23,160,986
KR (T)	rep1	34,926,706	28,174,146	22,975,134
	rep2	32,963,336	28,548,450	23,747,834
	rep3	32,474,320	28,474,746	22,322,760

[a)] (N) means without acetamiprid treatment, and (T) means with acetamiprid treatment (0.08 ppm and 0.5 ppm for the susceptible and resistant clone, respectively). [b)] The number of raw reads, filtered reads, and reads mapped to the reference transcript sequences are shown for three biological replicates (rep1, rep2, and rep3) of each clone treated without or with acetamiprid.

Table 4-3. Selected genes identified by RNA-seq that were differentially transcribed at a significant level between the insecticide-resistant *A. gossypii* clone (KR) and the insecticide-susceptible clones (NS and MS).

Gene ID[a]	CDS length (bp)	ID of top-hit NCBI-nr protein	Description of top-hit NCBI-nr protein	identity of top-hit (%)	Fold change of expression level				No. of tag counts[b]																
					KR/NS (N)	KR/MS (N)	KR/NS (T)	KR/MS (T)	NS (N)			NS (T)			MS (N)			MS (T)			KR (N)			KR (T)		
									rep1	rep2	rep3	rep1	rep2	rep3	rep1	rep2	rep3	rep1	rep2	rep3	rep1	rep2	rep3	rep1	rep2	rep3
c21228_g1	1542	XP_001948421	PREDICTED: cytochrome P450 6k1-like [Acyrthosiphon pisum]	78.35	46.21	4.35	38.05	3.71	53	10	23	50	23	25	411	374	262	612	542	243	1,166	1,654	943	1,516	1,086	1,521
c21368_g1	1542	XP_008184269	PREDICTED: probable cytochrome P450 6a13 [Acyrthosiphon pisum]	80.39	7.46	3.32	8.22	2.48	221	152	223	186	138	156	815	405	394	694	797	682	1,422	2,003	870	1,975	1,126	1,278
c29523_g2	420	XP_008184269	PREDICTED: probable cytochrome P450 6a13 [Acyrthosiphon pisum]	74.81	5.17	2.11	1.19	0.56	52	29	29	86	26	57	126	135	51	219	231	51	312	78	210	81	84	61
c22273_g1	1533	XP_001946384	PREDICTED: probable cytochrome P450 6a13 [Acyrthosiphon pisum]	91.59	3.68	9.06	1.21	1.99	161	153	168	83	50	79	80	72	77	61	62	52	598	429	752	65	119	99
c26291_g2	1536	XP_001952450	PREDICTED: probable cytochrome P450 6a13 [Acyrthosiphon pisum]	76.45	3.01	19.84	2.99	1.99	2,111	2,289	2,422	134	79	94	332	312	555	219	223	191	7,763	4,927	8,128	312	340	363
c26291_g1	1518	XP_001952450	PREDICTED: probable cytochrome P450 6a13 [Acyrthosiphon pisum]	81.98	2.66	45.25	1.93	1.88	465	384	546	52	27	29	44	28	26	55	78	21	1,727	341	1,842	67	71	92
c4974_g1	1533	XP_008188450	PREDICTED: uncharacterized protein LOC100168454 [Acyrthosiphon pisum]	88.34	2.43	3.94	5.39	1.84	478	407	484	153	112	95	502	218	296	629	476	352	1,188	1,158	943	768	729	663
c27644_g1	1554	XP_001947920	PREDICTED: cytochrome P450 6a2-like [Acyrthosiphon pisum]	74.81	1.59	4.26	3.43	0.83	785	699	974	113	56	72	490	413	189	622	665	112	1,495	1,015	1,447	310	255	347
c23819_g1	288	XP_001951034	PREDICTED: cytochrome P450 4C1-like [Acyrthosiphon pisum]	78.12	0.48	0.79	3.18	3.16	5	5	2	6	2	3	6	2	1	5	2	8	7	0	0	8	24	8

[a] The amino acid sequence identities of each gene compared with *Acyrthosiphon pisum* P450 sequences acquired from the NCBI-nr protein sequence database are shown. b)(N), without acetamiprid treatment; (T), with acetamiprid treatment (0.08 ppm for the susceptible clones and 0.5 ppm for the resistant clone).

Red cells indicate statistically significant differential upregulation (FDR < 0.05 and fold change ≥2) between the two clones. The values of FDR and the fold changes of expression levels were calculated using the iDEGES/edgeR method with tag counts (mapped paired-end reads) of two groups of RNA-seq data. The numbers of tag counts (mapped paired-end reads) for each P450 gene are shown for three biological replicates (rep1, rep2, and rep3) of each clone treated with or without acetamiprid. Accession numbers and database sequence identifiers are as follows: c21228_g1 (LC223821), c21368_g1 (LC223822), c29523_g2 (LC223823), c22273_g1 (LC223824), c26291_g2 (LC223825), c26291_g1 (LC223826), c4974_g1 (LC223827), c27644_g1 (LC223828), and c23819_g1 (LC223829).

A. gossypii *P450 expression and CYP6-mediated metabolism*

The expression levels of CYP6CY22 (c21228_g1) and CYP6CY13 (c21368_g1) were highly upregulated in the insecticide-resistant KR clone as compared with their levels in the insecticide-susceptible NS and MS clones (Table 4-3). We, therefore, attempted to express these two P450 genes using a *Drosophila* expression system to assess their metabolic activities. CYP6CY22 (c21228_g1) and CYP6A13 (c21368_g1) expression was detected in cells incubated in CYP expression medium 48 hr after transfection (Figure 4-1); however, they were weakly expressed in normal medium (SDM containing 10% FBS) (Figure 4-1).

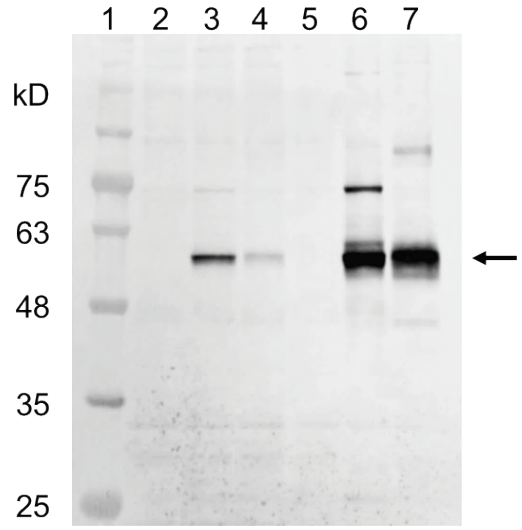

Figure 4-1. Expression of *A. gossypii* CYP6CY22 and CYP6CY13 genes in transfected *D. melanogaster* S2 cells. Lane 1 = molecular weight standards. Lanes 2 and 5 = negative control, cells transfected only with the pAc5.1 vector without inserted genes. Lanes 3 and 4 = cells transfected with c21228_g1 and c21368_g1 genes and cultured in normal medium (Schneider's *Drosophila* Medium with 10% FBS). Lanes 6 and 7 = cells transfected with c21228_g1 and c21368_g1 genes (59 kDa) and cultured in CYP expression medium (Insectagro DS2 medium supplemented with 0.1 mM ferric citrate, 0.1 mM 5-aminolevulinic acid, and 4 mM Ala-Glu without FBS).

All neonicotinoid insecticides were almost completely recovered after they were incubated with untransfected *D. melanogaster* S2 cells (Table 4-4). However, when acetamiprid or imidacloprid was incubated with *D. melanogaster* S2 cells expressing CYP6CY22 (c21228_g1), little of the parent compound was recovered. In contrast, moderate amounts of the parent compounds were recovered from cultures of the CYP6CY13 (c21368_g1) transfectant. LC-MS analyses of *D. melanogaster* S2 cell extracts showed that acetamiprid was converted to *N*-desmethyl acetamiprid (Figure 4-2A–C), and imidacloprid was converted to a hydroxylated metabolite (Figure 4-2C). LC-MS analyses identified acetamiprid and its main metabolite *N*-desmethyl acetamiprid (Figure 4-2A, B). The retention times and m/z values of the components detected were consistent with those of the reference substance. Recoveries of thiacloprid, clothianidin, thiamethoxam, nitenpyram, and dinotefuran from cultures of cells expressing CYP6CY22 (c21228_g1) were 8.5%, 55.2%, 42.8%, 69.3%, and 55.8%, respectively (Table 4-4). Recoveries of thiacloprid, clothianidin, thiamethoxam, nitenpyram, and dinotefuran from cultures of cells expressing CYP6CY13 (c21368_g1) were 32.8%, 74.5%, 69.3%, 77.1%, and 51.2%, respectively (Table 4-4). In contrast, sulfoxaflor was almost completely recovered from cultures of cells expressing CYP6CY22 (c21228_g1) or CYP6CY13 (c21368_g1). Lower and higher concentrations of the insecticides and their metabolites, respectively, were detected in cultures of *D. melanogaster* S2 cells that expressed CYP6CY22 (c21228_g1) vs. CYP6CY13 (c21368_g1) (Table 4-4).

Table 4-4. Metabolism of test compounds by *D. melanogaster* S2 cells expressing CYP6CY22(c21228_g1) and CYP6CY13 (c21368_g1) genes.

	c21228_g1 (CYP6CY22)			c21368_g1 (CYP6CY13)				
	%Recovery (avg. ± S.D.)[a)]		%Metab.	%Recovery (avg. ± S.D.)[a)]		%Metab.	RF1[b)]	RF2[c)]
	Control	+transfection		Control	+transfection			
Acetamiprid	102.2 ± 0.2	26.0 ± 0.1	84.0	99.5 ± 1.0	38.8 ± 1.0	61.2	65.4	104
Thiacloprid	99.8 ± 0.7	8.5 ± 0.7	91.5	95.6 ± 0.3	32.8 ± 0.8	67.2	23.8	17
Sulfoxaflor	99.6 ± 0.6	95.6 ± 0.6	4.4	101.2 ± 1.9	98.3 ± 2.8	1.7	22.6	
Imidacloprid	101.5 ± 0.4	7.5 ± 0.4	92.5	98.5 ± 1.2	60.0 ± 1.0	40.0	216	253
Clothianidin	98.2 ± 1.5	55.2 ± 3.0	44.8	96.5 ± 0.4	74.5± 1.1	25.5	394	687
Thiamethoxam	95.6 ± 1.1	42.8 ± 1.3	57.2	98.2 ± 0.2	69.3 ± 0.3	30.7	295	246
Nitenpyrum	97.5 ± 1.2	69.3 ± 1.0	30.7	96.5 ± 1.3	77.1 ± 2.3	22.9	253	43
Dinotefuran	103.4 ± 1.2	55.8 ± 5.9	44.2	101.3 ± 2.1	51.2 ± 7.5	48.8	237	199

[a)]% Recovery 72 hr after incubation compared with time 0. Data represent the mean ± SD (n = 3).

[b)]Resistance factor (LC_{50} MK clone/LC_{50} NS clone). The resistance factor of sulfoxaflor was determined by method described previously (Hirata et al., 2015).

[c)]Resistance factor (LC_{50} MK clone/LC_{50} MS clone) (Matsuura and Nakamura, 2014).

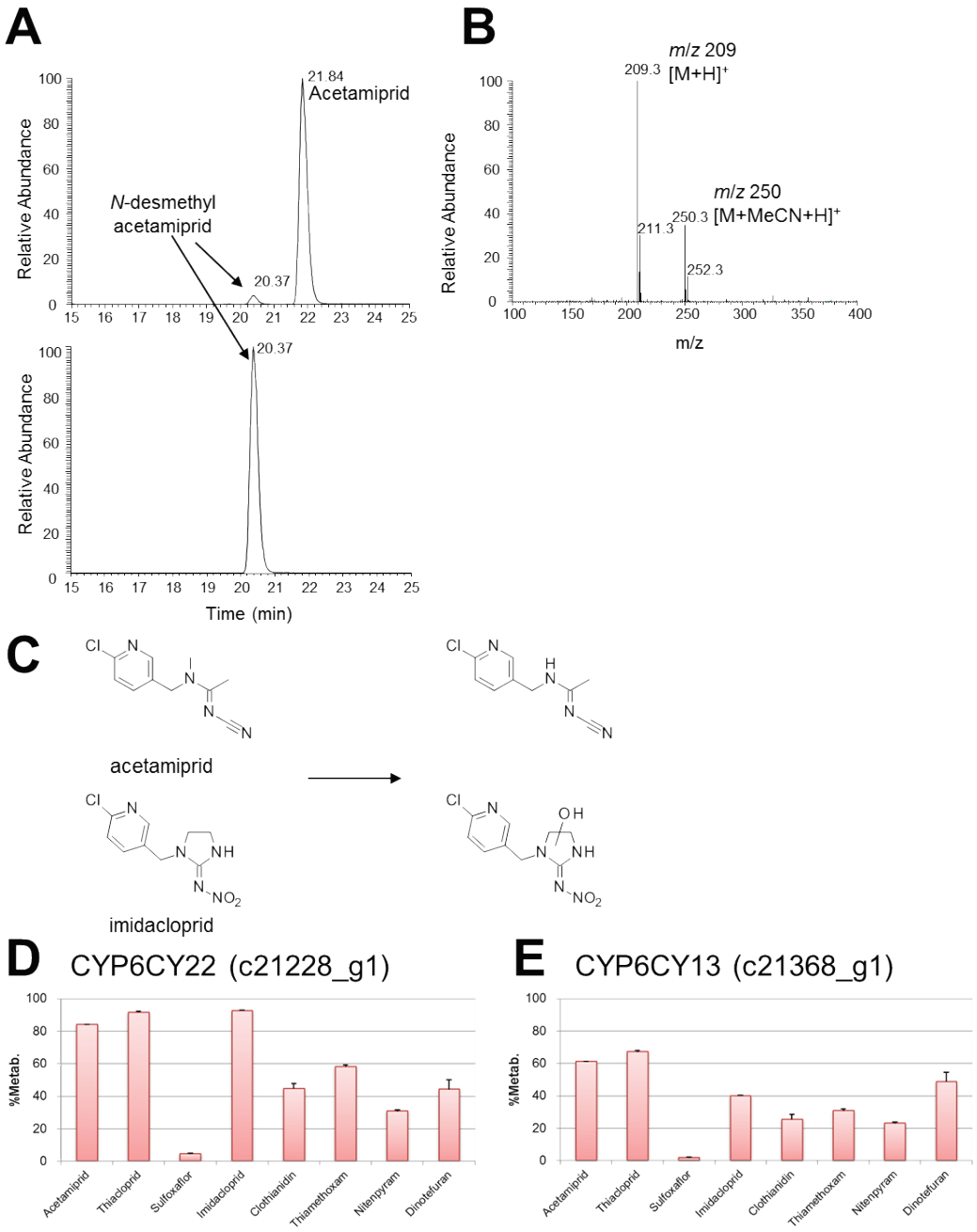

Figure 4-2. ESI-LC-MS spectra of acetamiprid and imidacloprid, structures of the metabolites, and percentages of metabolites. (A) LC elution profile of acetamiprid in extracts of *D. melanogaster* S2 cells expressing the c21228_g1 gene (12 hr after test compound was added). (B) LC-MS spectrum of acetamiprid in an extract of *D. melanogaster* S2 cells expressing the c21368_g1 gene. (C) Structures of the metabolites of acetamiprid and imidacloprid. (D) Metabolism of test compounds in cultures of cells expressing the c21228_g1 gene. (E) Metabolism of test compounds in cultures of cells expressing the c21368_g1 gene. Data are the mean ± SD (n = 3)

Discussion

In the present study, we performed RNA-seq analysis and NGS to identify P450 genes involved in the metabolism of neonicotinoid insecticides by *A. gossypii*. The author identified nine upregulated cytochrome P450 genes that were expressed at significantly higher levels by the insecticide-resistant KR clone as compared with those of insecticide-susceptible clones (Table 4-3). Genes encoding detoxification enzymes such as GST and COE were not similarly upregulated. Moreover, we established an *A. gossypii* P450 expression method in the S2 insect cell expression system to generate functionally active P450 by improving transient expression methods. This approach will enable the generation of ample quantities of insect P450 for insecticide resistance studies and structural analysis of metabolites of insecticides.

The P450 genes c21228_g1 and c21368_g1 were highly upregulated in the KR clone in the presence or absence of acetamiprid, as compared with the levels of upregulation in the insecticide-susceptible clones NS and MS (Table 4-3). The sequences of the c21228_g1 and c21368_g1 genes are similar to those of the *A. gossypii* genes encoding CYP6CY22 and CYP6CY13, respectively. Numerous P450s catalyze a highly restricted set of reactions, although some metabolize diverse compounds. In insects, members of the CYP4, -6, -9, and -12 families are implicated in biological detoxifying functions in the environment, and members of the CYP4 and CYP6 subfamilies are most commonly involved in the metabolism of and resistance to xenobiotics (Berenbaum, 2002; Li et al., 2007).

The CYP6CY22 (c21228_g1) gene was overexpressed 46-fold in the KR clone, as compared with the NS clone, and 4-fold, as compared with the MS clone when

aphids were treated without acetamiprid. Similarly, the CYP6CY13 (c21368_g1) gene was expressed at a 7-fold higher level by the KR clone vs. the NS clone and a 3-fold higher level by the KR clone vs. the MS clone under the same conditions. The findings were similar for acetamiprid treatment. The levels of the two P450 genes expressed by the KR clone were significantly increased as compared with those of the NS clone. P450 genes were not upregulated in the KR clone in the presence or absence of acetamiprid, indicating constitutive upregulation, as compared with the insecticide-susceptible clones.

The NS clone has been maintained at the Odawara Research Center without insecticide selection since 1993. In contrast, the levels of the two P450 genes expressed by the KR clone were moderately increased as compared with those of the insecticide-susceptible MS clone, and the levels of the latter were higher as compared with those of the NS clone. The MS clone was collected in a field in Miyazaki Prefecture, Japan, and is likely to have been exposed to more insecticides, as compared with the NS clone. This may explain the difference in expression levels between the two insecticide-susceptible clones, as insecticide exposure likely induced the expression of P450 genes (Markussen and Kristensen, 2010). Furthermore, differences in expression levels between these two insecticide-susceptible clones are explained by the exchange of host plants (Li et al., 2002; Scott et al., 1998). However, although the expression levels of the two P450 genes of the two susceptible strains were significantly different, the resistance factors (LC_{50} resistant clone/LC_{50} susceptible clone) for neonicotinoid insecticides of the KR/NS clones are similar to those of the KR/MS clones (Hirata et al., 2015; Matsuura and Nakamura, 2014).

The contribution of P450-mediated detoxification to metabolism is indicated by

the use of piperonyl butoxide (PBO), an inhibitor of metabolic enzymes, including P450s. Further, PBO pretreatment reduces the LC_{50} values of neonicotinoid insecticides, and the synergistic factors of acetamiprid and imidacloprid = 3.6 and 6.0, respectively (Hirata et al., 2015). Furthermore, the two *A. gossypii* P450 genes metabolize neonicotinoid insecticides (Figure 4-2, Table 4-4). These findings suggest that these P450s affect neonicotinoid resistance.

The neonicotinoids examined here were metabolized to varying degrees by *D. melanogaster* S2 cells expressing *A. gossypii* CYP6CY22 (c21228_g1) and CYP6CY13 (c21368_g1) (Table 4-4, Figure 4-2D, E). Under the conditions applied here, acetamiprid, thiacloprid, and imidacloprid were more extensively metabolized than the other neonicotinoids (Table 4-4, Figure 4-2), which is consistent with the findings of a previous study (*D. melanogaster* CYP6G1) (Sparks et al., 2012). However, these results differ from those observed for the monooxygenase CYP6CM1vQ, which is associated with the imidacloprid resistance of *B. tabaci* (Roditakis et al., 2011).

Imidacloprid, thiacloprid, and clothianidin are metabolized by CYP6CM1vQ, but not acetamiprid and thiamethoxam (Roditakis et al., 2011). In the present study, all compounds were metabolized, although sulfoxaflor was a poor substrate for *A. gossypii* CYP6CY22 and CYP6CY13 (Table 4-4, Figure 4-2D, E), which is consistent with results obtained for *D. melanogaster* CYP6G1 (Sparks et al., 2012). Furthermore, CYP6G1 metabolizes structurally diverse insecticides such as DDT, malathion, and pyrethroids (Jones et al., 2010). Thus, *A. gossypii* CYP6CY22 and CYP6CY13 may have broader substrate specificities. The incubation of *D. melanogaster* S2 cells expressing *A. gossypii* CYP6CY22 or CYP6CY13 with acetamiprid and imidacloprid produced a metabolite with a hydroxyl group on the imidazolidine ring and

N-desmethyl acetamiprid, respectively (Figure 4-2A–C) (Brunet et al., 2005; Nauen et al., 1999; Nishiwaki et al., 2004). Hydroxylation and *N*-dealkylation are likely the key reactions catalyzed by *A. gossypii* CYP6CY22 and CYP6CY13, respectively.

In conclusion, The author used RNA-seq to identify nine differentially upregulated P450 genes involved in the metabolism of neonicotinoids by the *A. gossypii* KR clone. Among them, genes encoding CYP6CY22 and CYP6CY13 were the most highly upregulated. Furthermore, we constructed *A. gossypii* CYP6CY22 and CYP6CY13 expression vectors and used them to transfect an insect cell line to study P450-mediated insecticide metabolism, although it was difficult to determine the catalytic constants (e.g., K_m and K_{cat}) of these recombinant P450s. Moreover, we did not determine the P450 activities of microsomal membrane fractions. Nevertheless, these findings contribute compelling evidence that these P450s may contribute to aphids' resistance to neonicotinoids in the future.

Summary

In this study, the author investigated the mechanism of action of the compound that acts on Vssc and nAChR, and the associated mechanism of resistance, mainly using an electrophysiological method.

The voltage-sensitive sodium (Na^+) channel (Vssc) is the target site of pyrethroid insecticides. Pest insects develop resistance to this class of insecticide by acquisition of one or multiple amino acid substitution (s) in this channel. In Southeast Asia, two major Vssc types confer pyrethroid resistance in the dengue mosquito vector *Aedes aegypti*, namely, S989P+V1016G and F1534C. The author expressed several types of Vssc in *Xenopus* oocytes and examined the effect of amino acid substitutions in Vssc on pyrethroid susceptibilities. S989P+V1016G and F1534C haplotypes reduced the channel sensitivity to permethrin by 100- and 25-fold, respectively, while S989P+V1016G+F1534C triple mutations reduced the channel sensitivity to permethrin by 1100-fold. S989P+V1016G and F1534C haplotypes reduced the channel sensitivity to deltamethrin by 10- and 1-fold (no reduction), respectively, but S989P+V1016G+F1534C triple mutations reduced the channel sensitivity to deltamethrin by 90-fold. These results imply that pyrethroid insecticides are highly likely to lose their effectiveness against *A. aegypti* if such a Vssc haplotype emerges as the result of a single crossing-over event; thus, this may cause failure to control this key mosquito vector.

The *Aphis gossypii* clone, Kushima, which was first discovered in Miyazaki Prefecture, Japan, exhibits significant resistance to neonicotinoid insecticides. The author investigated the resistance mechanism involved by sequencing the nicotinic

acetylcholine receptor (nAChR) gene, by electrophysiological analysis, and by insecticidal tests in the presence or absence of the oxidase inhibitor, piperonyl butoxide. The Kushima clone showed higher resistance to nitro-substituted neonicotinoids, such as imidacloprid, than to cyano-substituted neonicotinoids, such as acetamiprid. Sequencing of the nAChR subunit genes of a susceptible clone and the Kushima clone revealed an R81T mutation in loop D of the β1 subunit in the resistant clone. This mutation led to a significant shift in the pEC_{50} value of imidacloprid for the *Drosophila melanogaster* Dα2-chicken β2 subunit, while it barely affected the concentration-response curves of acetylcholine and acetamiprid.

Neonicotinoid insecticides and sulfoxaflor have generally shown excellent control of *A. gossypii*, but these aphids have recently developed resistance against neonicotinoid insecticides. The Kushima clone harbors the R81T mutation in the nicotinic acetylcholine receptor (nAChR) β1 subunit; this mutation is the source of neonicotinoid insecticide resistance. In the chapter 3, electrophysiological analyses and molecular modeling were employed to investigate the differential effects of the R81T mutation on cyano- and nitro-substituted neonicotinoids and sulfoxaflor. The author isolated full-length coding sequences of *A. gossypii* nAChR α1, α2, and β1 subunits. When co-expressed in *Xenopus laevis* oocytes with chicken β2 nAChR, A. gossypii α1 evoked inward currents in a concentration-dependent manner in response to acetylcholine (ACh) and showed sensitivity to neonicotinoid and sulfoxaflor. Additionally, the chicken β2 T77R+E79V (equivalent double mutant of R81T) mutation resulted in a lower effect to cyano-substituted neonicotinoids and sulfoxaflor than to nitro-substituted neonicotinoids. Electrophysiological data and nAChR homology modeling analysis suggested that the Kushima clone exhibited different levels of resistance to cyano- and

nitro-substituted neonicotinoid insecticides.

The Kushima clone was resistant to neonicotinoid insecticides (23.8- to 394-fold). RNA-seq and next-generation sequence analyses were conducted to identify nine cytochrome P450 (CYP) genes that were significantly upregulated in the Kushima clone as compared with those in the insecticide-susceptible clone. *A. gossypii* P450s were transiently and efficiently expressed in S2 cell to show that CYP6CY22 (c21228) and CYP6CY13 (c21368), which were the most upregulated of the nine P450s in the Kushima clone, did not degrade sulfoxaflor, a new class of insecticides acting on insect nAChRs, but markedly metabolized all of the neonicotinoids tested. Hence, P450s are likely to underpin neonicotinoid resistance in other aphids as well in the future, and the P450 expression protocol established here will prompt studies on P450-medidated insecticide resistance and structural analyses of relevant metabolites. These findings contribute compelling evidence that these P450s may contribute to aphids' resistance to neonicotinoids in the future.

In the present study, the mechanism of resistance to pyrethroids in *A. aegypti*, that to neonicotinoids in *A. gossypii* were clarified. We also demonstrated that similar compounds that interacted on the same target with slightly different substituents exhibited different effects on the target molecule with different amino acid residues at the activity site of insect ion channels. The author believe that the findings of studies on the mechanisms of action of neurotoxic insecticides and resistance to them will contribute to the research and development of new insecticides, including ones effective against insecticide-resistant insects, and to the establishment of appropriate and effective measures for avoiding resistance.

Reference

World Population Prospects 2015 – Data Booklet (ST/EST/SER.A/377). Population Divisions, Department of Economic and Social Affairs, United Nations, New York, NY (2015).

Amichot, M., Tarès, S., Brun-Barale, A., Arthaud, L., Bride, J.-M., Bergé, J.-B., 2004a. Point mutations associated with insecticide resistance in the *Drosophila* cytochrome P450 *Cyp6a2* enable DDT metabolism. *European Journal of Biochemistry* **271**, 1250-1257.

Aponte, H.A., Penilla, R.P., Dzul-Manzanilla, F., Che-Mendoza, A., López, A.D., Solis, F., Manrique-Saide, P., Ranson, H., Lenhart, A., McCall, P.J., Rodríguez, A.D., 2013. The pyrethroid resistance status and mechanisms in *Aedes aegypti* from the Guerrero state, Mexico. *Pesticide Biochemistry and Physiology* **107**, 226-234.

Bai, D., Lummis, S.C.R., Leicht, W., Breer, H., Sattelle, D.B., 1991. Actions of imidacloprid and a related nitromethylene on cholinergic receptors of an identified insect motor neurone. *Pesticide Science* **33**, 197-204.

Bass, C., Puinean, A.M., Andrews, M., Cutler, P., Daniels, M., Elias, J., Paul, V.L., Crossthwaite, A.J., Denholm, I., Field, L.M., Foster, S.P., Lind, R., Williamson, M.S., Slater, R., 2011. Mutation of a nicotinic acetylcholine receptor beta subunit is associated with resistance to neonicotinoid insecticides in the aphid *Myzus persicae*. *BMC Neuroscience* **12**, 51.

Bass, C., Puinean, A.M., Zimmer, C.T., Denholm, I., Field, L.M., Foster, S.P., Gutbrod, O., Nauen, R., Slater, R., Williamson, M.S., 2014. The evolution of insecticide resistance in the peach potato aphid, *Myzus persicae*. *Insect Biochemistry and Insect Molecular Biology* **51**, 41-51.

Berenbaum, M.R., 2002. Postgenomic Chemical Ecology: From genetic code to ecological interactions. *Journal of Chemical Ecology* **28**, 873-896.

Bergé, J., Feyereisen, R., Amichot, M., 1998. Cytochrome P450 monooxygenases and insecticide resistance in insects. Philosophical Transactions of the Royal Society of London. Series B: *Biological Sciences* **353**, 1701-1705.

Bezanilla, F., Armstrong, C.M., 1977. Inactivation of the sodium channel. I. Sodium current experiments. *The Journal of General Physiology* **70**, 549-566.

Bloomquist, J.R., 1996. Ion channels as targets for insecticides. *Annual Review of Entomology* **41**, 163-190.

Bogwitz, M.R., Chung, H., Magoc, L., Rigby, S., Wong, W., O'Keefe, M., McKenzie, J.A., Batterham, P., Daborn, P.J., 2005. *Cyp12a4* confers lufenuron resistance in a natural population of *Drosophila melanogaster*. *Proceedings of the National Academy of Sciences of the United States of America* **102**, 12807-12812.

Bolger, A.M., Lohse, M., Usadel, B., 2014. Trimmomatic: a flexible trimmer for Illumina sequence data. *Bioinformatics* **30**, 2114-2120.

Brown, L.A., Ihara, M., Buckingham, S.D., Matsuda, K., Sattelle, D.B., 2006. Neonicotinoid insecticides display partial and super agonist actions on native insect nicotinic acetylcholine receptors. *Journal of Neurochemistry* **99**, 608-615.

Brunet, J.-L., Badiou, A., Belzunces, L.P., 2005. *In vivo* metabolic fate of [^{14}C]-acetamiprid in six biological compartments of the honeybee, *Apis mellifera L*. *Pest Management Science* **61**, 742-748.

Burton, M.J., Mellor, I.R., Duce, I.R., Davies, T.G., Field, L.M., Williamson, M.S., 2011. Differential resistance of insect sodium channels with *kdr* mutations to deltamethrin, permethrin and DDT. *Insect Biochemistry and Insect Molecular Biology* **41**, 723-732.

Casida, J.E., Durkin, K.A., 2013. Neuroactive insecticides: targets, selectivity, resistance, and secondary effects. *Annual Review of Entomology* **58**, 99-117.

Changeux, J.-P., 2012. The nicotinic acetylcholine receptor: the founding father of the pentameric ligand-gated ion channel superfamily. *Journal of Biological Chemistry* **287**, 40207-40215.

Corringer, P.J., Le Novere, N., Changeux, J.P., 2000. Nicotinic receptors at the amino acid level. *The Annual Review of Pharmacology and Toxicology* **40**, 431-458.

Davies, T.G., Field, L.M., Usherwood, P.N., Williamson, M.S., 2007. DDT, pyrethrins, pyrethroids and insect sodium channels. *IUBMB Life* **59**, 151-162.

Du, Y., Nomura, Y., Luo, N., Liu, Z., Lee, J.E., Khambay, B., Dong, K., 2009. Molecular determinants on the insect sodium channel for the specific action of type II pyrethroid insecticides. *Toxicology and Applied Pharmacology* **234**, 266-272.

Du, Y., Nomura, Y., Satar, G., Hu, Z., Nauen, R., He, S.Y., Zhorov, B.S., Dong, K., 2013. Molecular evidence for dual pyrethroid-receptor sites on a mosquito sodium channel. *Proceedings of the National Academy of Sciences of the United States of America* **110**, 11785-11790.

Eddy, S.R., 2011. Accelerated Profile HMM Searches. *PLoS computational biology* **7**, e1002195.

Elbert, A., Haas, M., Springer, B., Thielert, W., Nauen, R., 2008. Applied aspects of neonicotinoid uses in crop protection. *Pest Management Science* **64**, 1099-1105.

Elbert, A., Nauen, R., 2000. Resistance of *Bemisia tabaci* (Homoptera: Aleyrodidae) to insecticides in southern Spain with special reference to neonicotinoids. *Pest Management Science* **56**, 60-64.

Feng, G., Deak, P., Chopra, M., Hall, L.M., 1995. Cloning and functional analysis of tipE, a novel membrane protein that enhances *drosophila* para sodium channel function. *Cell* **82**, 1001-1011.

Feyereisen, R., Koener, J.F., Farnsworth, D.E., Nebert, D.W., 1989. Isolation and sequence of cDNA encoding a cytochrome P-450 from an insecticide-resistant strain of the house fly, *Musca domestica*. *Proceedings of the National Academy of Sciences* **86**, 1465-1469.

Gammon, D.W., Brown, M.A., Casida, J.E., 1981. Two classes of pyrethroid action in the cockroach. *Pesticide Biochemistry and Physiology* **15**, 181-191.

Gao, J.-R., Yoon, K.S., Lee, S.H., Takano-Lee, M., Edman, J.D., Meinking, T.L., Taplin, D., Clark, J.M., 2003. Increased frequency of the T929I and L932F mutations associated with knockdown resistance in permethrin-resistant populations of the human head louse, *Pediculus capitis*, from California, Florida, and Texas. *Pesticide Biochemistry and Physiology* **77**, 115-124.

Gorman, K., Devine, G., Bennison, J., Coussons, P., Punchard, N., Denholm, I., 2007. Report of resistance to the neonicotinoid insecticide imidacloprid in *Trialeurodes*

vaporariorum (Hemiptera: Aleyrodidae). *Pest Management Science* **63**, 555-558.

Grabherr, M.G., Haas, B.J., Yassour, M., Levin, J.Z., Thompson, D.A., Amit, I., Adiconis, X., Fan, L., Raychowdhury, R., Zeng, Q., Chen, Z., Mauceli, E., Hacohen, N., Gnirke, A., Rhind, N., di Palma, F., Birren, B.W., Nusbaum, C., Lindblad-Toh, K., Friedman, N., Regev, A., 2011. Full-length transcriptome assembly from RNA-Seq data without a reference genome. *Nature Biotechnology* **29**, 644-652.

Grutter, T., Changeux, J.-P., 2001. Nicotinic receptors in wonderland. *Trends in Biochemical Science*s **26**, 459-463.

Gubler, D.J., 1998. Dengue and dengue hemorrhagic fever. *Clinical Microbiology Reviews* **11**, 480-496.

Harris, A.F., Rajatileka, S., Ranson, H., 2010. Pyrethroid resistance in *Aedes aegypti* from Grand Cayman. *The American Journal of Tropical Medicine and Hygiene* **83**, 277-284.

Hemingway, J., Hawkes, N.J., McCarroll, L., Ranson, H., 2004. The molecular basis of insecticide resistance in mosquitoes. *Insect Biochemistry and Molecular Biology* **34**, 653-665.

Hirata, K., Jouraku, A., Kuwazaki, S., Shimomura, H., Iwasa, T., 2017. Studies on *Aphis gossypii* cytochrome P450s CYP6CY22 and CYP6CY13 using an *in vitro* system. *Journal of Pesticide Science* **42**, 97-104.

Hirata, K., Kiyota, R., Matsuura, A., Toda, S., Yamamoto, A., Iwasa, T., 2015. Association between the R81T mutation in the nicotinic acetylcholine receptor β1 subunit of *Aphis gossypii* and the differential resistance to acetamiprid and imidacloprid. *Journal of Pesticide Science* **40**, 25-31.

Ho, S.N., Hunt, H.D., Horton, R.M., Pullen, J.K., Pease, L.R., 1989. Site-directed mutagenesis by overlap extension using the polymerase chain reaction. *Gene* **77**, 51-59.

Hu, Z., Du, Y., Nomura, Y., Dong, K., 2011. A sodium channel mutation identified in *Aedes aegypti* selectively reduces cockroach sodium channel sensitivity to type I, but not type II pyrethroids. *Insect Biochemistry and Molecular Biology* **41**, 9-13.

Huang, J., Kristensen, M., Qiao, C.L., Jespersen, J.B., 2004. Frequency of *kdr* gene in

house fly field populations: correlation of pyrethroid resistance and kdr frequency. *Journal of Economic Entomology* **97**, 1036-1041.

Hurst, R., Rollema, H., Bertrand, D., 2013. Nicotinic acetylcholine receptors: From basic science to therapeutics. *Pharmacology & Therapeutics* **137**, 22-54.

Ihara, M., Brown, L.A., Ishida, C., Okuda, H., Sattelle, D.B., Matsuda, K., 2006. Actions of imidacloprid, clothianidin and related neonicotinoids on nicotinic acetylcholine receptors of american cockroach neurons and their relationships with insecticidal potency. *Journal of Pesticide Science* **31**, 35-40.

Ihara, M., Matsuda, K., Otake, M., Kuwamura, M., Shimomura, M., Komai, K., Akamatsu, M., Raymond, V., Sattelle, D.B., 2003. Diverse actions of neonicotinoids on chicken α7, α4β2 and *Drosophila*–chicken SADβ2 and ALSβ2 hybrid nicotinic acetylcholine receptors expressed in *Xenopus laevis* oocytes. *Neuropharmacology* **45**, 133-144.

Ihara, M., Matsuda, K., Shimomura, M., Sattelle, D.B., Komai, K., 2004. Super agonist actions of clothianidin and related compounds on the SADβ2 nicotinic acetylcholine receptor expressed in *Xenopus laevis* oocytes. *Bioscience, Biotechnology, and Biochemistry* **68**, 761-763.

Ihara, M., Okajima, T., Yamashita, A., Oda, T., Asano, T., Matsui, M., Sattelle, D.B., Matsuda, K., 2014a. Studies on an acetylcholine binding protein identify a basic residue in loop G on the β1 strand as a new structural determinant of neonicotinoid actions. *Molecular Pharmacology* **86**, 736-746.

Ihara, M., Okajima, T., Yamashita, A., Oda, T., Hirata, K., Nishiwaki, H., Morimoto, T., Akamatsu, M., Ashikawa, Y., Kuroda, S., Mega, R., Kuramitsu, S., Sattelle, D.B., Matsuda, K., 2008. Crystal structures of *Lymnaea stagnalis* AChBP in complex with neonicotinoid insecticides imidacloprid and clothianidin. *Invertebrate Neuroscience* **8**, 71-81.

Jeschke, P., Nauen, R., 2008. Neonicotinoids—from zero to hero in insecticide chemistry. *Pest Management Science* **64**, 1084-1098.

Jones, R.T., Bakker, S.E., Stone, D., Shuttleworth, S.N., Boundy, S., McCart, C., Daborn, P.J., ffrench-Constant, R.H., van den Elsen, J.M.H., 2010. Homology modelling

of *Drosophila* cytochrome P450 enzymes associated with insecticide resistance. *Pest Management Science* **66**, 1106-1115.

Kagabu, S., Nishiwaki, H., Sato, K., Hibi, M., Yamaoka, N., Nakagawa, Y., 2002. Nicotinic acetylcholine receptor binding of imidacloprid-related diaza compounds with various ring sizes and their insecticidal activity against *Musca domestica*. *Pest Management Science* **58**, 483-490.

Kao, P.N., Dwork, A.J., Kaldany, R.R., Silver, M.L., Wideman, J., Stein, S., Karlin, A., 1984. Identification of the alpha subunit half-cystine specifically labeled by an affinity reagent for the acetylcholine receptor binding site. *Journal of Biological Chemistry* **259**, 11662-11665.

Karlin, A., 2002. Emerging structure of the nicotinic acetylcholine receptors. *Nature Reviews Neuroscience* **3**, 102-114.

Kasai, S., Komagata, O., Itokawa, K., Shono, T., Ng, L.C., Kobayashi, M., Tomita, T., 2014. Mechanisms of pyrethroid resistance in the dengue mosquito vector, *Aedes aegypti*: target site insensitivity, penetration, and metabolism. *PLOS Neglected Tropical Diseases* **8**, e2948.

Kasai, S., Ng, L.C., Lam-Phua, S.G., Tang, C.S., Itokawa, K., Komagata, O., Kobayashi, M., Tomita, T., 2011. First detection of a putative knockdown resistance gene in major mosquito vector, *Aedes albopictus*. *Japanese journal of infectious diseases* **64**, 217-221.

Kasai, S., Weerashinghe, I.S., Shono, T., 1998. P 450 monooxygenases are an important mechanism of permethrin resistance in *Culex quinquefasciatus* say larvae. *Archives of insect biochemistry and physiology* **37**, 47-56.

Kawada, H., Higa, Y., Komagata, O., Kasai, S., Tomita, T., Yen, N.T., Loan, L.L., Sánchez, R.A.P., Takagi, M., 2009. Widespread distribution of a newly found point mutation in the voltage-gated sodium channel in pyrethroid-resistant *Aedes aegypti* populations in Vietnam. *PLOS Neglected Tropical Diseases* **3**.

Kusano, K., Miledi, R., Stinnakre, J., 1982. Cholinergic and catecholaminergic receptors in the *Xenopus* oocyte membrane. *The Journal of Physiology* **328**, 143-170.

Lawrence, L.J., Casida, J.E., 1982. Pyrethroid toxicology: Mouse intracerebral structure-toxicity relationships. *Pesticide Biochemistry and Physiology* **18**, 9-14.

Li, X., Berenbaum, M.R., Schuler, M.A., 2002. Plant allelochemicals differentially regulate *Helicoverpa zea* cytochrome P450 genes. *Insect Molecular Biology* **11**, 343-351.

Li, X., Schuler, M.A., Berenbaum, M.R., 2007. Molecular mechanisms of metabolic resistance to synthetic and natural xenobiotics. *Annual Review of Entomology* **52**, 231-253.

Lin, Y.-H., Tsen, W.-L., Tien, N.-Y., Luo, Y.-P., 2013. Biochemical and molecular analyses to determine pyrethroid resistance in *Aedes aegypti*. *Pesticide Biochemistry and Physiology* **107**, 266-276.

Liu, Z., Williamson, M.S., Lansdell, S.J., Denholm, I., Han, Z., Millar, N.S., 2005. A nicotinic acetylcholine receptor mutation conferring target-site resistance to imidacloprid in *Nilaparvata lugens* (brown planthopper). *Proceedings of the National Academy of Sciences of the United States of America* **102**, 8420-8425.

Liu, Z., Williamson, M.S., Lansdell, S.J., Han, Z., Denholm, I., Millar, N.S., 2006. A nicotinic acetylcholine receptor mutation (Y151S) causes reduced agonist potency to a range of neonicotinoid insecticides. *Journal of Neurochemistry* **99**, 1273-1281.

Lyne, P.D., Lamb, M.L., Saeh, J.C., 2006. Accurate prediction of the relative potencies of members of a series of kinase inhibitors using molecular docking and MM-GBSA scoring. *Journal of Medicinal Chemistry* **49**, 4805-4808.

Marcombe, S., Mathieu, R.B., Pocquet, N., Riaz, M.-A., Poupardin, R., Sélior, S., Darriet, F., Reynaud, S., Yébakima, A., Corbel, V., David, J.-P., Chandre, F., 2012. Insecticide resistance in the dengue vector *Aedes aegypti* from martinique: distribution, mechanisms and relations with environmental factors. *PLOS ONE* **7**, e30989.

Markussen, M.D.K., Kristensen, M., 2010. Cytochrome P450 monooxygenase-mediated neonicotinoid resistance in the house fly *Musca domestica L*. *Pesticide Biochemistry and Physiology* **98**, 50-58.

Massova, I., Kollman, P.A., 2000. Combined molecular mechanical and continuum solvent approach (MM-PBSA/GBSA) to predict ligand binding. *Perspectives in Drug Discovery and Design* **18**, 113-135.

Matsuda, K., Buckingham, S.D., Freeman, J.C., Squire, M.D., Baylis, H.A., Sattelle,

D.B., 1998. Effects of the α subunit on imidacloprid sensitivity of recombinant nicotinic acetylcholine receptors. *British Journal of Pharmacology* **123**, 518-524.

Matsuda, K., Buckingham, S.D., Kleier, D., Rauh, J.J., Grauso, M., Sattelle, D.B., 2001. Neonicotinoids: insecticides acting on insect nicotinic acetylcholine receptors. *Trends in Pharmacological Sciences* **22**, 573-580.

Matsuda, K., Kanaoka, S., Akamatsu, M., Sattelle, D.B., 2009. Diverse actions and target-site selectivity of neonicotinoids: structural insights. *Molecular Pharmacology* **76**, 1-10.

Matsuda, K., Shimomura, M., Ihara, M., Akamatsu, M., Sattelle, D.B., 2005. Neonicotinoids show selective and diverse actions on their nicotinic receptor targets: electrophysiology, molecular biology, and receptor modeling studies. *Bioscience, Biotechnology, and Biochemistry* **69**, 1442-1452.

Matsuura, A., Nakamura, M., 2014. Development of neonicotinoid resistance in the cotton aphid *Aphis gossypii* (Hemiptera: Aphididae) in Japan. *Applied Entomology and Zoology* **49**, 535-540.

Millar, N.S., Denholm, I., 2007. Nicotinic acetylcholine receptors: targets for commercially important insecticides. *Invertebrate Neuroscience* **7**, 53-66.

Narahashi, T., 1986. Toxins that modulate the sodium channel gating mechanisma. *Annals of the New York Academy of Sciences* **479**, 133-151.

Narahashi, T., 1996. Neuronal ion channels as the target sites of insecticides. *Pharmacology & Toxicology* **79**, 1-14.

Narahashi, T., 2000. Neuroreceptors and ion channels as the basis for drug action: past, present, and future. *Journal of Pharmacology and Experimental Therapeutics* **294**, 1-26.

Nauen, R., Denholm, I., 2005. Resistance of insect pests to neonicotinoid insecticides: current status and future prospects. *Archives of Insect Biochemistry and Physiology* **58**, 200-215.

Nauen, R., Denholm, I., Dennehy, T., Nichols, R., 2008. News from the front line: reports from the global workshop on the stewardship of neonicotinoid insecticides,

Honolulu, Hawaii, 5-6 June 2008. *Pest Management Science* **64**, 1082-1083.

Nauen, R., Reckmann, U., Armborst, S., Stupp, H.-P., Elbert, A., 1999. Whitefly-active metabolites of imidacloprid: biological efficacy and translocation in cotton plants. *Pesticide Science* **55**, 265-271.

Nikou, D., Ranson, H., Hemingway, J., 2003. An adult-specific CYP6 P450 gene is overexpressed in a pyrethroid-resistant strain of the malaria vector, *Anopheles gambiae*. *Gene* **318**, 91-102.

Nishiwaki, H., Nakagawa, Y., Kuwamura, M., Sato, K., Akamatsu, M., Matsuda, K., Komai, K., Miyagawa, H., 2003. Correlations of the electrophysiological activity of neonicotinoids with their binding and insecticidal activities. *Pest Management Science* **59**, 1023-1030.

Nishiwaki, H., Sato, K., Nakagawa, Y., Miyashita, M., Miyagawa, H., 2004. Metabolism of imidacloprid in houseflies. *Journal of Pesticide Science* **29**, 110-116.

Pridgeon, J.W., Liu, N., 2003. Overexpression of the cytochrome c oxidase subunit I gene associated with a pyrethroid resistant strain of German cockroaches, *Blattella germanica* (*L*.). *Insect Biochemistry and Molecular Biology* **33**, 1043-1048.

Puinean, A.M., Denholm, I., Millar, N.S., Nauen, R., Williamson, M.S., 2010. Characterisation of imidacloprid resistance mechanisms in the brown planthopper, *Nilaparvata lugens* Stål (Hemiptera: Delphacidae). *Pesticide Biochemistry and Physiology* **97**, 129-132.

Rauch, N., Nauen, R., 2003. Identification of biochemical markers linked to neonicotinoid cross resistance in *Bemisia tabaci* (Hemiptera: Aleyrodidae). *Archives of Insect Biochemistry and Physiology* **54**, 165-176.

Roditakis, E., Morou, E., Tsagkarakou, A., Riga, M., Nauen, R., Paine, M., Morin, S., Vontas, J., 2011. Assessment of the *Bemisia tabaci CYP6CM1vQ* transcript and protein levels in laboratory and field-derived imidacloprid-resistant insects and cross-metabolism potential of the recombinant enzyme. *Insect Science* **18**, 23-29.

Saavedra-Rodriguez, K., Strode, C., Flores Suarez, A., Fernandez Salas, I., Ranson, H., Hemingway, J., Black, W.C., 2008. Quantitative trait loci mapping of genome regions controlling permethrin resistance in the mosquito *Aedes aegypti*. *Genetics* **180**,

1137-1152.

Scott, J.G., 1999. Cytochromes P450 and insecticide resistance. *Insect Biochemistry and Molecular Biology* **29**, 757-777.

Scott, J.G., Liu, N., Wen, Z., 1998. Insect cytochromes P450: diversity, insecticide resistance and tolerance to plant toxins1. Comparative Biochemistry and Physiology Part C: *Pharmacology, Toxicology and Endocrinology* **121**, 147-155.

Shimomura, M., Satoh, H., Yokota, M., Ihara, M., Matsuda, K., Sattelle, D.B., 2005. Insect-vertebrate chimeric nicotinic acetylcholine receptors identify a region, loop B to the N-terminus of the *Drosophila* Dα2 subunit, which contributes to neonicotinoid sensitivity. *Neuroscience Letters* **385**, 168-172.

Shimomura, M., Yokota, M., Ihara, M., Akamatsu, M., Sattelle, D.B., Matsuda, K., 2006. Role in the selectivity of neonicotinoids of insect-specific basic residues in loop D of the nicotinic acetylcholine receptor agonist binding site. *Molecular Pharmacology* **70**, 1255-1263.

Shimomura, M., Yokota, M., Matsuda, K., Sattelle, D.B., Komai, K., 2004. Roles of loop C and the loop B-C interval of the nicotinic receptor alpha subunit in its selective interactions with imidacloprid in insects. *Neuroscience Letters* **363**, 195-198.

Sparks, T.C., DeBoer, G.J., Wang, N.X., Hasler, J.M., Loso, M.R., Watson, G.B., 2012. Differential metabolism of sulfoximine and neonicotinoid insecticides by *Drosophila melanogaster* monooxygenase CYP6G1. *Pesticide Biochemistry and Physiology* **103**, 159-165.

Sparks, T.C., Nauen, R., 2015. IRAC: Mode of action classification and insecticide resistance management. *Pesticide Biochemistry and Physiology* **121**, 122-128.

Srisawat, R., Komalamisra, N., Eshita, Y., Zheng, M., Ono, K., Itoh, T.Q., Matsumoto, A., Petmitr, S., Rongsriyam, Y., 2010. Point mutations in domain II of the voltage-gated sodium channel gene in deltamethrin-resistant *Aedes aegypti* (Diptera: Culicidae). *The journal Applied Entomology and Zoology* **45**.

Stenhouse, S.A., Plernsub, S., Yanola, J., Lumjuan, N., Dantrakool, A., Choochote, W., Somboon, P., 2013. Detection of the V1016G mutation in the voltage-gated sodium channel gene of *Aedes aegypti* (Diptera: Culicidae) by allele-specific PCR assay, and its

distribution and effect on deltamethrin resistance in Thailand. *Parasites & Vectors* **6**, 253.

Sun, J., Nishiyama, T., Shimizu, K., Kadota, K., 2013. TCC: an R package for comparing tag count data with robust normalization strategies. *BMC Bioinformatics* **14**, 219.

Talley, T.T., Harel, M., Hibbs, R.E., Radic, Z., Tomizawa, M., Casida, J.E., Taylor, P., 2008. Atomic interactions of neonicotinoid agonists with AChBP: molecular recognition of the distinctive electronegative pharmacophore. *Proceedings of the National Academy of Sciences of the United States of America* **105**, 7606-7611.

Tamura, K., Stecher, G., Peterson, D., Filipski, A., Kumar, S., 2013. MEGA6: molecular evolutionary genetics analysis version 6.0. *Molecular Biology and Evolution* **30**, 2725-2729.

Tan, J., Galligan, J.J., Hollingworth, R.M., 2007. Agonist actions of neonicotinoids on nicotinic acetylcholine receptors expressed by cockroach neurons. *Neurotoxicology* **28**, 829-842.

Tan, J., Liu, Z., Nomura, Y., Goldin, A.L., Dong, K., 2002. Alternative splicing of an insect sodium channel gene generates pharmacologically distinct sodium channels. The *Journal of Neuroscience* **22**, 5300-5309.

Tan, P., Tong, L., 2004. Identification of delamination in a composite beam using integrated piezoelectric sensor/actuator layer. *Composite Structures* **66**, 391-398.

Tatebayashi, H., Narahashi, T., 1994. Differential mechanism of action of the pyrethroid tetramethrin on tetrodotoxin-sensitive and tetrodotoxin-resistant sodium channels. *Journal of Pharmacology and Experimental Therapeutics* **270**, 595-603.

Thackeray, J.R., Ganetzky, B., 1995. Conserved alternative splicing patterns and splicing signals in the *Drosophila* sodium channel gene *para*. *Genetics* **141**, 203-214.

Thany, S.H., Lenaers, G., Raymond-Delpech, V., Sattelle, D.B., Lapied, B., 2007. Exploring the pharmacological properties of insect nicotinic acetylcholine receptors. *Trends in Pharmacological Sciences* **28**, 14-22.

Tomizawa, M., Casida, J.E., 2001. Structure and diversity of insect nicotinic

acetylcholine receptors. *Pest Management Science* **57**, 914-922.

Tomizawa, M., Casida, J.E., 2005. NEONICOTINOID INSECTICIDE TOXICOLOGY: mechanisms of selective action. *Annual Review of Pharmacology and Toxicology* **45**, 247-268.

Toshima, K., Ihara, M., Kanaoka, S., Tarumoto, K., Yamada, A., Sattelle, D.B., Matsuda, K., 2008. Potentiating and blocking actions of neonicotinoids on the response to acetylcholine of the neuronal α4β2 nicotinic acetylcholine receptor. *Journal of Pesticide Science* **33**, 146-151.

Toshima, K., Kanaoka, S., Yamada, A., Tarumoto, K., Akamatsu, M., Sattelle, D.B., Matsuda, K., 2009. Combined roles of loops C and D in the interactions of a neonicotinoid insecticide imidacloprid with the alphα4betα2 nicotinic acetylcholine receptor. *Neuropharmacology* **56**, 264-272.

Unwin, N., Fujiyoshi, Y., 2012. Gating movement of acetylcholine receptor caught by plunge-freezing. *Journal of Molecular Biology* **422**, 617-634.

Vais, H., Williamson, M.S., Goodson, S.J., Devonshire, A.L., Warmke, J.W., Usherwood, P.N.R., Cohen, C.J., 2000. Activation of *Drosophila* sodium channels promotes modification by deltamethrin. reductions in affinity caused by knock-down resistance mutations. *Journal of General Physiology* **115**, 305-318.

Vontas, J., Kioulos, E., Pavlidi, N., Morou, E., della Torre, A., Ranson, H., 2012. Insecticide resistance in the major dengue vectors *Aedes albopictus* and *Aedes aegypti*. *Pesticide Biochemistry and Physiology* **104**, 126-131.

Wang, B., Li, L., Hurley, T.D., Meroueh, S.O., 2013. Molecular recognition in a diverse set of protein-ligand interactions studied with molecular dynamics simulations and end-point free energy calculations. *Journal of Chemical Information and Modeling* **53**, 2659-2670.

Wang, N.X., Watson, G.B., Loso, M.R., Sparks, T.C., 2016. Molecular modeling of sulfoxaflor and neonicotinoid binding in insect nicotinic acetylcholine receptors: impact of the *Myzus* β1 R81T mutation. *Pest Management Science* **72**, 1467-1474.

Wang, W., Lim, W.A., Jakalian, A., Wang, J., Wang, J., Luo, R., Bayly, C.I., Kollman, P.A., 2001. An analysis of the interactions between the Sem−5 SH3 domain and its

ligands using molecular dynamics, free energy calculations, and sequence analysis. Jour*nal of the American Chemical Society* **123**, 3986-3994.

Watson, G.B., Loso, M.R., Babcock, J.M., Hasler, J.M., Letherer, T.J., Young, C.D., Zhu, Y., Casida, J.E., Sparks, T.C., 2011. Novel nicotinic action of the sulfoximine insecticide sulfoxaflor. *Insect Biochemistry and Molecular Biology* **4**1, 432-439.

Zewen, L., Zhaojun, H., Yinchang, W., Lingchun, Z., Hongwei, Z., Chengjun, L., 2003. Selection for imidacloprid resistance in *Nilaparvata lugens*: cross-resistance patterns and possible mechanisms. *Pest Management Science* **59**, 1355-1359.

Zhao, G., Liu, W., Brown, J.M., Knowles, C.O., 1995. Insecticide resistance in field and laboratory strains of western flower thrips (Thysanoptera: Thripidae). *Journal of Economic Entomology* **88**, 1164-1170.

Zhao, J.-Z., Bishop, B.A., Grafius, E.J., 2000. Inheritance and synergism of resistance to imidacloprid in the colorado potato beetle (Coleoptera: Chrysomelidae). *Journal of Economic Entomology* **93**, 1508-1514.

Zlotkin, E., 1999. The insect voltage-gated sodium channel as target of Iinsecticide. *Annual Review of Entomology* **44**, 429-455.

Acknowledements

This study was carried out at the Odawara Research Center, Nippon-soda Co. Ltd. The author would like to express his gratitude to Kazuhiko Matsuda for his kind guidance and warm encouragement during the course of this study. The author is also greatly indebted to Takashi Tomita, Shinji Kasai, Osamu Komagata, Kentaro Itokawa (National Institute of Infectious Diseases), Akira Matsuura (Miyazaki Agricultural Research Institute), Satoshi Toda (NARO Institute of Fruit Tree Science) for their kind suggestions and support for this research.

Finally, the author would like to offer special thanks to the members of Nippon-soda Co. Ltd., who created a beneficial work environment and supported this research. The work on nAChR and the neonicotinoid resistance of *Aphis gossypii* was supported by a grant from the Ministry of Agriculture, Forestry, and Fisheries of Japan (Genomics-based Technology for Agricultural Improvement, PRM-003).

List of Publication

Main publication

Koichi Hirata, Osamu Komagata, Kentaro Itokawa, Atsushi Yamamoto, Takashi Tomita, Shinji Kasai
A single crossing-over event in voltage-sensitive Na^+ channel genes may cause critical failure of dengue mosquito control by insecticides
PLOS Neglected Tropical Diseases., **8**, e3085, (2014).

Koichi Hirata, Ryotaro Kiyota, Akira Matsuura, Satoshi Toda, Atsushi Yamamoto, Takao Iwasa
Association between the R81T mutation in the nicotinic acetylcholine receptor β1 subunit of *Aphis gossypii* and the differential resistance to acetamiprid and imidacloprid
Journal of Pesticide Science., **40**, 25-31 (2015).

Koichi Hirata, Akiya Jouraku, Seigo Kuwazaki, Hajime Shimomura, Takao Iwasa
Studies on *Aphis gossypii* cytochrome P450s CYP6CY22 and CYP6CY13 using an in vitro system
Journal of Pesticide Science., **42**, 97-104 (2017).

Koichi Hirata, Akiya Jouraku, Seigo Kuwazaki, Jun Kanazawa, Takao Iwasa
The R81T mutation in the nicotinic acetylcholine receptor of *Aphis gossypii* is associated with neonicotinoid insecticide resistance with differential effects for cyano- and nitro-substituted neonicotinoids
Pesticide Biochemistry and Physiology., **143**, 57-65 (2017).

Related publication

Ikuya Ohno, Koichi Hirata, Chiharu Ishida, Makoto Ihara, Kazuhiko Matsuda, Shinzo Kagabu
Proinsecticide candidates *N*-(5-methyl-2-oxo-1,3-dioxol-4-yl)methyl derivatives of imidacloprid and 1-chlorothiazolylmethyl-2-nitroimino-imidazolidine
Bioorganic & Medicinal Chemistry Letters., **17**, 4500-4503 (2007).

Makoto Ihara, Koichi Hirata, Chiharu Ishida, Shinzo Kagabu, Kazuhiko Matsuda
Blocking actions of alkylene-tethered bis-neonicotinoids on nicotinic acetylcholine receptors expressed by terminal abdominal ganglion neurons of *Periplaneta americana*
Neuroscience Letters., **425**, 137-140 (2007).

Lijun Liu, Mohammad Sayed Alam, Koichi Hirata, Kazuhiko Matsuda, Yoshihisa Ozoe
Actions of quinolizidine alkaloids on *Periplaneta americana* nicotinic acetylcholine receptors
Pest Management Science., **64**, 1222-1228 (2008).

Koichi Hirata, Chiharu Ishida, Yoko Eguchi, Kazuto Sakai, Fumio Ozoe, Yoshihisa Ozoe, Kazuhiko Matsuda
Role of a serine residue (S278) in the pore-facing region of the housefly L-glutamate-gated chloride channel in determining sensitivity to noncompetitive antagonists
Insect Molecular Biology., **17**, 341-350 (2008)

Saori Kataoka, Syogo Furutani, Koichi Hirata, Hideo Hayashi, Kazuhiko Matsuda
Three austin family compounds from *Penicillium brasilianum* exhibit selective blocking action on cockroach nicotinic acetylcholine receptors
Neurotoxicology., **32**, 123-129 (2011).

Koichi Hirata, Saori Kataoka, Syogo Furutani, Hideo Hayashi, Kazuhiko Matsuda
A fungal metabolite asperparaline a strongly and selectively blocks insect nicotinic acetylcholine receptors: the first report on the mode of action
PLoS One, **6**, e18354 (2011).

Koichi Hirata
Studies on the mode of action of neurotoxic insecticides
Journal of Pesticide Science., **41**, 87-94 (2016).

Shinji Kasai, Koichi Hirata, Osamu Komagata, Kentaro Itokawa, Takashi Tomita
Molecular mechanisms underlying pyrethroid resistance in dengue mosquito vectors collected from Singapore. *Acta Horticulturae.* **1169**, 87-92 (2017).